FROM QTL TO QTG:
MOLECULAR AND BIOCHEMICAL STUDIES TOWARD UNDERSTANDING THE INFLUENCE OF A MOUSE CHROMOSOME 1 LOCUS ON ALCOHOL WITHDRAWAL VULNERABILITY

By

DeAunne Lenay Denmark

A DISSERTATION

Presented to the Neuroscience Graduate Program

and the Oregon Health & Science University

School of Medicine

in partial fulfillment of

the requirements for the degree of

Doctor of Philosophy

August 2009

School of Medicine

Oregon Health & Science University

CERTIFICATE OF APPROVAL

This is to certify that the Ph.D. dissertation of

DeAunne Lenay Denmark

has been approved

Kari Buck	Mentor
Robert Hitzemann	Committee Chair
Dennis Koop	Committee Member
Joseph Quinn	Committee Member
Aaron Janowsky	Committee Member

TABLE OF CONTENTS

LIST OF TABLES AND FIGURES

Tables

Figures

Acknowledgements

Where to begin when there are so many incredible people to thank for their role and accompaniment on this journey? How lucky and grateful I am. Of course, the most heartfelt appreciation to my mentor, Dr. Kari Buck, for accepting me into her lab as a graduate student and allowing me this immense opportunity for discovery, growth, learning, and challenge. Kari's supreme standards of scientific excellence, work ethic, values of respect and integrity are outstanding. Her rare agility and persistence in balancing professional accomplishment and scientific progress with personal fulfillment outside her career provide a model I have rarely seen, but have aspired to emulate from the very beginning. Added to her breadth of experience and knowledge in diverse fields, and encouraging, optimistic, and supportive ways of providing guidance, she is a brilliant example of mentorship that I will continue to channel for the rest of my life. Integral to my success along this path was Nikki Walter who took on the perhaps daunting dask of imparting to the new graduate student her extensive expertise in molecular biology, a role from which she was never able to get out from under. Her patience, generosity, and ability to listen and teach are some of the most superior I have encountered. Dr. Laura Kozell, for her steadfast and endless supply of encouraging words, supportive hugs, and both personal and professional wisdom invariably available at exactly the right time. Dr. Renee Shirley, for her razor-sharp intellect, superb organizational skills, wise practicality, and calming reassurance that everything would, indeed, come to completion. All the members of my committee: Bob Hitzemann, Joe Quinn, Dennis Koop, and Aaron Janowsky, each of whom will continue to motivate and inspire me well into the future. A very special thanks to the director of the OHSU MD/PhD Program, Dr. David Jacoby, whose sincere investment in the career development, success, and advancement of each individual student, as well as concern for our well-being, is extraordinary and invaluable. My dear friend, the lovely Sarah Alexander, whose tremendous friendship, humor, laughter, and smiles have carried me through so many difficult moments over the last four years, and without which my life would not be so bright nor my focus so steady. Ms. Laurie Tull for her superb animal handling skills and relentless willingness to help with anything and everything, but particularly "certain" tasks that were sometimes too hard on my very soft heart. The lab technical support of the highest quality provided by Greg Auger, Nate Spofford, and Dimitri Boss, without whom the demanding and labor-intensive animal management could never run so smoothly, and camaraderie of my fellow graduate student and "the better sister," Ms. Lauren Milner. Countless, warmest, and most appreciative thanks are owed to my amazing friends, in particular Julie Lyons, Stephanie Draper, Marisa Brandt, Lynsey Gammon, Shannon Strumpfer, Jon Wilson, Jonah Bishop, Josh Walker, Ryan Lougeay, Jan Boitz, Gretchen Newmark, and Eric Tonsfeldt who bring pure joy to my life and remind who I am when I have fallen and forgotten. My incredible dog and four-legged best friend, Hobie, who truly makes every single one of my days better. And my utmost appreciation and humble gratitude for my parents, Linda and Steve, and my little brother, Kammer - you give me more than I can ever repay you, and inspire me in the most precious of ways. Thank you all for making this work possible.

ABSTRACT

Alcoholism/alcohol dependence is a widespread public health concern of international importance. A complex host of biological (genetic) and environmental factors interact throughout the addictive process to influence alcohol use/abuse has significantly hindered treatment and prevention of this disease. While the large genetic component of alcohol dependence is well-established, the identification of specific genetic determinants has been severely limited. Physiological dependence and associated withdrawal episodes in humans constitute a powerful motivational force that contributes to relapse and perpetuates continued alcohol use/abuse despite adverse physical, social and economic consequences. Physical signs of dependence and withdrawal in mice are remarkably similar to those seen in humans, and segregate in severity among inbred strains and their derivative populations. Thus, preclinical models utilizing these genetically tractable subtypes are extremely valuable tools for the discovery and/or verification of relevant genetic sources contributing to complex human diseases like alcoholism. This dissertation presents studies focused on a region of mouse Chromosome 1 syntenic with human chromosome 1q23.2-23.3 where quantitative trait loci (QTLs) with large effects on predisposition to physical dependence and associated withdrawal severity following chronic and acute alcohol exposure (*Alcdp1/Alcw1*) have recently been localized to a 1.1 Mb interval. First, a systematic molecular analysis of all the genes within this interval was performed to identify the most promising candidates that may underlie the QTL effect. Seventeen candidates, with known roles in a diverse spectrum of cellular functions, were identified as high priority based on validated genotype-dependent brain expression and/or non-synonymous coding sequence variation. Second, to assist in candidate prioritization, genome-wide expression data were further analyzed for *trans*-regulatory effects and putative network structure. As a functional category, genes related to mitochondrial function and oxidative homeostasis appeared distinctly overrepresented both among high priority candidates residing within the QTL interval, as well as among those located elsewhere in the genome. qRT-PCR on selected genes preliminarily confirmed an interaction between the *Alcdp1/Alcw1* QTL interval and a larger gene network involved in cellular stress response pathways. Damaging effects on brain mitochondrial bioenergetics and oxidative stress are some of the most well-known consequences of ethanol exposure, and is a highly plausible mechanism by which vulnerability to ethanol may be genetically influenced. Third, a biochemical approach was used to directly assess whether the mitochondrial respiratory chain exhibits genotype-dependent features before or after ethanol exposure and subsequent withdrawal. This work represents a substantial advancement toward identification of the gene(s) underlying *Alcdp1/Alcw1*, and suggests a promising neurobiological mechanism for its phenotypic effects. It is my sincere hope that this work will continue to improve understanding and future research directed toward identifying the specific genetic determinants of alcoholism.

I. GENERAL INTRODUCTION

I.A. Alcohol dependence/alcoholism

In the United States, it is estimated that 17.6 million people, about 1 in every 12 adults, abuse alcohol or are alcohol dependent (http://www.niaaa.nih.gov.liboff.ohsu.edu). Dependence is defined by the current Diagnostic and Statistical Manual-IV (DSM-IV) as “a maladaptive pattern of substance use, leading to clinically significant impairment or distress,” and commonly manifests as tolerance to the intoxicating or desired effects of alcohol accompanied by the appearance of adverse symptoms when it is discontinued. The use of alcohol occurs in virtually every facet of our society and internationally, over many age groups, and is a leading cause of morbidity and premature death in this country[1].

Physical dependence on alcohol and associated withdrawal are thought to constitute a powerful motivational force that perpetuates continued use/abuse and contributes to relapse. Seizure or convulsive activity (tonic and/or tonic-clonic) is a well-known consequence of physical dependence and is one of the most feared manifestations of the withdrawal syndrome in alcoholics. The withdrawal syndrome is often considered to be a "rebound" phenomenon, occurring subsequent to the largely depressive effects of alcohol on the ligand- and voltage-gated ion channels driving neurotransmission. During extended exposure, compensatory (homeostatic) processes develop in the CNS that lead to the development of functional tolerance in the presence of ethanol, and cross-tolerance to other depressants. When the ethanol is abruptly withdrawn (i.e., use is discontinued), these previously compensatory neuroadaptive processes exhibit over-compensation, leading to the CNS hyperexcitability signs (e.g., anxiety, psychomotor agitation, tachycardia, seizures) characteristic of the withdrawal syndrome[2].

In humans, the brain stem is known to play an important role in withdrawal seizures, and contributes to a pathophysiologic mechanism distinct from other clinically important seizure types[2]. While it is clear that other structures are most certainly involved, the underlying

neurocircuitry and cellular substrates are still mostly unknown. Rodent models mimicking the human withdrawal syndrome (Section I.C) have been highly useful in elucidating contributory CNS physiology, and typically involve eliciting convulsions audiogenically or by handling after some ethanol exposure paradigm. In these models, audiogenic seizures appear to be mediated largely in the brainstem, with a critical role played by the inferior colliculus[3] and propagation possibly supported by the hippocampus[4]. Conversely, handling-induced convulsions seem to require a broader neuronal circuitry, incorporating regions of the extended amygala, hippocampus, cortex, and basal ganglia and is strongly influenced by genetic factors[5-7].

I.B. Human genes for alcohol dependence and withdrawal

The importance of genetic factors in alcohol dependence has been supported for many years, arising largely through repeated observations that 1) relatives of alcoholics carry a several-fold increased risk of developing dependence, 2) identical twins of alcohol-dependent patients carry a higher risk than fraternal twins or full siblings, 3) children of alcoholics adopted to other families carry the same enhanced risk as do offspring raised by the affected parent[8]. Decades of research have contributed to the accepted estimation that 40-60% of disease risk can be genetically explained, making alcohol abuse/dependence one of the most highly heritable addictive conditions[9]. It is, however, clearly a complex disorder comprised of many behavioral phenotypes, and influenced by multiple genes that likely interact with each other as well as multi-factorial environmental components to ultimately impact disease development.

In general, identification of genes involved in alcohol use disorders has been pursued in affected populations through attempting to either establish an association, or linkage, between a chromosomal region and an alcohol-related phenotype, or by directly genotyping a candidate gene of interest. The large collection of pedigree data available through the collaborative study on the genetics of alcoholism (COGA) has identified regions associated with alcohol dependence on several chromosomes[10]. These have been most consistently replicated for a Chromosome 4q region containing a cluster of gamma-aminobutyric acid (GABA) receptor

genes[11], and 7q31-35 where high priority candidates include receptors involved in bitter taste sensitivity[12] and cholinergic muscarinic neurotransmission[13]. Candidate gene studies rely on a certain degree of *a priori* information regarding potential involvement in the trait under study, and were used to identify polymorphisms in the metabolic enzymes alcohol dehydrogenase (ADH), also located on 4q, and acetaldehyde dehydrogenase (ALDH2) as strongly associated with risk for dependence in several populations (reviewed by[10]). Similarly, primary alcohol effects have long been known to involve dopamine, serotonin, and GABA neurotransmission, and led to the discovery that variation in several genes related to these systems are associated with alcohol dependence in certain populations (reviewed by[10]).

While these studies have been made significant and critical headway, the confident identification of genes underlying dependence has been severely limited. Attempts to genetically dissect particular components of dependence are complicated in humans by genetic heterogeneity, complex inheritance, diagnostic uncertainties, and environmental factors. Accordingly, almost no information regarding specific genetic contributions to the withdrawal syndrome as an aspect of dependence is available, except that symptoms have a genetic predisposition[14, 15] and aggregate in families[16]. Animal models with alcohol phenotypes similar to humans can therefore be particularly useful for providing genetic clues that will improve the efficiency and confidence of gene identification. While it may not be possible to develop a comprehensive model, a deeper understanding of the neurobiology underlying specific traits (i.e., withdrawal) that closely approximate the clinical situation is essential for advancing elucidation of gene networks involved in the human disease condition.

I.C. Animal models for withdrawal in alcohol genetics research

Physical signs of alcohol withdrawal in animals are remarkably similar to those seen in humans. These include autonomic overactivity, tremor and other motoric dysfunction[17, 18], as well as potentially life-threatening convulsions that are seen in all mammalian species during severe withdrawal. Because other signs of withdrawal are highly correlated with convulsive

activity[19, 20], common practice is to use convulsive activity as the primary index of ethanol withdrawal syndrome severity. The handling-induced convulsion (HIC), so called because it is elicited by picking up a mouse by the tail, is a well-accepted method that provides a quantitative and reproducible index of motor seizure severity associated with ethanol withdrawal[21] (Table 1).

While several variations exist, two general versions of exposure/withdrawal paradigms are the most widely used in animal studies: chronic and acute. Chronic models of withdrawal commonly utilize continuous ethanol exposure induced through diet or inhalation over multiple days and are the most commonly used protocols to study physical dependence and associated withdrawal in animals[22]. In the acute model, withdrawal is monitored over the 12 hr following a single hypnotic dose of ethanol (4 g/kg ip), and has the advantages that neither monitoring nor stabilization of blood ethanol concentrations (BECs) is necessary, since BECs typically vary little across genotype after a single injection. The chronic model has advantages in that withdrawal is more intense, allowing for more accurate quantitation of individual differences. Perhaps for this reason, the heritability is also higher for the chronic model.

Table 1. Handling-Induced Convulsion (HIC) Scale used to index withdrawal severity

Handling-induced convulsion rating scale

Symptom	Score
No convulsion or facial grimace after gentle 180° spin	0
A facial grimace is seen after gentle 180° spin	1
No convulsion when lifted by the tail, but a tonic convulsion is elicited by a gentle 180° spin	2
Tonic-clonic convulsion after a gentle 180° spin	3
Tonic convulsion upon lifting by the tail	4
Tonic-clonic convulsion when lifted by the tail, often with the onset delayed up to 1-2 seconds	5
Severe, tonic-clonic convulsion when lifted by the tail, with a quick onset and long duration, often continuing for several seconds after the mouse is released	6
Severe, tonic-clonic convulsion elicited prior to lifting by the tail, with a quick onset and long duration, often continuing for several seconds after the mouse is released	7

The C57BL/6J (B6) and DBA/2J (D2) mouse strains are the most widely studied genetic models of severe and mild ethanol withdrawal, respectively. Extrapolated from BXD recombinant inbred (RI) strain data to the F_2, the estimated heritability (h^2_{F2}; index of the proportion of the total variation due to genetic sources) is 0.38 for the chronic model[23, 24] and 0.24 for the acute model[25]. It appears that the longer ethanol treatment duration of the chronic model allows additional genes to come into play compared to the acute model, so the genetic differences are qualitative as well as quantitative. The modest genetic correlation (r=0.48) between these two models among BXD RI strains indicates that 23% of the genetic variance is shared. Similar comparisons across standard inbred strains show 30% shared genetic variance and similar heritabilities[26].

An estimate of genetic correlation indexes the degree to which any pair of traits share common genetic influences, a condition termed pleiotropy[27, 28]. It is well-established that severity of withdrawal from ethanol in inbred strains has a significant proportion of genetic influence in common with withdrawal from other sedative-hypnotics having abuse liability, including pentobarbital, zolpidem, and diazepam [27, 29-31]. Furthermore, genetic relationships exist in these strains between withdrawal severity and other alcohol traits including preference drinking, conditioned taste aversion, tolerance to ethanol-induced hypothermia, and ethanol-stimulated activity [32, 33]. Portions of this pleiotropic influence have more recently been localized to particular chromosomal regions [30, 31, 34, 35], and will continue to be increasingly useful for the intricate process of candidate gene identification in animal models.

I.D. Quantitative trait loci (QTLs)

A QTL is a chromosomal site that influences a quantitative trait, which most often refers to a behavioral or physiological phenotype, but can formally include any biological manifestation that occurs over a range of measurable values. Due to their polygenic and polyenvironmental determination, quantitative traits are also called complex traits. In recent years, gene expression levels themselves have been recognized as quantitative traits influenced by eQTLs that display

similar mechanisms of complicated inheritance and genetic influence as classical phenotypic traits, and whose patterns of relationship may be exploited to better understand their role in shaping behavior and physiology[36, 37]. A primary objective of contemporary genetics research in biomedicine is to precisely locate the genetic information that influences a trait or disease of interest so its underlying mechanism can be rigorously studied.

QTL mapping has proved to be an extremely successful method for locating specific genomic regions amidst considerable "noise" from other QTLs and nongenetic sources of individual variation as uniquely influential on a complex trait. Increasingly sophisticated in technologies to greatly improve resolution of defined genome-wide polymorphisms, and the development of statistical methods to map QTLs from marker and trait data, have substantially enhanced the efficiency with which QTLs can be discovered[38]. To date, thousands of QTLs have been discovered in mice, traversing the entire spectrum of normal and pathological variation (Mouse Genome Informatics, www.informatics.jax.org). Chromosomal regions where marker allelic and trait variation covary implicates the presence of a QTL. This method has proven to be successful in identifying QTLs associated with several alcohol phenotypes, including those responsible for significant proportions of genetic variance in acute and chronic withdrawal severity on mouse Chromosomes (Chr) 1, 4, 11, and 19[34, 35].

I.E. B6 and D2: Diversity in ethanol-related and other traits

As described above, the B6 and D2 inbred mouse strains differ widely in withdrawal severity after both acute and chronic ethanol exposure. Not surprisingly, they also exhibit extensive variation in several other ethanol-related traits, mostly centered in preference and behavioral sensitivity. As early as 1959, it was demonstrated that B6 mice will readily consume ethanol in a standard two-bottle choice paradigm, while D2 mice display strong avoidance[39]. Since then, these two inbred strains have repeatedly demonstrated large divergences in the locomotor[40], hypnotic[41], ataxic[42], and reinforcing[43] effects of ethanol, as well as traits related to consumption (reviewed by[1]). Interestingly, QTLs for several of these have been localized to the same general

region of distal Chromosome 1 as the acute and chronic alcohol withdrawal loci mentioned above (Section II.A).

In addition to those related to ethanol, the B6 and D2 strains differ in a wide array of other behavioral and physiological traits. Oxidative, metabolic, and other stressors are emerging as important themes for the mechanisms contributing to genetic influence, and are often observed in studies related to aging. D2 have a significantly shorter lifespan compared with B6 (average 21 vs 29 months)[44], highly contrasting hematopoietic stem cell cycling characteristics[45], and reduced effectiveness of calorie restriction to extend longevity[46]. In the latter study, D2 also maintained less brain antioxidative capacity than B6 over the lifespan, and subsequently displayed higher metabolic rates in heart and skeletal muscle[47]. These strains exhibit drastically different phenotypes in the context of global mitochondrial superoxide dismutase (MnSOD) deficiency[48], and large disparities in susceptibility to a wide variety of lung pathogens known to act through oxidative mechanisms[44].

Predictably, genome-wide expression studies have also revealed inherently distinct gene networks in these strains and their derivative mapping populations[49-52]. Extensive interactive databases are now available cataloging these strain-specific expression traits (e.g., GeneNetwork, www.genenetwork.org) that will continue to serve as an extremely valuable resource for candidate gene identification studies. Misra *et al.*[44] recently observed an increase in several stress-response cascades in aging D2 mice, including upregulation of oxidative stress response genes involving detoxification and xenobiotic metabolism, and preservation of the heat shock response network in the lung. These stress protective programs were distinctly not engaged in B6; in fact, heat shock genes were selectively downregulated in this strain, while the IGF-I signaling pathway involved in longevity was preserved. Of particular relevance to our work, differential gene regulatory networks have been observed in B6 and D2 brain during withdrawal from both acute and chronic alcohol involving selective strain-specific activation of several programs central to cell survival, growth, and injury response[50, 53]. Furthermore, D2 mice

demonstrate higher brain expression than B6 of specific alcohol-related mitochondrial and oxidative stress genes, including *Aldh2*[54], glutathione reductase (*Gsr*; Buck lab, unpublished), and nicotinamide nucleotide transhydrogenase (*Nnt*)[55], but lower relative levels of metallothionein II (*Mt2*)[56] and a respiratory complex I subunit (*Ndufb8*)[57].

I.F. QTL discovery is only a first step on the path toward quantitative trait gene (QTG) identification

Identification of the specific genes underlying QTLs (quantitative trait genes, QTGs) is a major challenge in the translation of preclinical research[38]. QTL mapping, while critical to localizing influential regions with any confidence in a non-biased genome-wide approach, has historically done so with relatively low resolution. Intervals on the order of a few dozen centimorgans (cM) were the rule rather than the exception, and usually contained hundreds of genes, any number of which could play a plausible role in the phenotype of interest. Clearly, additional methods aiming to narrow the QTL interval are vital if the specific genetic variations truly involved in phenotypic expression are to be realistically determined.

The potentially complex genetic architecture of a QTL is becoming increasingly appreciated[36, 58, 59]. A major finding to emerge from mouse QTG cloning attempts is that, in most cases, a single genetic effect detected in inbred strain crosses is due to the combined small effects of several physically linked genes[38] sometimes with opposite effects, and perhaps inherited as a haplotype. Fine mapping can resolve closely linked loci[60], and has realized considerable success in many disease models through application of congenic techniques. In the interval specific strategy, defined chromosomal regions are introgressed by recombination between strains that display highly divergent traits, allowing the study of specific genetic intervals in relative isolation, i.e., in a new congenic line (ISCL, heterozygote for donor allele) or strain (ISCS, homozygote for donor allele) that has only the introgressed interval on a >98% uniform genomic background. Positive trait expression (capture) by the ISCL/S defines the critical interval, while simultaneously filtering out potentially large stretches of genomic

landscape by congenics that remain unaffected. Such congenics have been developed for many chromosomal regions, several of which have proven particularly useful for alcohol genetics research (reviewed in[61]).

Despite significant progress in detecting numerous QTLs and and narrowing some of these, only about 30 genes are currently accepted as QTGs for complex traits in mammals[62, 63]. These successes have relied upon evidence from several sources, and many have used congenic strains to their advantage [64-67]. In most cases, QTGs were identified using a stepwise process that eliminated all other possibilities by narrowing the region and comparing its composite molecular variation, then demonstrating the existence of allelic differences associated with the trait of interest. Additional strongly supportive evidence has often come from testing for a phenotypic effect using transgenics or knockouts whereby a biological mechanism of a gene's influence can be directly observed. Considering that these resources also have associated difficulties and caveats to interpretation that are well-known[68], and that even further challenges to QTG identification emerge when a QTL interval contains enhanced genetic diversity and/or gene density (Sections I.G, 2.D), the integration of mechanistic studies that can more completely elucidate underlying trait biology is a valuable complimentary approach for definitive nomination and validation of candidate genes.

I.G. Identification and fine mapping of acute (*Alcw1*) and chronic (*Alcdp1*) ethanol withdrawal QTLs on mouse Chromosome 1 (Chr 1)

Buck and colleagues initially mapped a QTL for acute alcohol withdrawal (*Alcw1*) to a large (20-50 cM) region of distal Chr 1[34] using mapping populations derived from the B6 and D2 progenitor strains. Fisher's method was used to calculate a combined *P* value for experiments using BXD recombinant inbred (RI) strains, B6D2 F_2, lines selectively bred to diverge in acute alcohol withdrawal severity, and congenic strain data, and identified a significant QTL using logarithm of odds scores (LOD) on distal Chr 1 ($p=2x10^{-10}$, LOD=8.8) accounting for 26% of the genetic variance in acute ethanol withdrawal severity. A QTL for chronic ethanol withdrawal

(*Alcdp1*) was also mapped to Chr 1[35]. Fisher's method was used to calculate a combined *P* value for experiments testing the same hypothesis using BXD strains, B6D2 F_2 mice, and congenic strain data, again identifying a significant QTL on distal Chr 1 ($P=2x10^{-9}$, LOD=7.6) that also accounted for approximately 26% of the genetic variance in chronic ethanol withdrawal severity.

Recently, Kozell *et al*. (2008) used an interval specific congenic strain approach to fine map both *Alcdp1* and *Alcw1*. A conventional congenic strain with an approximately 15 Mb introgressed interval (B6.D2-*Mtv7*) was crossed to B6 strain mice to yield F_1 (B6.D2-*Mtv7* X B6) mice, which were then backcrossed to B6 mice. Individual progeny were genotyped using markers in or flanking the QTL interval to identify mice harboring a recombination(s) within the starting congenic interval mice and define the boundaries of the introgressed region. Individual recombinant mice were backcrossed to B6 mice, resulting in multiple offspring with the same recombination, an ISCL. These were then intercrossed to generate donor interval homozygotes, ISCS. A panel of several Chr 1 ISCSs were behaviorally tested for chronic and acute ethanol withdrawal severity, and the phenotypic results, are shown in Figure 1. The B6.D2-*Mtv*, ISCS4, ISCS6, and ISCS8 (R8) all show more severe ethanol withdrawal than B6 background strain mice in acute and chronic models, thereby fine-mapping the critical region affecting both phenotypes to a minimal 1.1 Mb (172.8-173.9 Mb) interval of distal Chr 1.

These results substantially reduced the size of the QTL intervals, particularly for *Alcw1,* whose 1 LOD confidence region was originally 50 cM (approximately 100 Mb)[69]. Perhaps even more striking is the reduced number of potential candidate genes that, while well above several hundred before fine mapping, can now be confined to only a few dozen. Notably, this interval is one of the most gene-dense across all mouse chromosomes, containing ~4-5x the number of genes than expected based on calculations of average gene density (Section II.C.1). Additionally, genetic variation is extensive in much of this region; over 2000 B6/D2 single

nucleotide polymorphisms (SNPs) are present within just the 1.1 Mb minimal interval[70], while the boundary region just proximal is almost identical-by-descent between these strains.

Critically, while the original *Alcdp1* and *Alcw1* QTLs both lie within the same broad region of distal Chr 1 as a QTL (*Pbw1*) demonstrating a large effect on pentobarbital withdrawal[71], the R8 congenic does not display more severe withdrawal from pentobarbital than the B6 background strain[69]. These results indicate that *Pbw1* lies outside the 1.1 Mb fine-mapped interval, and were the first to confirm a fine mapped locus for alcohol withdrawal that does not influence barbiturate withdrawal. Additionally, a distal Chr 1 QTL for maximal electroshock seizure threshold[72] was localized to the region immediately distal to *Alcdp1*/Alcw1[73] and most recently shown to contain the entire *Pbw1* effect[74]. These results highlight the utility of ISCSs in dissociating related and physically linked QTL, as well as the complexity of genetic architecture in this region of Chr 1. The widespread influence of this region on several alcohol-related and other behavioral, physiological, and immunological traits (Mouse Phenome Database, phenome.jax.org/pub-cgi/phenome/mpdcgi; Sections I.E., II.A), and its synteny with an alcohol dependence-associated region of distal human Chr 1 that also contains influential genes for other human conditions modeled in mice (reviewed by[75]), designate it as a highly important subject for detailed investigation in alcohol and other genetics research.

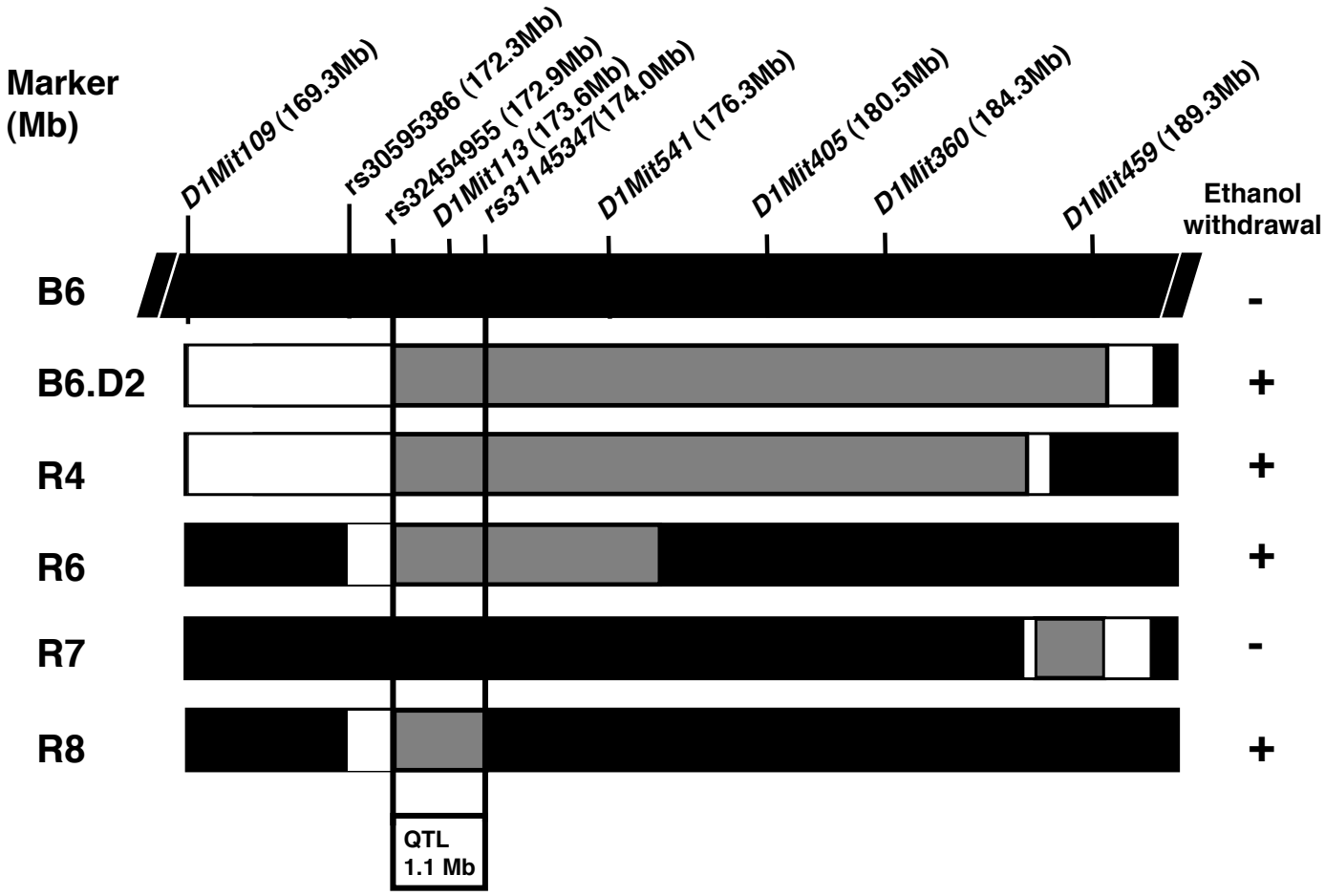

Figure 1. **Congenic strains (ISCSs) used to fine map the Chr 1 ethanol withdrawal QTL.**
In addition to the starting B6.D2 congenic strain, four recombinant ISCSs (R4, R6, R7 and R8) were developed and tested to attain higher resolution QTL mapping. The genetic markers examined to establish the congenic interval boundaries, and locations (in Mb), are indicated. For each congenic strain, the donor D2D2 segment is shown in gray; chromosomal regions homozygous for the B6 background strain allele are shown in black and the boundaries between the B6 and D2 regions are shown in white. Congenic mice that showed significantly more severe withdrawal than B6 background strain mice, i.e., QTL capture within the introgressed interval, are noted (+). Taken together, these data narrow *Alcdp1*/*Alcw1* to a minimal 1.1 Mb (172.9–174.0 Mb) interval; the maximal interval (172.3–174.0 Mb) includes a 0.6 Mb proximal boundary region. This directly corresponds to the R8 introgressed interval. (+) = QTL captured; (-) = QTL not captured. Adapted from Kozell *et al.* (2008)

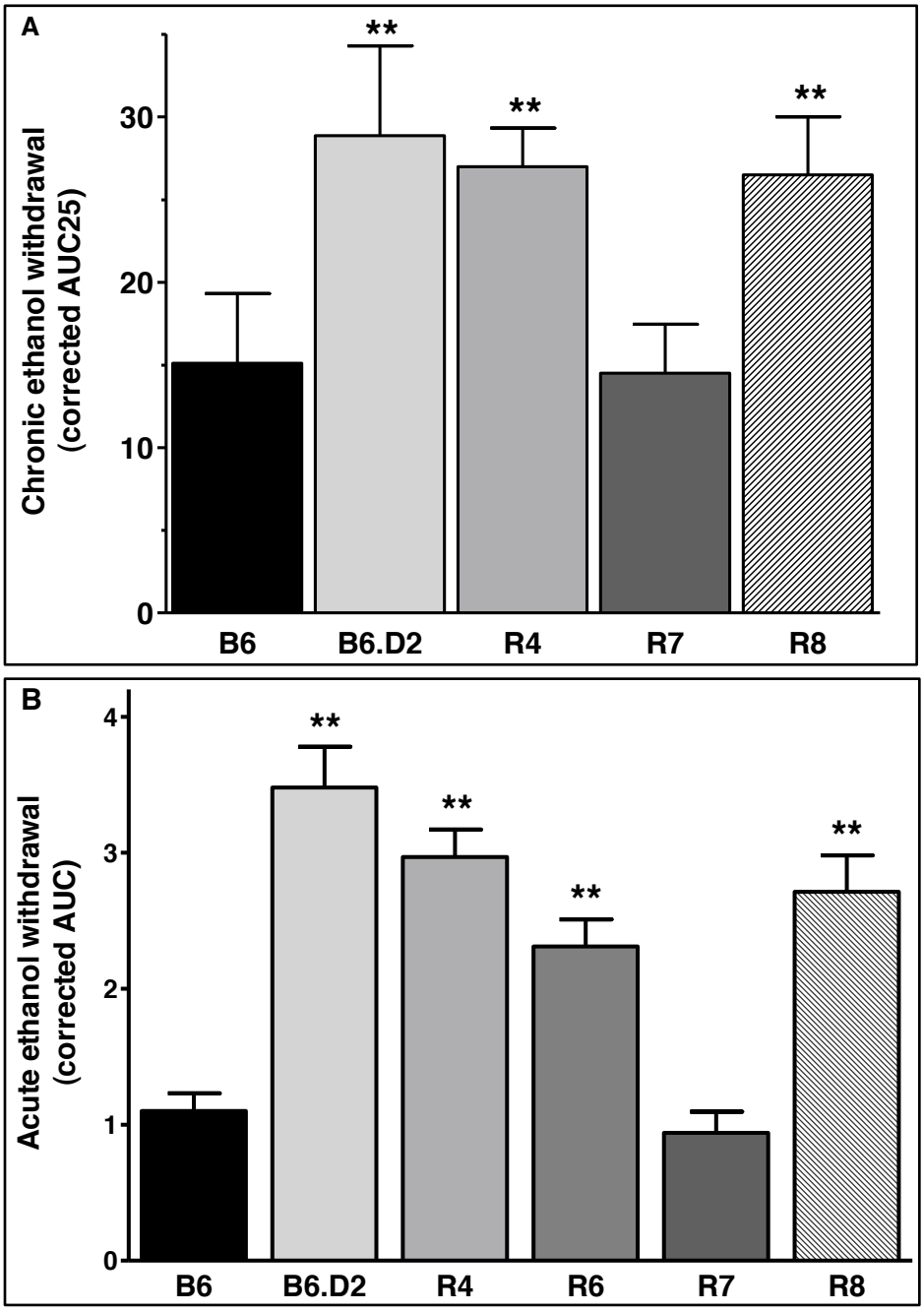

Figure 2. R8 congenic mice show significantly more severe withdrawal than background B6 mice. (A) Chronic ethanol withdrawal severity for the B6.D2, three ISCSs (R4, R7 and R8), and B6 background strain mice are shown, and was significantly different across strains ($H_{4,147}$=10.6, P=0.03). Ethanol withdrawal was more severe in B6.D2 (P=0.044, n=14), R4 (P=0.041, n=73) and R8 (P=0.048, n=33) than in B6 background strain mice (n=16). In contrast, chronic ethanol withdrawal severity did not differ from background strain mice for R7 (P=0.62, n=11). (B) Acute ethanol withdrawal severity for the B6.D2, four ISCSs, and B6 background strain mice are shown, and was significantly different across strains ($H_{[df=7]}$=85.2, $P<1 \times 10^{-15}$). Ethanol withdrawal was significantly more severe in B6.D2 ($P<1 \times 10^{-9}$, n=89), R4 ($P=6 \times 10^{-8}$, n=194), R6 ($P=1.4 \times 10^{-3}$, n=140) and R8 ($P=6.4 \times 10^{-5}$, n=119) mice than in background strain mice (n=126). In contrast, ethanol withdrawal severity did not differ from background strain mice for R7 (P=0.98, n=51). For details, please refer to Kozell *et al*. (2008). **P<0.05 (two-tailed)

I.H. Overall Goal

A decisive goal of QTL-to-QTG identification in animal models is the establishment of confident targets for research on human disease, in our case, alcoholism. In some fortunate cases the QTG will be the same in mouse and man[76], or QTL research will identify relevant gene networks involved in similar biology across species. Regardless, a comprehensive understanding of genetic variation in humans and animal models is crucial to establish relationships between genotype and biological function[77]. Furthermore, detailed knowledge of the neurobiological mechanisms underlying a behavior of interest is critical to validating the proposed QTG influence[78], or even confidently nominating particular candidates to pursue in the case that several are identified as promising. This thesis describes the following work that was undertaken as an effort in these directions: 1) A systematic, detailed, and unbiased molecular analysis of primary genetic variation within the fine mapped ethanol withdrawal QTL (*Alcdp1/Alcw1*) to identify the most promising candidate QTGs, 2) Interpretation of these results and integration of preliminary evidence to implicate the involvement of a larger gene network with primary functions of mitochondrial and cellular stress response activities, and 3) Application of a biochemical approach to directly assess whether the mitochondrial respiratory chain exhibits genotype-dependent features at baseline, and/or after ethanol exposure and subsequent withdrawal. It is my sincere hope that this work will contribute to an improved understanding of the means by which genetic variation at the *Alcdp1/Alcw1* QTG(s) exerts its effects on ethanol withdrawal severity in mouse and other animal models, and perhaps inform human studies directed toward identifying the specific genetic determinants of alcoholism.

II. MOLECULAR ANALYSES AND IDENTIFICATION OF PROMISING CANDIDATE GENES FOR LOCI ON MOUSE CHROMOSOME 1 AFFECTING ALCOHOL PHYSIOLOGICAL DEPENDENCE AND ASSOCIATED WITHDRAWAL

II.A. INTRODUCTION

The genetic determinants of alcoholism are largely unknown, significantly hindering effective treatment and prevention. Only a few genes have consistently demonstrated a role in alcoholism or associated endophenotypes in human studies, and can thus be nominated as candidate vulnerability genes. These include isoforms of the alcohol metabolizing enzymes *ADH1*, *ADH4, and ALDH2,* and neurotransmitter receptor subunits *GABRB1*, *GABRA2,* and *CHRM2*[79,80]. However, identification of these genes relied heavily on *a priori* knowledge of physiological responses to ethanol, and has not wholly explained the complex genetic susceptibility to alcoholism. Thus, unbiased and systematic approaches to gene discovery are critical if novel genes and mechanisms underlying alcohol dependence are to be discovered and translated to improved treatment and prevention.

No animal model can duplicate alcoholism in humans, but robust animal models for specific traits, including alcohol withdrawal, are valuable genetic resources. Detection of QTLs in these models is fundamental to an unbiased genome-wide search for candidate genes. In an accompanying set of experiments[69], Kozell *et al.* mapped QTLs (*Alcdp1* and *Alcw1*) affecting alcohol physical dependence and associated withdrawal following chronic and acute alcohol exposure to a minimal 1.1 Mb interval of mouse chromosome 1 syntenic with human chromosome 1q23.2-23.3. QTLs affecting alcohol-conditioned aversion[81], alcohol preference drinking[82], and alcohol-induced locomotor activation[83] and hypothermia[29] are also detected on distal Chr 1. The possibility that *Alcdp1/Alcw1* plays an important role in such diverse responses to alcohol makes it an important target. Moreover, at least four studies have identified markers on human chromosome 1q associated with alcoholism or associated endophenotypes[84-87] and, while still only localized to large regions, carry the potential to overlap with sytenic stretches on distal mouse Chr 1. Therefore, detailed analyses of *Alcdp1/Alcw1* candidate genes may inform

developing models for genetic influences on human alcoholism.

To date, few QTGs have been identified for the thousands of detected QTLs[38], and only one QTG (*Mpdz*) has been convincingly determined to influence alcohol withdrawal[67]. A comprehensive understanding of genetic variation in humans and informative animal models is crucial to establish relationships between genotype and biological function[88]. Here, we identify a list of high priority QTG candidates for *Alcdp1/Alcw1* using an integrative and unbiased strategy to systematically assess the molecular genetic variation within this interval.

II.B. METHODS

II.B.1. Animals

All animals used were bred in our colony at the Portland VA Medical Center. C57BL/6J (B6) and DBA/2J (D2) inbred strain breeders were purchased from the Jackson Laboratory (Bar Harbor, ME). Breeder stock for two chromosome 1 congenic strains (R8 and R4) were provided by Drs. John Hofstetter and Aimee Mayeda at the Indianapolis VA Medical Center. Detailed descriptions and capture of the increased ethanol withdrawal severity phenotype by R4 and R8 congenics can be found in[69]. Mice were group-housed 2-5 per cage by strain and sex. Mouse chow (Purina #5001) and water were available *ad libitum*, and lights were on from 6:00 AM to 6:00 PM in a colony room maintained at 22.0 ± 1.0°C. All procedures were approved by the Oregon Health & Science University and VA Medical Center Care and Use Committees in accordance with USDA and USPHS guidelines.

II.B.2. Candidate genes and brain expression analyses

The Ensembl (www.ensembl.org, NCBI Build 36, April 2006) and UCSC Genome Browser (www.genome.ucsc.edu, mm8, February 2006) databases were used to identify as many known and predicted genes as possible within the 1.1 Mb *Alcdp1/Alcw1* interval. Ensembl mouse transcript and NCBI RefSeq sequences were used as consensus sequences in subsequent gene and probe set alignments.

The Unigene (NCBI, www.ncbi.nlm.nih.gov/entrez/query, November 2006) and Allen Brain Atlas (ABA, www.brainatlas.org/aba, February 2008) databases were searched to obtain brain expression information for each known and predicted gene within *Alcdp1/Alcw1*. Additionally, genes for which public information was absent, minimal, or conflicting, were screened with transcript-specific PCR on a panel of mouse brain cDNAs (whole brain, brainstem, cerebellum, cortex, frontal cortex, hippocampus, hypothalamus, medulla, pons, thalamus) as in previous work[67]. Unigene is the largest organized resource for mouse transcriptome information,

including source cDNA. All genes were queried by MGI accession number and/or gene ID, and considered expressed only if "brain" or any brain region was listed as a cDNA source. Annotations of "whole head/neck," "eye," or "retina" were not considered evidence of brain expression. ABA is a database of genome-wide *in situ* hybridization mouse brain mRNA expression data superimposed on a detailed and interactive anatomical atlas. All *Alcdp1/Alcw1* genes were queried by gene ID and/or MGI accession number and analyzed individually in both 2D slice and 3D BrainExplorer modes. Expression patterns and densities were visually assessed for each of the major anatomical divisions curated by ABA and a qualitative expression rating assigned for a region based on non-isotopic ISH signal as detected and annotated by the database. Details of the methods used to derive relative expression level and density annotations can be found at www.brain-map.org/pdf/InformaticsDataProcessing.pdf.

II.B.3. Microarray expression analyses

Naïve R4 chromosome 1 congenic and B6 background strain mice (males 60-90 days of age) were euthanized by cervical dislocation, and the whole brain rapidly dissected and flash frozen in liquid nitrogen. The genetic composition of the R4 strain is >99.5% B6, except for an introgressed 5 Mb donor interval (172.97–177.97 Mb) spanning *Alcdp1/Alcw1* derived from the D2 strain[69]. Total RNA was isolated from pseudo-randomly chosen left or right hemispheres using TRIzol® reagent (Invitrogen) in a one-step guanidine isothiocyanate procedure as in previous work[53]. The extracted RNA was purified using the RNeasy kit (Qiagen) and evaluated by ultraviolet spectroscopy for purity and concentration. Samples containing 10 µg of total RNA were sent to the OHSU Gene Microarray Shared Resource facility for further quality control and microarray analysis. After labeling, individual RNA samples (n=6 per strain) were hybridized to Affymetrix MOE430A chips as specified by Affymetrix and detailed at www.ohsu.edu/gmsr/amc/services/serv_labeling.htm.

Position-dependent nearest neighbor (PDNN) analysis[89] using default settings was implemented using PerfectMatch software (Li Zhang, v2.1, http://odin.mdacc.tmc.edu/~zhangli/

PerfectMatch). Quantile normalization was performed with PDNN to enhance low-level analysis; this method incorporates hybridization efficiencies of individual probes and does not include mismatch probe data in the analysis.

II.B.4. Quantitative real-time PCR (qRT-PCR) expression analyses

Naïve R8 congenic and B6 background strain mice (males 60-90 days of age) were euthanized by cervical dislocation, and whole brains removed immediately by rapid dissection. The genetic composition of the R8 strain is >99.5% B6, except for a small interval donated from the D2 strain that entirely captures the *Alcdp1/Alcw1* effect on withdrawal severity[69]. The minimal R8 introgressed interval is 1.1 Mb (172.97-174.06 Mb). The maximal interval includes a proximal 0.6 Mb boundary region (172.37-172.97 Mb) currently undifferentiated between B6 and D2 due to strong identity by descent (data not shown), and thus not likely to contain positional QTG candidates[90]. The left or right hemisphere of individual animals (n=10-12 per strain) was chosen pseudo-randomly and placed in 500 μl RNAlater (Qiagen) for storage at 4°C until RNA extraction. Total RNA from half-brains was isolated with RNeasy (Qiagen) and mRNA purified with Oligotex (Qiagen). Prior to first-strand cDNA synthesis with High Capacity cDNA Archive Kit (ABI), aliquots of mRNA were treated with DNase (Promega) at 37°C for 30 minutes to eliminate potential contaminating genomic DNA.

qRT-PCR was used to confirm promising expression results obtained by microarray, as well as to assess those genes within the QTL interval that were not represented on the MOE430A chip. Relative expression was measured using validated gene-specific TaqMan assays (ABI), most of which span an intron as an additional control against contaminating genomic DNA. Reactions (20 μl) were performed in an ABI Prism7500 thermal cycler (ABI) using Two-Step PCR Master Mix. Threshold values (C_t) for target (candidate) gene expression levels were determined automatically by the standard TaqMan software package and normalized to reference gene (mouse *Hmbs*, Mm00660262_g1) expression. The comparative ($\Delta\Delta C_t$) method[91] was used for relative quantification, which powerfully corrects for run-to-run variability (e.g.,

pipetting errors, cDNA concentration or quality differences) by normalization of sample target and reference gene expression to expression levels of a calibrator sample (n=6 B6 and n=6 R8 mRNA aliquots pooled for synthesis of a single cDNA) included on each run.

II.B.5. Single nucleotide polymorphism (SNP) annotation

We compiled several public SNP datasets to annotate all known SNPs within the 1.1 Mb *Alcdp1/Alcw1* interval between the B6 and D2 progenitor strains as recently described[92]. This compilation includes D2 strain sequence data from the NIEHS/Perlegen Mouse Resequencing Project, the Mouse Phenome Database SNP Tool (http://www.jax.org/phenome/snp.html), and the Sanger resequencing SNPs from Ensembl. Direct sequencing of selected exons was conducted in-house when *in silico* D2 data were absent, low quality, or based on single reads. Sequence-specific primers were designed to amplify cDNA products of 0.1-1.0 kb based on consensus transcripts, and where possible, to span an intron for control against genomic contamination. PCR products were analyzed on ethidium bromide-stained 2% agarose gels, and selected bands excised, purified (QiaQuick, Qiagen), and submitted to the OHSU sequencing core facility. Details of the sequencing protocol used can be found at www.ohsu.edu/research/core/dseq/. Sequencing was performed on both strands for all products and raw reads reassembled in-house using Sequencher (v4.5, Gene Codes) DNA analysis software. The sequences have been deposited in dbSNP.

All probes and target sequences were aligned with SNP annotation to assess the potential impact of allelic differences on gene expression results. Affymetrix probe set target sequences and locations of individual probes were obtained at www.affymetrix.com (R20, July 2006). Since this information for TaqMan assays is proprietary, amplicon sequences were approximated from ABI (www2.appliedbiosystems.com) by assuming that the provided base number coordinate approximately corresponds to the amplicon's center nucleotide and taking into account the provided amplicon length. All probe sets spanning a SNP(s) were masked from the microarray analyses using a masking algorithm developed in our laboratory[92]. Alternative gene-specific

TaqMan assays were used when B6/D2 SNPs were detected in the initial probe's target sequence. Only expression results obtained using probes free of known SNPs are reported.

II.B.6. Data Analysis

All Affymetrix microarray (post low-level analysis with PDNN) and qRT-PCR data were analyzed for strain-dependent expression (B6 *vs.* R4 or R8, respectively) using a two-tailed (Student's) *t*-test implemented by Excel (Microsoft Office, 2003). Significance level for expression differences was set at $\alpha<0.05$ to increase the probability that the maximum of potentially true genotype-driven variation would be detected.

II.C. RESULTS

II.C.1. Identification of candidate genes within the 1.1 Mb Alcdp1/Alcw1 interval

Using mouse genome databases (Ensembl, UCSC) we identified as many known and predicted transcripts as possible within the 1.1 Mb QTL interval. As shown in Table 2, the minimal 1.1 Mb QTL contains a total of 37 known and three novel (predicted) protein-coding genes, as well as three non-coding RNAs and one pseudogene. These results distinguish the *Alcdp1/Alcw* interval as remarkably gene-dense (one known or predicted gene every 27.5kb) compared to estimates of the draft mouse genome (one per 113.6 kb)[93].

We used evidence for brain expression as an initial filter in prioritizing potential candidate genes because convulsions are centrally mediated, and handling-induced convulsions are an index of alcohol withdrawal severity for which pharmacokinetic factors are not crucially important[29, 94]. Using the Unigene and ABA databases, as well as a PCR-based screen on a panel of mouse brain cDNAs including whole brain and nine specific regions (data not shown), we confirmed expression in mouse brain for 33 of the 40 coding genes mapped within the *Alcdp1/Alcw1* interval, and established these as primary candidates (Table 2). Additionally, while absolute quantitation of expression levels is currently not possible with ABA, we used this resource to derive qualitative pattern and relative expression density information for primary candidates in the major brain regional subdivisions as a first step toward resolving cellular substrates of *Alcdp1/Alcw1*-influenced withdrawal (Table 2).

Table 2. Genes within the 1.1 Mb *Alcdp1/Alcw1* interval and evidence for brain expression.

GENE SYMBOL	DESCRIPTION	Entrez Gene ID	Uni Gene[a]	ABA regional expression[b]													
				CTX	OLF	HIP	RHP	AMY	STd	STv	LSX	PAL	TH	HY	MB	P	MY	CB
Fcgr3	Fc receptor, IgG, low affinity III	14131	+	-/+	-/+	-/+	-	-/+	-	-/+	-	-/+	-	-/+	-/+	-/+	-/+	-/+
1700009P17Rik	RIKEN cDNA 1700009P17 gene	75472	+	-/+	+	-/+	-/+	-	-/+	+	++	-/+	-/+	-	+	-/+	+	+
Sdhc	succinate dehydrogenase complex, subunit C	66052	+	+	+	++	+	+	+	+	+	+	+	+	+	+	-	+
Mpz	myelin protein zero	17528	+	+	+	+	+	-	+	-	-	-	-	-	-/+	-/+	+	+
Pcp4l1	Purkinje cell protein 4-like 1	66425	+	++	++	++	++	++	++	++	++	++	++	++	++	++	++	++
Nr1i3	nuclear receptor subfamily 1, group I, member 3	12355	+	+	+	+	+	+	+	+	-	+	-/+	+	+	+	+	+
Tomm40l	translocase of outer mitochondrial membrane 40 homolog-like (yeast)	641376	+								*nd*							
Apoa2	apolipoprotein A-II	11807	+	-	-/+	-/+	-	-	-	-	-	-	-	-	-	-/+	-/+	-
Fcer1g	Fc receptor, IgE, high affinity I, gamma polypeptide	14127	+								*nd*							
Ndufs2	NADH dehydrogenase (ubiquinone) Fe-S protein 2	226646	+	++	++	++	++	+	+	++	+	++	++	++	++	++	++	++
Adamts4	a disintegrin-like and metallopeptidase (reprolysin type) with thrombospondin type 1 motif, 4	240913	+	+	+	+	+	+	+	+	+	+	++	+	+	+	+	+
B4galt3	UDP-Gal:betaGlcNAc beta 1,4-galactosyltransferase, polypeptide 3	57370	+	++	++	++	++	+	+	+	+	+	++	++	+	+	+	+
Ppox	protoporphyrinogen oxidase	19044	+	+	+	++	+	+	-	+	-	-/+	+	+	+	+	+	+
Usp21	ubiquitin specific peptidase 21	30941	+	++	++	++	++	+	++	++	+	+	++	++	++	+	+	++
Ufc1	ubiquitin-fold modifier conjugating enzyme 1	66155	+	+	+	++	+	-/+	+	+	-	+	++	+	+	+	++	+
novel[c]	ENSMUSG00000079137		*nd*								*nd*							
Dedd	death effector domain-containing	21945	+	++	++	++	++	++	++	+	++	++	++	++	++	++	++	++
Nit1	nitrilase 1	27045	+	+	+	+	-	-	-	-	-	-	-/+	-	-	+	+	+
Pfdn2	prefoldin 2	18637	+	++	++	++	++	+	+	+	+	+	+	+	+	+	+	+
Klhdc9	kelch domain containing 9, 1190002J23Rik	68874	+	+	+	+	+	-	+	+	-	+	+	+	+	+	+	+
Pvrl4	poliovirus receptor-related 4	71740	+	++	++	++	+	+	+	+	+	+	+	+	+	+	+	+
Arhgap30	Rho GTPase activating protein 30	226652	-	-	-	-	-	-	-	-	-	-	-	-	-	-	-	-
Usf1	upstream transcription factor 1	22278	+	++	++	++	++	+	+	+	+	+	++	+	+	+	+	+
F11r	F11 receptor	16456	+	+	+	-	+	-	-/+	-/+	-	-	-/+	-	-/+	+	+	-/+
snRNA	U5		*nd*								*nd*							
Refbp2	RNA and export factor binding protein 2	56009	+								*nd*							
novel[c]	ENSMUSG00000038218		*nd*								*nd*							
Itln1[c]	intelectin 1	16429	-								*nd*							
Cd244[c]	CD244 natural killer cell receptor 2B4	18106	-								*nd*							
Ly9[c]	lymphocyte antigen 9	17085	-	-	-	-	-	-	-	-	-	-	-	-	-	-	-	-
Slamf7	SLAM family member 7	75345	-	+	+	+	+	+	+	+	-	+	+	+	-/+	+	+	-/+
Cd48	CD48 antigen	12506	+	-	+	-	-	-	-	-	-	-	-	-	-	+	+	-
novel	ENSMUSG00000059058, pseudogene		*nd*								*nd*							
snRNA	U6		*nd*								*nd*							
Slamf1[c]	SLAM family member 1	27218	-	-	-	-	-	-	-/+	-	-	-	-	-	-	-	-	-
Cd84	CD84 antigen	12523	+	-	-	-	-	-	-	-	-	-	-	-	-	-	-	-
Q3UP30[c]	novel, ENSMUSG00000073492		*nd*								*nd*							
miRNA	mmu-mir-680-3		*nd*								*nd*							
Slamf6	SLAM family member 6	30925	+	+	-/+	+	-/+	-	-/+	+	-	-/+	-	-	-	-/+	+	+
Ltap	loop tail associated protein 2	93840	+	-/+	+	-/+	-/+	-	-/+	-/+	-	-	-/+	-/+	-	-/+	-/+	+
Nhlh1	nescient helix loop helix 1	18071	+	-/+	+	+	+	-/+	-	-	-	-/+	-/+	-	-/+	-/+	-	-
Ncstn	nicastrin	59287	+	+	+	++	+	+	+	+	-/+	-/+	+	+	+	-/+	+	-/+
Copa	coatomer protein complex subunit alpha	12847	+	+	++	++	++	++	+	+	+	+	+	++	+	+	++	+
Pex19	peroxisome biogenesis factor 19	19298	+	++	+	++	+	-/+	+	-/+	-/+	-/+	+	-	-	-/+	-/+	+

Table 2. Genes within the 1.1 Mb *Alcdp1/Alcw1* interval and evidence for brain expression. The Ensembl and UCSC public genome databases were used to identify 37 known, 3 predicted, 1 pseudogene, and 3 non-coding RNA genes as all candidate genes within the 1.1 Mb QTL interval. The Unigene and ABA databases contain evidence of brain expression for 33 of these (bold face type) which represent the primary candidates for *Alcdp1/Alcw1* evaluated in subsequent studies. [a] Evidence of brain expression in Unigene: (+) 'brain' or brain region listed as cDNA source; (-) 'brain' or brain region not listed as cDNA source; (nd) no data available. [b] Evidence of regional brain expression in ABA: (-) no signal; (-/+) minimal signal, indistinguishable from artifact or extremely restricted expression; (+) moderate signal, significant expression present; (++) strong signal, dense and/or high level expression present; (*nd*) no data available. CTX=cerebral cortex, OLF=olfactory areas, HIP=hippocampal region, RHP=retrohippocampal region, AMY=amygdalar nuclei, STd=dorsal striatum, STv=ventral striatum, LSX=lateral septal complex, PAL=pallidum, TH=thalamus, HY=hypothalamus, MB=midbrain, P=pons, MY=medulla, CB=cerebellum. [c] Not detected by PCR on panel of mouse brain region cDNAs.

II.C.2. Microarray analyses

The Affymetrix database (http://www.affymetrix.com/) was queried using the basic local alignment search tool (BLAST) search to determine the microarray probe set(s) representing each of the confirmed candidate genes. To ensure that all brain regions potentially relevant to the behavioral expression of withdrawal were included in the analyses, and to increase power through biological replication, arrays were run on whole brain samples obtained from individual animals from the chromosome 1 congenic (R4) and B6 background strains (*n*=6 per strain). Comparison of gene expression between the R4 congenic and B6 background strains affords substantially increased confidence that expression differences detected for transcripts physically mapped within *Alcdp1/Alcw1* are *cis*-mediated, as would be expected for a true QTG. In the present studies, we decided to nominate candidates based on inherent genotype-dependent expression for three reasons: (1) Many more genes are differentially expressed between ethanol-naïve B6 and D2 mice than after a single injection of ethanol[50, 53]; (2) most of the ethanol-induced B6/D2 expression differences are already apparent before ethanol exposure [50]; and (3) the 4-7 hour timeframe post-ethanol injection is shorter than that generally thought to be required for the majority of gene expression changes to show the corresponding changes in protein critical for behavioral expression of differential withdrawal severity, increasing the likelihood that the relevant gene expression disparity(s) is pre-existing.

Thirty-one of the 33 primary candidates were represented by at least one high-quality probe set on the Affymetrix MOE430A chip, of which 11 (represented by 12 probe sets) showed evidence of inherent genotype-dependent brain expression (Figure 3). Nine out of eleven (82%) genes showed evidence of lower expression in R4 congenic vs. B6 background strain mice, while only two genes (*Ndufs2, Sdhc*) were apparently more highly expressed in congenic than background strain animals. None of the detected expression differences approached 50%, highlighting the importance of performing sensitive low-level analyses and potentially accepting

less-stringent false-positive or false discovery rates, and performing confirmation analyses (e.g., qRT-PCR), in initial microarray assessments of genome-wide brain expression[95].

II.C.3. Confirmatory candidate gene expression analyses

Gene- and transcript-specific qRT-PCR was performed for confirmation testing of genotype-dependent expression of the 11 microarray-implicated candidates, as well as the three candidates not represented on the Affymetrix MOE430A chip. Subsequent to microarray analyses, we identified a small donor segment congenic (R8) with a minimal 1.1 Mb donor interval, which entirely captured the *Alcdp1/Alcw1* effect on alcohol withdrawal following chronic and acute alcohol exposure at a magnitude equivalent to R4[69]. Therefore, qRT-PCR studies compared gene expression between R8 congenic and B6 background strain animals, even further increasing confidence that all detected differences are due to allelic variation contained within the *Alcdp1/Alcw1* interval. Because microarray results indicated no evidence for genotype-dependent expression for any gene within the 0.6 Mb proximal R8 boundary region and we have detected no B6/D2 allelic variation to-date (i.e., the region is highly identical by descent; data not shown), these genes were not assessed further.

Relative quantitation analyses confirmed genotype-dependent brain expression for 8 of the 11 microarray-implicated candidates (*Sdhc*, *Apoa2*, *Ndufs2*, *Adamts4*, *Ppox*, *Ufc1*, *Ncstn*, *Copa*; $p<0.02$), as well as for two of the three candidates not represented on the MOE430A array (*Klhdc9*, *Refbp2(b)*; $p<0.0007$; Table 3). This is an unusually high number of genes for such a small region to show baseline strain-specific expression, particularly since they are structurally unrelated, and corroborates earlier findings of disproportionately frequent basal expression differences between the B6 and D2 strains for genes in this region of Chr 1, even after correction for the increased gene density[50]. The direction of effect was consistent in all cases (B6 > congenic: *Apoa2*, *Adamts4*, *Ppox*, *Ufc1*, *Ncstn*, *Copa*; congenic > B6: *Sdhc*, *Ndufs2*), and while there was an increase in magnitude when compared to the microarray (Figure 3), only one

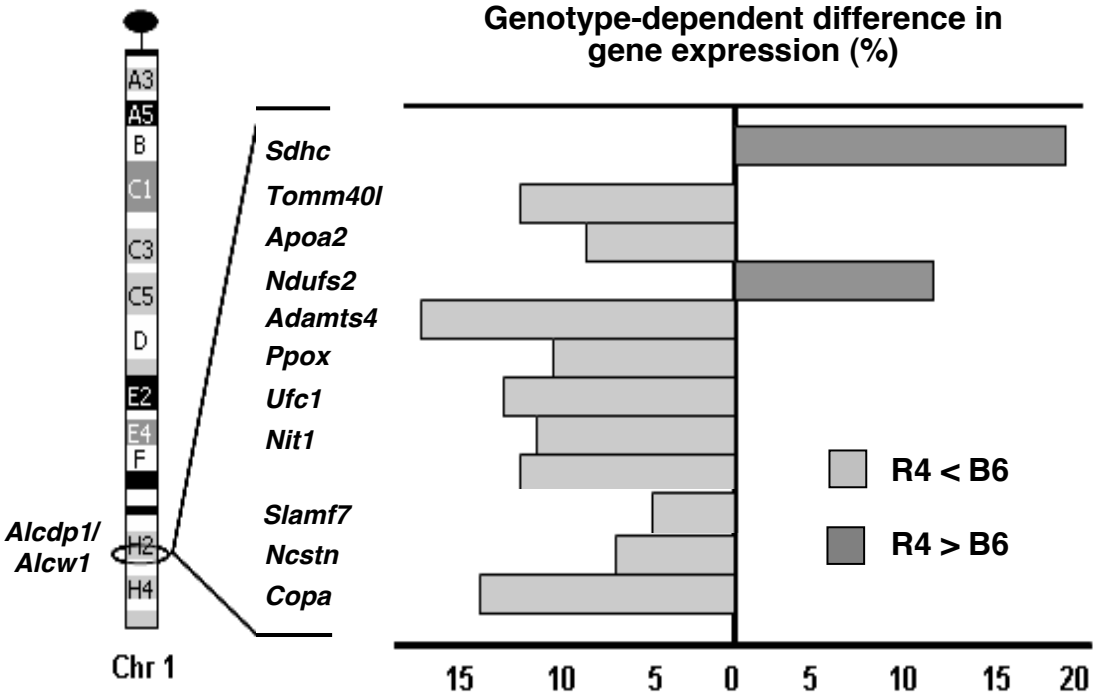

Figure 3. *Alcdp1/Alcw1* candidate genes with microarray evidence for differential expression between congenic (R4) and background strain (B6) mice. Genome-wide expression analyses were performed on R4 chromosome 1 congenic and background strain (B6) whole brain RNA with Affymetrix MOE430A chips (n=6 per strain). Thirty-one brain-expressed genes within the 1.1 Mb QTL interval were represented by at least one high quality probe-set; 11 of these displayed differential expression between strains ($p \leq 0.03$). Bars shown in light gray denote B6 > R4 expression, and bars shown in dark gray denote R4 > B6 expression. *Nit1* was represented by two probe sets both showing differential expression.

candidate (*Apoa2*) showed a between-strains difference greater than 2-fold. Interestingly, recent independent genome-wide expression data sets for two populations (BXD, B6D2F2) used to initially map the *Alcw1/Alcp1* QTL to distal Chr 1 indicate *cis*-regulation (i.e., genotype at markers within the R8 interval is significantly associated with expression level) for six of the eight candidates implicated by microarray and subsequently confirmed by qRT-PCR to exhibit genotype-dependent expression (*Sdhc*, *Apoa2*, *Ndufs2*, *Adamts4*, *Ufc1*, *Copa*; www.genenetwork.org).

qRT-PCR did not confirm genotype-dependent expression of three genes implicated by microarray (*Tomm40l*, *Nit1, Slamf7*; $p>0.4$), all of which showed initial evidence of lower expression in R4 congenic compared to the B6 background strain. Because Affymetrix probes are designed to match the reference B6 strain, this bias may have been caused by SNPs in the target sequences resulting in spuriously low hybridization signals for non-B6 alleles. It was recently demonstrated that at least 16% of the probe sets on the MOE430A microarray harbor SNPs between the B6 and donor (D2) strains, and that application of a SNP mask based on public database D2 sequence mitigates potentially false expression differences detected by microarray[92]. We applied this SNP mask to assess the impact of known SNPs between the congenic and B6 background strains on our microarray results, and observed no alteration in detected expression differences for genes within the *Alcdp1/Alcw1* interval (data not shown). However, it should be kept in mind that the public D2 sequence is not yet complete and cryptic SNPs may still exist between the two strains that have the potential to impact hybridization-based methods of assessing gene expression.

gene symbol	Taqman probe ID	R8/B6
1700009P17Rik	Mm00512620_m1	0.98
Sdhc	**Mm00481172_m1**	**1.49[d]**
Tomm40l	Mm01290711_g1	1.06
Apoa2	**Mm01290539_g1**	**0.01[d]**
Ndufs2	**Mm00467605_g1**	**1.58[c]**
Adamts4	**Mm00556068_m1**	**0.73[d]**
Ppox	**Mm00447232_m1**	**0.59[a]**
Ufc1	**Mm00502923_m1**	**0.83[a]**
Nit1	Mm00449588_m1	1.02
Klhdc9	**Mm01295280_g1**	**0.75[c]**
Refbp2(a)	Mm00727241_s1	*nd*
Refbp2(b)	**Mm01309506_s1**	**0.62[b]**
Slamf7	Mm00513807_m1	*nd*
Ncstn	**Mm01293326_g1**	**0.73[b]**
Copa	**Mm01283371_m1**	**0.60[d]**

Table 3. qRT-PCR confirms genotype-dependent expression between R8 chromosome 1 congenic and background (B6) strains for ten *Alcdp1/Alcw1* candidates. Bold face type indicates genes for which expression in R8 is statistically different than B6 as detected by the listed TaqMan assay and described in terms of percentage B6 level: [a] $p \leq 0.016$; [b] $p < 0.001$; [c] $p < 0.0005$; [d] $p < 0.00005$. *nd*, not determined, expression levels beneath the threshold of reliable detection (mean $C_t \geq 33$), or only available probe contains B6/D2 SNP(s).

II.C.4. *Candidate gene coding sequence variation*

We began by utilizing public databases to systematically assess *in silico* which genes within the 1.1 Mb *Alcdp1/Alcw1* interval contain non-synonymous coding SNPs (i.e., that result in changes of predicted protein sequences) between the B6 and D2 progenitor strains. To date, high quality D2 sequence provides evidence for nine such genes (*Fcgr3*, *Ndufs2*, *Adamts4*, *Nit1*, *Klhdc9*, *Slamf7*, *CD48*, *CD84*, *Pex19*; Table 4), the majority of which did not display genotype-dependent expression and are thus additional QTG candidates. No B6/D2 coding polymorphism has been detected for any gene within the 0.6 Mb boundary region (data not shown).

Additionally, we performed direct sequencing of the D2 strain for selected exons in genes for which there was no *in silico* evidence of non-synonymous SNPs due to lack of coverage, or where evidence was based entirely on single or low-quality reads. This resulted in the addition of five genes verified to contain previously unannotated non-synonymous SNPs (*Sdhc*, *Usp21*, *Refbp2*, *Ncstn*, *Copa*; Table 4), and nominate a total of 14 genes in the QTL interval as high priority candidates on the basis of predicted amino acid differences. These experiments provide a sound and unbiased evaluation of all genes within *Alcdp1/Alcw1* for potential QTG candidacy based on either the expression or sequence variation criteria. For genes already nominated as candidates based upon genotype-dependent expression or sequence, 100% coverage of D2 coding sequence was not necessarily sought. More complete D2 coverage will likely require bacterial artificial chromosome sequencing in future work to fully interrogate potential mechanisms by which the causal quantitative trait nucleotide(s) (QTNs) influences withdrawal.

gene symbol	B6/D2 amino acid difference	public SNP identifier
Fcgr3	Trp217Gly	rs8242800
	Ser222Arg	rs8242799
	Ser244Ala	rs4222823
Sdhc	Phe4Leu	rs31116911[b]
	Ser10Gly	ENSMUSSNP5307558
	Leu253Val	rs31554163
Ndufs2	Arg8Gly	rs31541214
Adamts4	Gln30Arg	rs31538642
	Phe574Tyr	ENSMUSSNP6311765
Usp21	Gly461Val	*a*
	Asp463His	*a*
	Asp500Ser	*a*
Nit1	Thr21Ile	rs31552464
Klhdc9	Thr6Pro	rs31549115
	Glu115Gly	ENSMUSSNP4475076
Refbp2	Asn18Ser	rs31537262
	Arg37Ser	ENSMUSSNP4909206[b]
	Thr151Ala	rs31537260
Slamf7	Met248Thr	rs31080132
	Gly253Arg	rs32013887
Cd48	Ile4Arg	rs31533394
	Asn90Asp	rs3718911
Cd84	Val27Met	rs31528577
Ncstn	Ser21Phe	rs31580400[b]
	Thr678Ile	ENSMUSSNP4494825
	Val680Ile	ENSMUSSNP2251306
Copa	Asn984Ser	ENSMUSSNP1061247[b]
Pex19	Pro55Ser	rs32297387

Table 4. High priority candidate genes for *Alcdp1/Alcw1* based on non-synonymous B6/D2 coding sequence polymorphism. Predicted amino acid differences due to coding B6/D2 SNPs obtained through public databases and by direct in-house sequencing. [a] Novel B6/D2 SNP identified by direct sequencing. Public identifier is pending assignment in dbSNP; [b] Novel SNP identified by direct sequencing. Identifier previously assigned for allelic difference between reference (B6) and strain(s) other than D2.

II.D. DISCUSSION

QTLs for ethanol physical dependence and associated withdrawal are detected on distal mouse chromosome 1 in several mapping populations derived from the B6 and D2 progenitor strains, and underlie ~25% of the genetic variability displayed in acute (*Alcw1*) and chronic (*Alcdp1*) withdrawal severity[34, 35]. In accompanying work[69], Kozell *et al*. mapped *Alcw1* and *Alcdp1* to the same 1.1 Mb minimal interval. Here, we report a detailed molecular analysis identifying 17 genes as promising candidates to underlie these QTLs' effects on alcohol withdrawal. Seven of these display non-synonymous B6/D2 coding sequence variation, three show confirmed genotype-dependent brain expression between congenic and background strains, and the remaining seven exhibit both features. These types of genetic variation account for the majority of established QTGs[38], indicating that their thorough assessment is a key component of candidate QTG prioritization.

This work represents a substantial advance toward identification of a QTG(s) involved in ethanol dependence/withdrawal. Although there is considerable evidence that vulnerability to withdrawal from a variety of sedative-hypnotics has some genetic factors in common, *Alcdp1/Alcw1* apparently does not influence barbiturate withdrawal[74]. This is the first evidence for an alcohol withdrawal QTL that does not generalize to barbiturates, and is a crucial clue as to the identity of the *Alcdp1/Alcw1* QTG(s). Interpretation of the present results and future tests of promising candidates for their influence on withdrawal will likely be informed by probing for effects specific to ethanol and/or not influenced by barbiturates.

Copa is a high-priority candidate based on genotype-dependent expression and amino acid sequence. It encodes the largest (alpha-COP) of the seven-subunit coatomer protein complex, COPI, that mediates the essential retrieval pathway in early vesicular transport (reviewed by[96]). Interaction of COPI with subunits of various multimeric transmembrane proteins involved in both inhibitory and excitatory neurotransmission[97-102] is proposed to be a key trafficking checkpoint ensuring that only properly oligomerized complexes proceed through the secretory pathway for

plasma membrane expression. Ethanol has direct effects on COP-mediated vesicular trafficking of sphingolipids[103], nascent glycoproteins and glycolipids[104], and decreases the expression of another coatomer protein, beta-COP[105]. Intriguingly, the first 25 amino acids of the mammalian *Copa* gene product are cleaved post-translationally to form xenin[106], a peptide that binds neurotensin receptors[107]. Xenin exhibits hypothalamic expression[108] and function consistent with neurotensin system activation[109], but little is known about its potential expression in other brain regions and broader neurobiological role. Because central neurotensinogenic function has been genetically and pharmacologically linked to hypnotic sensitivity to ethanol[110, 111], and specifically not to pentobarbital[112, 113], *Copa* is a particularly promising *Alcdp1/Alcw1* candidate. Interestingly, *Copa* mRNA expression (ABA; Table 1) is found in all major brain regions known to express neurotensin[114] and its' receptors[115, 116].

Our analyses also implicate oxidative stress and mitochondrial function as factors that potentially contribute to ethanol withdrawal. Ethanol exposure introduces intense oxidative stress *in vitro* and *in vivo* largely mediated by its effects on mitochondria[117, 118], and contrasts with evidence suggesting a neutral or anti-oxidative effect of pentobarbital exposure in brain[119-121]. While there has been little investigation, evidence from rat models suggests that ethanol withdrawal is accompanied by increases in reactive oxygen species that correlate with the severity of withdrawal behavior[122, 123]. Moreover, D2 mice maintain significantly higher brain levels of some oxidative stress markers than B6 mice[46], making this an attractive hypothesis for *Alcdp1/Alcw1* candidate analyses.

Three *Alcdp1/Alcw1* candidates (*Sdhc*, *Ndufs2, Ppox*) encode mitochondrial proteins involved in oxidative stress pathways. Two code for integral subunits of Complexes I (NDUFS2) and II (SDHC), the first enzymes of the mitochondrial respiratory chain (MRC). Proper and efficient MRC function is particularly critical to cells with high metabolic demand (e.g., CNS), since this activity generates the chemical gradient from which the majority of cellular energy is produced (Section IV.A.1). The third, protoporphyrin oxidase (PPOX), catalyzes the penultimate

step of heme biosynthesis, the prosthetic group required for the cytochrome function central to MRC activity and other cellular processes. NDUFS2 is crucial to the assembly and ubiquinone-reducing catalytic capacity of Complex I[124] and is highly conserved across prokaryotic and eukaryotic species. SDHC is the larger of two membrane-anchoring subunits and is required for proper functional assembly of Complex II[125], the point at which the Krebs Cycle and MRC converge to couple substrate metabolism to ATP-generating oxidative phosphorylation. Mutation in the *C. elegans Ndufs2* homolog (*gas-1*) creates hypersensitivity to ethanol and volatile anesthetics[126, 127] and increased oxidative stress[128, 129], while mutations in human *NDUFS2*[130] and *PPOX*[131] are causal for inherited diseases that include seizures as a prominent symptom. Lastly, expression changes for a number of oxidative stress and mitochondrial genes are hallmarks of the human alcoholic brain[132, 133].

Other candidates revealed by our analyses suggest both previously indicated and entirely novel aspects of neurobiology as potentially related to alcohol responses. *Adamts4* codes for aggrecanase-1, a glutamyl endopeptidase that functions largely within the extracellular matrix, is widely expressed in mammalian brain[134, 135], and plays an important role in regenerative neural plasticity through its actions on the synapse-stabilizing proteoglycan brevican[134, 136]. Interestingly, *Adamts4* null mutants display a strong neurological phenotype including increased sensitivity to pharmacologically-induced seizures (www.jaxmice.jax.org/strain). *Usp21* and *Ufc1* encode proteins involved in ubiquitin pathways, a complex protein degradation regulatory system implicated in alcoholism by human microarray studies[132, 133]. *Ncstn* codes for the largest subunit of gamma-secretase, an intracellular protease complex required for processing of several type I integral membrane brain proteins including amyloid precursor protein[137] and Notch[138]. The hundred-fold genotype-dependent difference in *Apoa2* expression is intriguing considering that even subtle gene expression changes in brain can be functionally important. While the *Apoa2* product, apolipoprotein A-II, is known almost entirely for its role in peripheral cholesterol metabolism and expression thought to be restricted to liver and intestine, protein

expression was recently detected in mouse[139] and human (B. Balgley 2007, www.humanproteinpedia.org) brain. Other apolipoproteins have primary roles in healthy and diseased brain states[140, 141], so *Apoa2* may have an as-yet unrecognized brain function that contributes to ethanol withdrawal. Lastly, several genes encoding proteins for immune function (*Fcgr3*, *CD48*, *CD84*, *Slamf7*), RNA-binding (*Refbp2*), and peroxisome genesis (*Pex19*), and one currently uncharacterized (*Klhdc9*), were identified as candidates that warrant further exploration.

These studies contribute significantly to progress in understanding the genetic determination of alcohol withdrawal and other behaviors, but there are some limitations. First, our genotype-dependent expression results are based on a survey of whole brain that, while an important first step, will need to be expanded in future studies assessing discrete brain regions and/or cell populations. New public resources containing genome-wide regional expression information (ABA and others), however, can potentially be useful in guiding these studies since the cellular resolution of *Alcdp1/Alcw1*-influenced withdrawal is currently unknown. Additionally, candidates were nominated based on comparisons of gene expression in naïve animals because several lines of evidence indicate that inherent genetic variation is primary to differential withdrawal vulnerability: many more genes are differentially expressed in naïve B6 and D2 animals than after acute ethanol exposure and most ethanol-induced differences are already present at baseline[50, 53] and lines selected to differ in chronic or acute withdrawal severity, but never exposed to alcohol, also identify QTLs in this region of Chr 1[34, 142]. No direct relationships have yet been established to delineate how acute ethanol-induced gene expression changes translate through protein levels to behavior. While such evidence might increase the value of potentially assessing gene expression during withdrawal in future studies, it is worth noting that no genes within *Alcdp1/Alcw1* have shown ethanol-induced B6/D2 differential expression[50, 53]. Finally, it is possible that the genetic factor(s) underlying *Alcdp1/Alcw1* is not a protein-coding gene. We identified three non-coding RNAs within the QTL interval; because reliable

quantitative techniques for their assessment are still evolving[143], these genes were not evaluated here. Although there is currently no evidence to suggest a role for non-coding RNAs in alcohol withdrawal, nor has any function been described for those mapped to *Alcdp1/Alcw1*, these entities remain of interest for future studies along with other genomic (non-protein-coding) elements to determine whether they play a role in withdrawal and/or other QTLs on distal Chr 1.

III. EVIDENCE FOR THE INFLUENCE OF *ALCDP1/ALCW1* ON GENE NETWORKS INVOLVED IN MITOCHONDRIAL FUNCTION AND RESPONSE TO CELLULAR STRESS

III.A. INTRODUCTION

Differences in mRNA expression are generated by the complex and dynamic interactions of several factors. A significant component is the result of heritable genetic variation, such that transcript expression qualifies as a quantitative trait (expression QTL, or eQTL) that can itself be subjected to genetic analysis. On a whole-genome scale, studies of this nature are termed genetical genomics and aim to understand how polymorphisms located both close to a gene (apparent *cis*-acting), as well as those distributed elsewhere throughout the genome (*trans*-acting), contribute and interact to direct overall levels of transcript expression. *Trans*-acting modulators of steady-state mRNA abundance include classical transcription factors, RNA helicases, ribozymes and other proteins involved in transcription, RNA processing and degradation, as well as many non-nuclear proteins that influence expression through extensive molecular cascades, feedback loops and large-scale networks[51].

Analyses of genome-wide expression differences for the presence of functionally related networks is a powerful method that can be used in a variety of applications to aid in characterizing the mechanism(s) by which a QTL exerts its influence. Applying these methods to gene expression data generated from congenic vs. background strain comparisons represents an especially promising opportunity to identify important *trans*-acting genetic modulators, particularly since quantitative traits, including eQTLs, are thought to be expressed predominantly through the collective influence of multiple small effects. Since the region of allelic variation in congenic strains is restricted to a defined chromosomal interval, and residual genomic “noise” effectively eliminated, all genotype-dependent expression differences for genes physically residing outside the interval can be fairly presumed the result of effectors acting *in trans*. While it is commonly accepted that the majority of these biologically relevant effectors may not actually be classical transcription factors[59], inherent variation in some genetic aspect at

this locus nonetheless drives the altered expression of distantly located genes and should thus be reasonably identifiable. Because individual *trans* effects are notoriously small, the general mechanism by which these effects act in aggregate may be more readily detectable, particularly with methods such as network analyses which incorporate established relationships and interactions on several biological levels into a systems-level view. Such methods may also illuminate entirely novel aspects of the mechanism, and specific associated genetic factors, that can then be probed directly for phenotypic involvement.

III.B. RESULTS AND INTERPRETATION

We originally performed microarray analysis on whole brain tissue from B6 background and Chr 1 congenic mice to assess large-scale pre-existing expression differences that may contribute to ethanol withdrawal susceptibility (Section II.C.2). These studies utilized the R4 congenic strain in which the introgressed region is a ~10 Mb interval of D2 origin that encompasses the entire R8 *Alcdp1/Alcw1* interval. Robust Multichip Analysis (RMA; www.bioconductor.org) was used in addition to PDNN (Section II.C.2) to efficiently analyze genome-wide genotype-dependent (R4 congenic *vs* B6 background strain) expression on the MOE430 2.0 array conditions that mask the influence of known SNPs between the B6 and D2 progenitor strains[92]. In addition to identifying promising candidates with genotype-dependent expression physically located within the QTL interval (apparent *cis*), these analyses revealed the presence of significant expression differences for an extensive set of genes residing outside the QTL (in *trans*), most often on other chromosomes. These results indicated that a considerable degree of widespread gene regulation is mediated through B6/D2 allelic variation within or very near the *Alcdp1/Alcw1* QTL interval.

As a first step in characterizing the mechanism(s) by which the Chr 1 QTL influences ethanol withdrawal and other phenotypes, preliminary analyses were performed to determine whether differences were related through a network of coordinated gene expression. Microarray results were overlaid with high confidence, curated protein-protein, protein-DNA, protein-RNA

and protein-compound interaction data to determine the underlying connectivity for network analysis. Initial results produced significant evidence for highly connected network structure, and functional enrichment for genes more broadly involved in mitochondrial function and cellular stress responses, specifically oxidative ($p=1.02x10^{-5}$). These results are especially intriguing considering that data variability within the sample set (N=6 arrays per strain, each representative of one individual) was sufficient to render only 60% power to detect differences smaller than 2-fold, and indicate that even modest increases in sample size will substantially enhance the informative value of network analyses in future microarray studies.

Development of the R8 congenic strain and demonstration of ethanol withdrawal QTL capture was completed subsequent to initiation of microarray analysis. This strain was used to more robustly confirm with qRT-PCR whether allelic variation specifically within the *Alcdp1/Alcw1* interval*,* affects gene expression *in trans* as suggested on microarray analyses (Walter, N.A.R., Denmark, D.L., in preparation). Conditions were identical to those described for *cis*-regulated genes (Section II.C.2). Notably, significantly higher expression was observed in whole brain from naïve R8 congenic *vs* B6 background strain mice (N=9 per strain) for several genes whose protein products are central to mitochondrial function and pathways activated under oxidative, ER, and nutrient/amino acid stress (Integrative Stress Response): eIF2α (*Eif2a* – eukaryotic translation initiation factor 2A) is phosphorylated in response to various cellular stressors thereby inhibiting general protein translation while simultaneously activating translation of specific mRNAs involved in protection, adaptation, and cell survival[144]; GRP78/BiP (*Hspa5* – glucose-regulated protein, 78kDa) is a Hsp70-type chaperone abundantly present in the ER lumen whose dissociation with transmembrane ER surface proteins, including the PKR-like ER kinase (PERK) that phosphorylates eIF2α, initiates downstream stress-coping intracellular signaling cascades[145]; ASNS (*Asns* – asparagine synthetase) catalyzes the glutamine- and ATP-dependent conversion of aspartic acid to asparagine, and its expression is highly regulated by amino acid or oxidative stress-induced eIF2α phosphorylation[146]; GCLC

(*Gclc* – γ-glutamate cysteine ligase catalytic subunit) comprises the first rate-limiting enzyme of glutathione synthesis, is induced transcriptionally by oxidative stressors including ethanol, and confers *in vivo* neuroprotection when upregulated under the stress of MRC inhibition[147]; and, mitochondrial Complex I subunits NDUFV1 (*Ndufv1*) and NDUFB6 (*Ndufb6*). Like *Ndufs2,* a promising *Alcdp1/Alcw1* QTG candidate identified by our molecular analyses (Section II), *Ndufv1* encodes an active site subunit of MRC Complex I that leads to severe neurological disorders when mutated in humans[148]. Also similar to *Ndufs2*, transgenic *C. elegans* strains expressing *Ndufv1* mutations demonstrate prototypical Complex I dysfunction, hypersensitivity to oxidative stress, and decreased cytochrome c oxidase (Complex IV) protein and activity[149], the latter highlighting an established interdependence of Complexes I and IV (Section IV.1).

These studies offer preliminary evidence that a potential network of stress-related genes distributed throughout the genome is affected by B6/D2 allelic variation, even when this variation is restricted to the *Alcdp1/Alcw1* interval. A central player in this network is activating transcription factor 4 (*Atf4*/ATF4), a member of the cAMP response element binding (CREB) protein family of basic-region leucine zipper (bZIP) transcription factors. Multiple pathways of intracellular stress (ER-related, amino acid deprivation, oxidant exposure) converge on eIF2α phosphorylation to preferentially upregulate translation of ATF4 mRNA while simultaneously inhibiting general protein synthesis, cell cycle progression, and transformation. Specific upregulation of ATF4 in turn activates an extensive gene regulatory program designed toward cellular adaptation in the face of nutrient, oxidative, metabolic or other challenges, including transcription of *Asns*[150]. While not surpassing the stringent significance thresholds established by multiple testing corrections ($p \leq 0.0014$), a trend toward higher levels of *Atf4* expression was detected in whole brain from R8 congenic *vs* B6 background strain mice ($p=0.0084$). Considering the distinct regional and temporal induction patterns observed in rodents for *Atf4,* as well as other ATF family members[151], this genotype-dependent expression may likely be more pronounced *in vivo* than is revealed in whole brain tissue preparations. Interestingly, under

in vitro conditions in both primary cerebellar cultures and SH-SY5Y neurolastoma cells, ethanol markedly potentiated the ATF4-mediated ER stress response induced by tunicamycin or thapsigargin through a mechanism appearing to involve oxidative stress[152].

An Integrated Stress Response gene network was also implicated in a recent study detecting reciprocal QTL for acute ethanol withdrawal and ethanol consumption in HS derived from four strains including B6 and D2[153]. In this report, selection for ethanol consumption produced lines with a negative relationship for acute withdrawal, as well as a significant association with distal Chr 1, as has been previously observed[32]. Most intriguingly, a reciprocal QTL detected on distal Chr 1 directly overlaps *Alcdp1/Alcw1.* Another ATF family member, ATF6α, was highlighted as a promising QTL candidate in this study due to appropriate haplotype structure and the presence of two non-synonymous SNPs, one of which occurs in a key functional domain. Two additional reciprocal QTLs out of the six others identified also contain genes central to ER stress-related networks. ATF6α appears to function as a transmembrane ER stress sensor upstream of eIF2α and in parallel to PERK, but also directly transcriptionally activates gene programs that can be either adaptive or apoptotic[154]. While *Atf6* lies just upstream of the minimal *Alcdp1/Alcw1* interval, it is localized within the proximal boundary region where allelic status in the R8 congenic is to date undetermined due to a dearth of B6/D2 SNPs in the immediate vicinity. qRT-PCR, however, detected a trend (p=0.007) for genotype-dependent expression *Atf6* in the same direction (R8 > B6) as the other stress network genes mentioned above (Walter, N.A.R., Denmark, D.L., in preparation).

Several recent studies support the involvement of the *Alcdp1/Alcw1* region of distal Chr 1 in influencing larger gene networks of gene expression[75, 155], one specifically involving the response to cellular stress.[156] This latter genome-wide study defined functional domains of physically associated genes on the basis of significant linkage disequilibrium (LD; combinations of co-inherited alleles occurring more often than expected by chance) among a set of 60 genetically diverse inbred strains including B6 and D2. A segment on distal Chr 1 (167-174 Mb)

was identified to contain separate examples of apparent gene duplications, tissue-specific coregulation of adjacent genes, and functional signaling between cell types, as well as the densest clustering of functionally related genes according to pathway analysis based on annotated physical, metabolic, and regulatory interactions. This domain was comprised of two subnetworks of 68 total genes, located both within the domain (in *cis*) and elsewhere (in *trans*), related through biological activity in immune, inflammatory, apoptotic, and cellular transformation pathways. Additionally, this domain showed highly significant LD with markers on separate chromosomes, particularly for a Chr 6 region containing several genes also known to be involved in the cell growth, cell cycle arrest, and apoptotic functions critical to orchestrating global responses to cellular stress. Genes controlling cell cycle and inflammatory signaling pathways have repeatedly shown strain-specific brain expression in previous microarray studies comparing B6 and D2 mice after either acute or chronic ethanol[50, 53, 157].

Collectively, these preliminary data combined with available literature evidence suggest a network of genes involved in the intracellular responses to a variety of stresses may be regulated *in trans* by allelic variation at *Alcdp1/Alcw1.* Considering the widespread cellular effects of ethanol exposure, and the well-known deleterious consequences on oxidative status and mitochondrial function, these mechanisms are a highly plausible source of genetic influence on the alcohol withdrawal phenotype.

IV. A POTENTIAL ROLE FOR THE MITOCHONDRIAL RESPIRATORY CHAIN IN GENETIC VULNERABILITY TO SEVERE ALCOHOL WITHDRAWAL

IV.A. INTRODUCTION

IV.A.1. Energy production by electron transport along the mitochondrial respiratory chain (MRC) and specific functions in the brain

The brain derives its energy almost exclusively from oxidative phosphorylation (OXPHOS) by the mitochondrial respiratory chain (MRC), which is organized as a branched chain of multi-protein complexes located in the inner mitochondrial membrane (IMM) that oxidizes reduced nicotinamide adenine dinucleotide (NADH) (complexes I, III, and IV) or reduced flavin adenine dinucleotide ($FADH_2$) (complex II). This oxidoreductase (redox) activity is coupled to the transfer of electrons, via the small carriers Ubiquinone (CoQ) and cytochrome c (*cyt c*), to oxygen and pumping of protons across the IMM, generating an electrochemical gradient that drives ATP synthesis by complex V. In addition to being the main energy source in most cell types, the OXPHOS system is central to the control of cellular redox homeostasis, as well as critical metabolic and signaling pathways ranging from the synthesis of pyrimidines to the regulation of apoptosis[158].

Each of the individual complexes is comprised of multiple protein subunits; mammalian complexes III (ubiquinol:cytochrome *c* oxidoreductase), IV (cytochrome *c* oxidase), and V (ATP synthase) include 10-20 different polypeptides each, while complex I (NADH:ubiquinone oxidoreductase) contains almost 50 (reviewed by[159]). These subunits are encoded by both nuclear and mitochondrial DNA, necessitating highly intricate and concerted transcription, translation, import, and assembly processes between both organelles that utilize a host of other cellular machinery and proteins still only beginning to be elucidated[160]. With just four subunits encoded entirely by nuclear DNA, Complex II (succinate-CoQ oxidoreductase) is the least structurally complicated portion of the MRC. The simplicity may end there, however, since two of these subunits have recently been implicated in functions other than respiration as part of a

multiprotein association conferring ATP-K^+ channel activity[161]. In addition to its role in the MRC, complex II contains the succinate dehydrogenase activity required by the tricarboxylic acid (TCA) cycle to convert succinate to fumarate, thus representing an important convergence point for amphibolic metabolism and OXPHOS.

This convergence point may be of particular importance in the brain, since TCA cycle activity plays a central role in the regulation of both glutamate and GABA levels. There is an especially tight coupling between activity, metabolism, and neurotransmitter expression in the CNS, and functional capacity of mitochondria to generate energy may differ by brain region and the state of activation at any given time[162]. Since GABAergic transmission is proportional to glutamatergic, and GABA synthesis uses 18% of neuronal TCA cycle flux, the energetic cost of tonic inhibition is becoming recognized as a significant contributor to regionally determined basal metabolic rates[163, 164]. Furthermore, metabolic compartmentalization of glutamate is regulated at the mitochondrial TCA and OXPHOS levels, and is channeled though different pathways (e.g., glycolysis or pyruvate carboxylase) in neurons and astrocytes[165].

In the brain, the MRC possesses a unique compensatory capacity to maintain sufficient energy production despite perturbation; cellular compromise does not result until activity inhibition surpasses a certain threshold of activity. Non-synaptic mitochondria have more excess capacity for inhibition (60-70% for CI, CIII, CIV)[166] than synaptic mitochondria, where 25% only inhibition of CI reduces ATP synthesis and oxygen consumption. This spare capacity is eliminated if mitochondrial glutathione is first depleted, attesting to the importance of antioxidant status in maintaining energy thresholds and the interplay between oxidative damage and energy production (reviewed by[167]).

IV.A.2. Ethanol induces significant effects on the MRC in the brain, including increased oxidative stress

The MRC is both a significant source and target of cellular oxidative stress, the disequilibrium created when reactive oxygen species (ROS) generated as by-products of normal and aberrant metabolic processes that utilize molecular oxygen cannot be balanced by antioxidant capacity. Damage to cells as a consequence of oxidative stress is a major pathological mechanism that contributes to a spectrum of diseases. The CNS is particularly vulnerable to imbalances in oxidative status due to its high oxygen metabolism, a relative underabundance of natural antioxidant defenses, and the high polyunsaturated fatty acid content of neural membranes that are a ready substrate for free radicals[118]. OXPHOS activity during even basal metabolism generates ROS, thought to derive primarily from electron leak at CI and CIII. Under normal conditions, this can be relatively balanced by natural antioxidant mechanisms, particularly via mitochondrial glutathione (GSH) and superoxide dismutase (MnSOD) activity. However, it is clear that environmental oxidative challenge or the accumulation of small oxidative damages pose a common and primary threat to healthy respiratory chain function that may initiate or perpetuate reaction cascades that amplify oxidative stress[168]. Furthermore, since mitochondria consume almost all O_2 available to the cells, they have been considered central O_2 sensors active along the entire spectrum of hypo/hyperoxic conditions[169]. Indeed, several neurodegenerative conditions associated with aging (Alzheimer's, Parkinson's, and Huntington's) share mitochondrial function and oxidative stress as common mechanisms of pathogenesis.

A surge in oxidative stress is a well-known effect of ethanol exposure on brain cells, although the exact mechanisms by which this occurs are still relatively unresolved, especially *in vivo*. Ethanol metabolism by brain mitochondrial-enriched CYP2E1 creates long-lived hydroxyethyl radicals that damage local molecules as well as diffuse away to critical target areas, induces acetaldehyde and ROS formation, and increases the $NADH/NAD^+$ ratio[170]

thereby driving respiration and further ROS generation. In the CNS, CYP2E1 can be induced by ethanol in a region and cell-specific pattern, thereby subjecting certain regions to a metabolic and oxidative surge[171]. Interestingly, the hippocampus and areas of the extended basal ganglia and are examples of such regions, and have also been demonstrated as central components of ethanol withdrawal brain circuitry[6, 7]. Ethanol metabolism increases ROS directly and indirectly in the immediate vicinity of lipid-rich mitochondrial membranes and proteins, including those of the MRC[170]. In chronically-exposed rats, notable formation of protein-acetaldehyde adducts were detected in brain, primarily in mitochondria of cortical and midbrain neurons, and granule cell layers of hippocampal dentate gyrus and cerebellum[172].

In liver, both nuclear and mitochondrial-encoded genes are affected by chronic alcohol consumption in rats, leading to a defect in the corresponding metabolic pathway expressed as decreases in CI and CIV levels and increases in mitochondrial stress-inducible chaperones[173]. Chronic alcohol consumption is responsible for hypoxia in some models[174], and subsequent increase in nitric oxide (NO) production that are responsible for mitochondrial damage caused by oxidative stress and decreased GSH levels[175]. Hypoxia can also down-regulate mitochondrial CI genes, implying that alcohol changes in oxygen tension could regulate mitochondrial DNA (mtDNA) gene expression[176]. A direct effect of ethanol on mtDNA has also been described in rat liver[177] and mouse brain[178]. In both cases, oxidative stress generated by the induction of CYP2E1 was postulated as the responsible factor for oxidative damage and then depletion of mtDNA. Ethanol exposure also directly impairs antioxidant defenses, including reduction of mitochondrial GSH levels[118].

In aggregate, these widespread effects produce significant oxidative stress thought to be a primary mechanism of cell death and tissue damage in both liver[179] and brain[180, 181] after chronic ethanol exposure. Also supporting this hypothesis are the repeatedly observed changes in lipids, proteins, and gene expression patterns as one of the outcomes most frequently

associated with alcohol administration in animal models (reviewed by[118]) and consumption in humans[132, 133].

IV.A.3. Is the MRC involved in ethanol withdrawal?

While the damaging effects of ethanol exposure and related oxidative stress on the MRC are well-established, there has been little investigation into whether these may play a role during ethanol withdrawal, perhaps due to an assumption that mitochondrial and oxidative balance is restored once the offending substance is removed. However, consequences of MRC stress and oxidative reactions often persist far longer than the initial exposure, frequently developing into self-perpetuating "vicious cycles" that result in continued and enhanced cell-wide stress oftentimes involving other organelles and membrane dynamics[118, 170].

Respiratory chain proteins may be particularly sensitive to oxidative stress, as emphasized by ethanol-induced lesions of CI and CIII that further enhance superoxide anion production[182], and decreases in CIV activity and mitochondrial membrane swelling during chronic withdrawal[183-186]. Additionally, significant regional brain lipid peroxidation has been observed during withdrawal[187]. The few studies focused on oxidative stress during the withdrawal period show increases in ROS in the brain several hours after acute and chronic ethanol exposure in rats[123], correlation of these levels to the degree of withdrawal seizures[188], and reduction of withdrawal severity and its associated brain protein oxidative modification after antioxidant administration[189]. Interestingly, intermittent hypoxia also demonstrated a protective preconditioning effect on ethanol withdrawal[185], perhaps occurring at least partially through the mtDNA regulatory interactions described above.

IV.A.4. MRC-related dysfunction and oxidative stress are associated with seizures

Neurological insults such as hypoxia, trauma, aging, and diseases such as stroke and Alzheimer's render the brain susceptible to seizures[190]. Each of these conditions have as common contributive factors mitochondrial dysfunction and increased oxidative stress,

supporting the idea that damage initiated by ROS can be both a cause and consequence of convulsive activity[190]. Even partial inhibition of one or more respiratory chain complexes by both exogenous (e.g., MPP^+ at CI) and endogenous (e.g., malonate at CII) substances can evoke seizures[191]. These are thought to be mediated via inhibitor-produced deficiencies in oxidative phosphorylation and ATP synthesis that result in the disruption of neuronal plasma membrane potential causing hyperexcitability[192]. Impaired energy metabolism at any level may generally enhance neuronal vulnerability to excitotoxic influence by deteriorating the mitochondrial membrane potential and decreasing capacity to buffer intracellular Ca2+[191]. Oxidative stress is known to directly raise plasma membrane excitability through damage to sensitive protein targets (e.g., astroglial and neuronal glutamate transporters) sufficient to increase seizure susceptibility[190]. Finally, seizures are one of the hallmarks of inherited mitochondrial diseases, many of which result from mutations in genes coding for a single respiratory complex subunit[130]. Mutations in other nuclear genes encoding MRC assembly factors, as well as mitochondrial-encoded genes and tRNAs, also cause a variety of hereditary encephalopathic conditions presenting with epilepsy[191].

IV.A.5. The importance of MRC organization

Two different models have been proposed to describe MRC organization *in vivo*. In the Random Diffusion or Fluid Model, individual complexes move randomly within the inner mitochondrial membrane with electron flow between them afforded by the mobile carriers ubiquinone (CoQ) and cytochrome *c* (Figure 4). Alternatively, the Solid Model proposes that individual complexes are assembled into larger structures within the inner mitochondrial membrane to enable rapid and efficient transport of electrons (reviewed by[193]). Based largely on kinetic studies, and the demonstration that the MRC complexes can be individually purified while retaining enzymatic activity, the fluid model gained general acceptance in the mid-80s[158]. However, several recent lines of evidence strongly support the view that MRC complexes preferentially and stably associate into supramolecular structures (supercomplexes; SCs) to

perform their functional role ("respirasomes") (Figure 4) and afford structural stabilization: a) a mild purification and separation protocol (Blue Native-PAGE; Section III.A.6) has produced consistent observations that different complexes co-migrate under native electrophoresis, and can be co-purified under immunoprecipitation conditions; b) flux control experiments favor SC organization over their individual occurrence; c) arrangement into SCs leads to improved stabilization of individual complexes; d) mutations leading to a loss of single subunits in one complex (e.g., CIII or CIV), or cytochrome *c,* can prevent SC formation and/or lead to secondary losses in other complexes (e.g., CI); e) SCs are present at defined stoichiometries *in vivo*; f) three-dimensional SC maps have been elucidated by single particle electron microscopy (reviewed by[194, 195]).

In addition to the importance of individual proteins and their interactions, several other determinants and consequences of intermolecular assembly influence MRC integrity and function. Mitochondrial membrane lipids are one such factor and may significantly modulate both the quantity and composition of inter-complex associations (reviewed by[196]). For example, a mitochondrial-specific phospholipid, cardiolipin (CL), has a unique headgroup that can act as a proton trap in OXPHOS and co-isolates with each of the MRC complexes. CL requirements for specific association between complexes[197] is exemplified by the human X-linked recessive disease Barth Syndrome whereby mutations in a CL synthesis gene, tafazzin, cause mitochondrial morphological abnormalities and respiratory dysfunction at CIII and CIV presenting in early childhood with usually fatal cardioskeletal myopathy, neutropenia, and aciduria[198]. While not absolutely required for OXPHOS *in vivo*, CL increases the dynamic range of conditions in which it can occur and significantly enhances the efficiency of energy production even under optimal conditions[199]. CL is also vulnerable to peroxidation by mitochondrial ROS following decreased electron transfer at CI and CIII, and may thereby deeply affect inter-complex assembly[200]. Additionally, the mobilization of *cyt c* out of mitochondria, a key apoptotic event, is tightly regulated by the oxidative state of CL[200]. Overall mitochondrial membrane

fluidity also certainly contributes to MRC association dynamics[196], and is highly influenced by peroxidation of lipids in addition to CL, as well as cholesterol content.

IV.A.6. Advantages of blue native polyacrylamide gel electrophoresis (BN-PAGE) to assess MRC organization and activity

Current knowledge of respiratory complexes is based on many decades of biochemical, enzymatic, genetic, and crystallographic studies. This knowledge has been greatly enhanced in the fifteen years by the development[201] and optimization[202] of blue native-PAGE (BN-PAGE), which has since become a standard procedure for the isolation and analysis of the multi-subunit MRC complexes. Extraction of the respiratory complexes requires disorganization of the inner mitochondrial membrane (IMM), in which they are integrally situated. BN-PAGE utilizes mild, non-ionic detergents to accomplish this, while still retaining inter- and intra-complex associations, and can thus resolve large (10 to >1000 kDa) complex associations. Furthermore, quasi-native solubilization and electrophoretic conditions preserve enzymatic capacity so that complex activity can be directly evaluated with addition of specific substrates. Use of the particularly mild detergent digitonin facilitates the detailed examination of higher order MRC organization; it interferes solely with IMM cholesterol moieties, thereby allowing retention of delicate inter-complex interactions that may be of utmost relevance *in vivo*. In combination, these techniques allow structural information on complex amount and assembly to be obtained simultaneously with isolated measurements of specific respiratory activity, a substantial advantage over traditional methods that typically assess respiratory function spectrophometrically within a mixed mitochondrial environment. Additionally, a host of downstream applications is readily available with which to evaluate specific subunits, post-translational and oxidative modifications, and involvement of auxillary non-OXPHOS proteins that are all highly influential on various aspects of MRC structure and function *in vivo*.

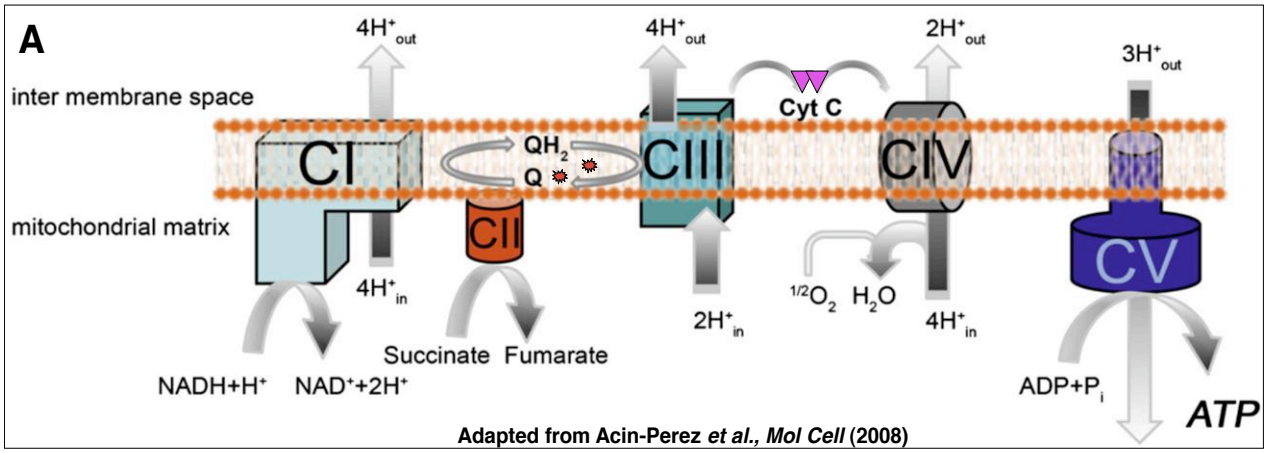

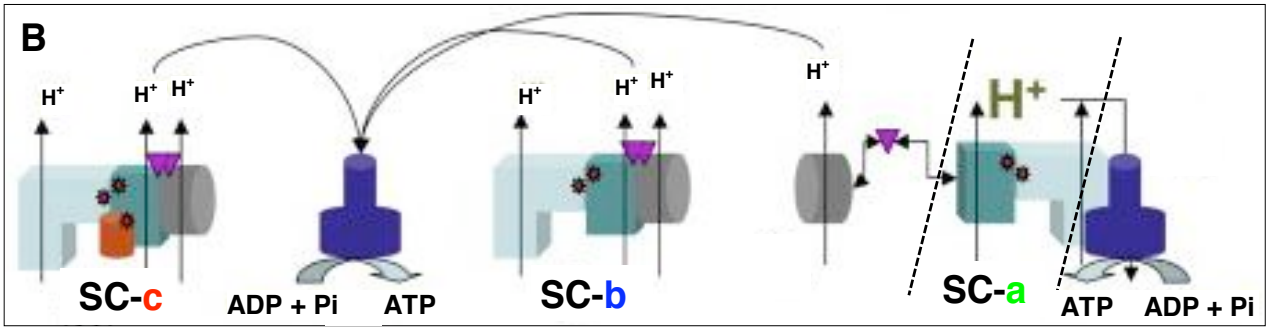

Figure 4. **Schematic representations of MRC organization and function.** The "classical" fluid model (A) of higher order MRC structure, and a recently developed "plasticity" model (B) merging the traditional solid-state and fluid models, whereby association into supercomplexes (SCs) can facilitate MRC efficiency. Only one complex unit of each type is represented in the different supercomplex (SC) assemblies, although the actual stoichiometry may vary, as has been previously reported (Schagger *et al.* 2001). SC-c and SC-b can be considered true respirasomes since they can transfer directly electrons from NADH to oxygen and contain mobile electron carriers. SC-a (indicated by dashed lines) may serve a strictly structural role, and can also form additional associations with ATPase/CV. (ubiquinone – red stars; cytochrome *c* – purple triangles). Adapted from Acin-Perez *et al.* (2008).

IV.A.7. Experimental Overview

The following work was undertaken as a mechanistic follow-up to our molecular analyses which systematically identified promising candidate genes potentially underlying the fine-mapped Chr 1 QTL with large effects on predisposition to both chronic (*Alcdp1*) and acute (*Alcw1*) ethanol withdrawal. Several mitochondrial genes are located within this QTL (Section II.C.1), three of which code for MRC-related proteins and show non-synonymous coding sequence variation between B6 and D2 progenitor strains and/or validated genotype-dependent expression differences in Chr 1 B6.D2 congenic vs. background strain mice. Damaging effects on mitochondrial bioenergetics, including MRC activity, and oxidative stress are some of the most well-known consequences of ethanol exposure, and may potentially contribute to genetically determined differences in risk for ethanol physiological dependence and associated withdrawal. Here we used BN-PAGE to evaluate whether inherent strain differences exist in brain MRC components and/or are apparent in ethanol-exposed mice. Due to their highly divergent ethanol withdrawal phenotypes, as well as available evidence regarding mitochondrial- and oxidative stress-related differences in gene expression and non-alcohol phenotypes, some of which have QTL localized to the general region of *Alcdp1/Alcw1*[75] (Gene Network, www.genenetwork.org), we focused initially on comparisons between naïve B6 and D2 strains, and the effects of chronic and acute ethanol on each. Furthermore, since the Chr 1 B6.D2 congenic (R8) defines the critical withdrawal QTL interval, we included naïve and chronically-exposed mice of this strain in comparisons to B6 to explore whether this chromosomal region in particular may have an observable effect on inherent or potential ethanol-related changes in MRC characteristics.

IV.B. METHODS

IV.B.1. Animals

All animals used were bred in our colony at the Portland VA Medical Center and all procedures approved by the Oregon Health & Science University and VA Medical Center Care and Use Committees in accordance with USDA and USPHS guidelines. C57BL/6J (B6) and DBA/2J (D2) inbred strain breeders were purchased from the Jackson Laboratory (Bar Harbor, ME). Breeder stocks for the R8 congenic strain were provided by Drs. John Hofstetter and Aimee Mayeda at the Indianapolis VA Medical Center. Mice were group-housed 2-5 per cage by strain and sex. Mouse chow (Purina #5001) and water were available *ad libitum*, and lights were on from 6:00 AM to 6:00 PM in a colony room maintained at 22.0 ± 1.0°C.

Ethanol withdrawal intensity has been previously measured in the B6, D2, and R8 congenic mouse strains used for the these studies, and was thus not measured here in order to avoid potentially confounding effects of seizure activity on the MRC variables of interest. Withdrawal convulsivity peaks approximately 7 hr post-ethanol injection[25] or removal from vapor chambers[35].

IV.B.2. Alcohol exposure/withdrawal paradigms

Chronic: Male mice (n=4-5 per strain, per treatment) were injected with a priming dose of ethanol (1.5 g/kg, i.p., 20% v/v in saline) or saline (control). Groups were placed in identical inhalation chambers and exposed to air (controls) or ethanol vapor (4.5-7.5 mg ethanol/l of air) adjusted to achieve equal blood ethanol concentrations (BECs) across strains, as measured daily in sentinel mice in each chamber using a gas chromatographic assay[22]. Physical dependence was induced by 72 hr of continuous exposure by ethanol vapor inhalation. Pyrazole HCl (68 mg/kg), an alcohol dehydrogenase inhibitor used to maintain BEC levels, is included in all initial injections and administered to all animals at 24 and 48 hr. At the end of the 72 hr ethanol exposure, a 20-µl blood sample was drawn from the tails of all ethanol exposed mice to determine individual BECs. Tails of all control (AP) mice were nicked, but blood samples not

collected. Half of each group was sacrificed by cervical dislocation upon immediate removal from the chambers for whole brain samples of ethanol-dependent and air/pyrazole control animals (E0; AP0). Since chronic withdrawal intensity peaks approximately 7 hr post-ethanol[35], the other half were returned to home cages and sacrificed 7 hr after removal from the chambers for whole brain samples of ethanol-withdrawn (E7) and control (AP7) animals. Only tissue from those mice with BECs between 1.0-2.0 mg ethanol/ml blood, within the range utilized in the *Alcdp1/Alcw1* mapping studies (~1.3-1.6 mg ethanol/ml blood)[23, 24], were used for protein biochemical assays.

Acute: Male mice (n=3-4 per strain, per treatment) were injected with ethanol (4 g/kg in 20% saline, ip) or vehicle (saline, 10 ml/kg), and returned to home cages. Since acute withdrawal intensity peaks approximately 7 hr post-ethanol injection[25], all groups were sacrificed by cervical dislocation 7 hours later for protein biochemical assessment of brain tissue.

IV.B.3. Mitochondria-enriched brain homogenates

To collect a mitochondrial-enriched fraction, pseudorandomly chosen half-brains were homogenized in ice-cold sucrose buffer (15 µl/mg tissue, 250 mM sucrose, 20 mM imidazole/HCl, pH 7.0). Each major experimental paradigm (naïve; acute and chronic models) was performed independently over the course of six months, and all strain and treatment groups within a paradigm prepared simultaneously to avoid variation potentially introduced by the purification procedure. Aliquots corresponding to 15 mg wet weight tissue were centrifuged at 20,000 x *g* for 10 min at 4°C, supernatants discarded, and the pellets frozen at -80°C. When ready for use, pellets were dissolved by swirling in 140 µl of solubilization buffer (50 mM NaCl, 50 mM imidazole/HCl, 2 mM 6-aminohexanoic acid, 1 mM EDTA, pH 7.0 at 4°C). Digitonin (20% in de-ionized water) was added in ratios (> 8 g detergent/ g protein) established in the literature (Schagger & Pfeiffer 2001) to obtain quantitative isolation of supercomplexes, and allowed to solubilize for 10 min. Samples were centrifuged at 100,000 x *g* for 15 min, and supernatants retained. Glycerol (85% in de-ionized water) and Coomassie blue G-250 (5% in 6-

aminohexanoic acid) were added to give a final concentration of 10% and 0.2%, respectively. Protein concentrations were determined by BCA quantitation (Pierce Protein Research Products, IL) either just prior to digitonin solubilization or addition of loading dye. Based on a standard curve determination of the linear range of integrated optical density (IOD) readings for the following staining and imaging conditions, 15-25 ug total crude mitochondrial protein (10-15 µl sample) was loaded in each well.

IV.B.4. BN-PAGE

The NativePAGE Novex system with 4-16% precast gels (Invitrogen, CA) was used to optimize resolution and visualization of 100-1500 kDa complexes, the established size range of MRC constituents. Electrophoresis was carried out (140 V, 4-4.5 hr, 4-7°C) in cathode buffer (50 mM Tricine, 7.5 mM imidazole, 0.02% Coomassie blue, pH 7.0), which was removed after 15 min and replaced by B/10 buffer (same as cathode buffer, except containing 0.002% Coomassie) to improve visualization of faint protein bands and native blotting. Immediately after electrophoresis, gels were soaked in de-ionized water for 5-10 min and stained to measure individual complex amount or activity.

IV.B.5. Coomassie blue & in-gel activity (IGA) staining

All statistical comparisons were made between samples run on the same gel. Samples from a single preparation were repeated on multiple gels, each treated with one of the following stains. For Coomassie Blue (COOM) assessment of band amount, gels were fixed and stained with Colloidal Blue Staining (Invitrogen, CA) for 10-12 hr, then destained in de-ionized water for 24 hr before imaging. Other gels were used to determine in-gel enzymatic activity (IGA) by the following histochemical reactions: (CI) 0.1M Tris-HCl, 0.14 mM NADH, 1.0 mg/ml nitro blue tetrazolium (NBT), pH 7.4; (CII) 50 mM phosphate buffer, 84 mM succinic acid, 0.2 mM phenazine methosulfate, 2.0 mg/ml NBT, 4.5 mM EDTA, 10 mM KCN, pH 7.4; (CIV) 50 mM phosphate buffer (pH 7.4), 0.5 mg/ml DAB (3,3'-diamonbenzidine), 24 units/ml catalase,

1 mg/ml cytochrome c, and 75 mg/ml sucrose. Enzymatic reactions were carried out at room temperature and stopped with fixation in 45% methanol/10% acetic acid for 15 min, then transferred to deionized water until imaging within 24 hr. ImageQuant software was used to obtain integrated optical density (IOD) readings under optimal visualization conditions that were maintained identically across all gels to minimize variation. Molecular weights of respiratory complexes have been repeatedly published[160, 203, 204], and are unique among each other, allowing identification in initial experiments using commercially available markers (NativeMark Unstained Protein Standard, Invitrogen, CA).

Reaction times for CI were determined in pilot studies to identify the linear range (20-40 min) based on loading amounts (20 µg protein) we empirically determined as linearly related to IOD readings. Staining for CII and CIV activity was much less sensitive; comparable IOD readings, particularly for CIV-containing SCs, could only be obtained after staining for 12-16 hr. CIV monomer (CIV-m) signal appeared maximal or near-maximal at this timepoint, however, precluding accurate comparisons of monomeric activity within the linear range but allowing valid, semi-quantitative utilization of this signal to normalize CIV IGA in super- and subcomplexes.

IV.B.6. Western blotting

Unfixed BN-PAGE gels were transferred with a semi-dry apparatus (Bio-Rad) immediately after separation to polyvinylidene Fluoride (PVDF) membranes (Millipore). After transfer, blots were washed briefly in methanol to remove residual Coomassie blue, and probed with mouse monoclonal antibodies for a subunit of CIII (UQCRC1; ubiquinol-cytochrome c reductase complex core 1 protein; 1:500) or CII (SDHB; succinate dehydrogenase iron-sulfur protein subunit, 30 kDa; 1:500) (Santa Cruz Biotechnology, CA).

IV.B.7. Statistical analysis

All gels were analyzed for strain- (B6 *vs*. D2 or R8 congenic strains, respectively) or treatment- (E *vs*. AP, or S) dependent differences using a two-tailed (Student's) *t*-test implemented by Prism (GraphPad v4, 2005). In the cases of normalized CIV activity in R8 congenic ethanol-dependent *vs* controls, and ethanol-withdrawn B6 *vs* R8, a one-tailed test was used for semi-quantitation based on the results obtained with D2/B6 comparisons indicating significant lower amounts (COOM), and CI and CIV activities, in ethanol-treated D2 mice. Due to a small, but significant, degree of technical variation between gels, only samples run on the same gel could be directly and statistically compared. Inter-gel qualitative comparisons, however, were deemed valid based on the consistency of band patterns observed over all experimental groups and mitochondrial protein preparations.

IV.C. RESULTS

IV.C.1. BN-PAGE reveals genotype-dependent higher order MRC organization in ethanol-naïve mice

B6 vs. D2 progenitor strains.

The B6 and D2 inbred strains are the most widely studied genetic models of alcoholism due to drastically different phenotypes in a variety of alcohol-related behaviors, including withdrawal severity. Buck and colleagues identified and fine-mapped a Chr 1 QTL (*Alcw1/Alcdp1*) estimated to direct 25-26% of the genetic variance in withdrawal severity between populations derived from these progenitor strains[34, 35]. This gene-dense QTL contains an overrepresentation of genes related to brain mitochondrial function and oxidative homeostasis, several of which were identified as promising QTG candidates (Section II). Furthermore, stress-response mechanisms related to mitochondrial or oxidative pathways are a common theme among the array of diverse behavioral and physiological traits that differ between these strains (Section I.E), and abundance of traits are influenced by a gene(s) within or near *Alcdp1/Alcw1*. Because B6 and D2 mice differ so drastically in withdrawal severity after acute as well as chronic ethanol, we hypothesized that they may exhibit observable baseline differences in MRC structure or function that could potentially be associated with increased withdrawal vulnerability.

Digitonin solubilization of naïve B6 whole brain mitochondria (n=5 per strain, samples representing one individual) and BN-PAGE with Coomassie staining (Figure 5, left lanes) yielded a band pattern reminiscent of that previously reported in mitochondria from various rat tissues including brain[160], and bovine heart[203, 205]. According to standard molecular weight markers for native proteins, (Section III.B.5), and previously published sizes of individual MRC complexes, bands corresponding to monomeric CII, CIV, CV, and CI could be clearly visualized. Additionally, two prominent high molecular weight bands (SC-a, SC-b) were observed that appear consistent with MRC supercomplexes (SCs) previously reported for mitochondria from bovine heart[203], various rat tissues[160], and mouse brain[204]. Supportive of this

is the very faint staining of the band corresponding to CI monomer, indicating that the majority of CI is present in some other configuration. Interestingly, when naïve D2 whole brain mitochondria were identically prepared, a different SC pattern was observed in that two additional high molecular weight bands (SC-c, SC-d) above those seen in B6 were present, suggesting that these two strains have inherently different higher order MRC organization.

The same samples (n=5 per strain) were prepared and stained for CI-specific NADH-oxidoreductase in-gel activity (IGA) (Figure 5, middle lanes), which confirmed the presence of CI in SC-a and SC-b, as well as the very small proportion of CI isolated as a monomer (CI-m). In D2, the two additional SC bands (SC-c, SC-d) also showed significant CI activity. A further high molecular weight band (SC-e), approximately 1200 kDa, was also detected to have CI activity in both strains. Upon close examination, several additional bands just slightly larger than SC-b were also observed in B6 after CI IGA staining, indicating the presence of multiple, slightly different CI-containing SC species. Only one of these was present in D2, slightly smaller than SC-c. Two of these additional B6 bands appear to be consistent with D2 SC-c and SC-d, but run at a slightly higher molecular weight, and have clearly reduced CI signal relative to SC-b, SC-a, D2 SC-c or D2 SC-d. These observations indicate that while Coomassie alone was not sensitive enough to detect these configurations in B6, a small amount is present and contains CI, but may also contain additional components or protein modifications (e.g., phosphorylation, glycosylation) which distinguish them from their D2 counterparts.

Specific IGA staining verifies the presence of CI in mitochondrial SCs in both strains, and is highly suggestive that SC-a is consistent with the SC repeatedly isolated with digitonin from several species and tissues ranging from Arabidopsis[206] and fungus[207], to bovine heart[203, 208], rat (brain, kidney, liver, heart, and muscle)[160], mouse (brain, spinal cord, and liver)[158, 204], and human cells[205], and verified to consist of a single CI and dimeric CIII (I_1III_2). Similarly, SC-b corresponds to the previously reported higher molecular weight SC containing dimeric CIII associated with one CI and CIV ($I_1III_2IV_1$), while the additional D2 bands are almost certainly

this same basic configuration with one (SC-c; $I_1III_2IV_2$) or two (SC-d; $I_1III_2IV_3$) supplemental copies of CIV[159, 194, 195].

Enzymatic staining for CIV activity (Figure 5, right lanes) further elucidates and verifies SC identities, since strong staining is clearly present in SC-b, SC-c, and SC-d, but not SC-a, and also confirms that the majority of CIV exists in monomeric form, as has previously been reported[204]. This enzymatic staining also revealed that several CIV-containing subcomplexes (*1, *2) of higher molecular weight than monomeric CIV, but smaller than SCs, are stable MRC configurations. These CIV-containing subcomplexes are consistent in size and relation to other complexes with those previously reported to contain $CIII_2$ associated with various copies of CIV[205].

Signal for CII was weak after Coomassie staining, as has been previously reported for mouse brain[204]. However, CII-specific IGA confirms the identity of this band and demonstrates its presence and activity in both strains at the predicted molecular weight (approximately 130 kDa).

Detailed investigation of the MRC in a variety of organisms, experimental conditions, and even human or animal model disease states, has been greatly enhanced by the development and more recent refinement[202] of the BN-PAGE technique. Even early on, a quantitative relationship between Coomassie or complex-specific IGA staining and IOD was established for MRC bands obtained after detergent solubilization and BN-PAGE separation[204, 209], facilitating measured comparisons of the amounts and activities of particular complexes of interest. We sought to take advantage of this method to quantitatively characterize genotype-dependent differences in MRC organization, and detect potential effects dependent on ethanol exposure and/or withdrawal.

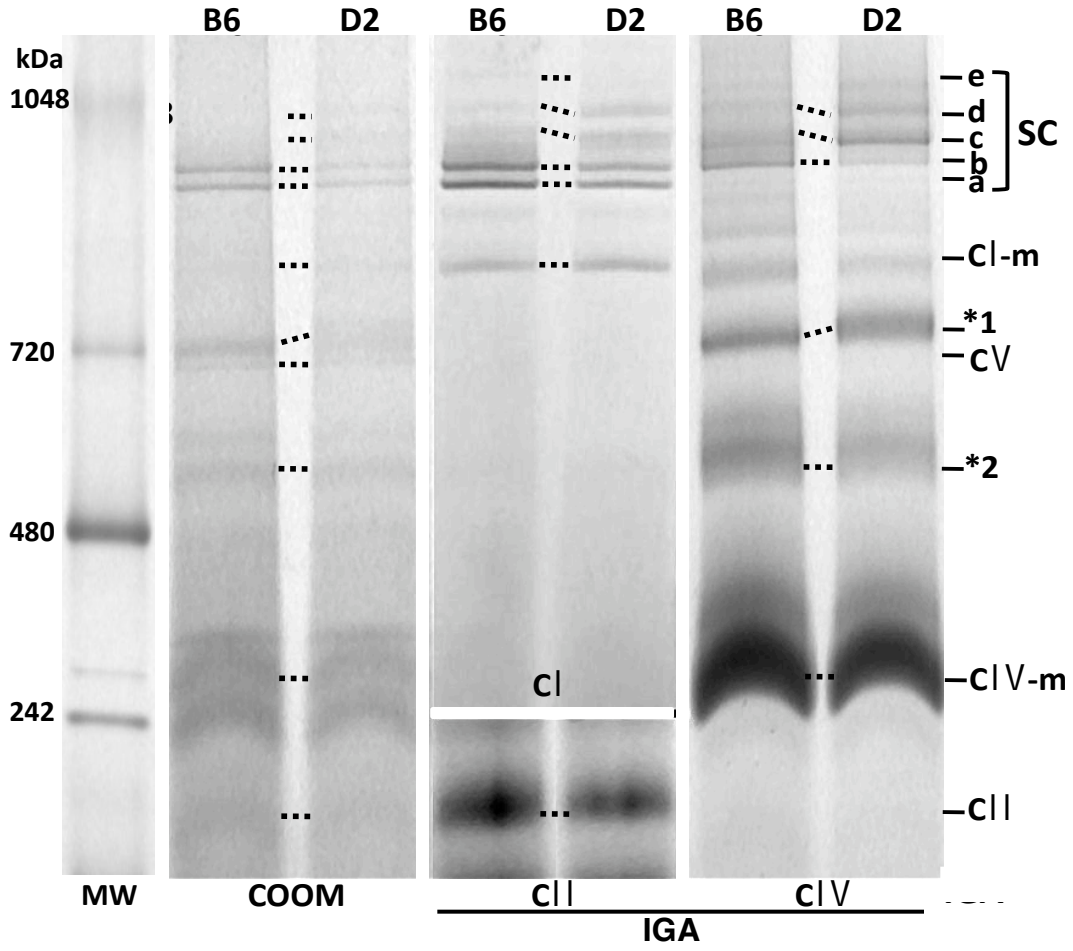

Figure 5. **BN-PAGE reveals distinct MRC organization in naïve B6 and D2 mice.** Solubilization of brain mitochondria from ethanol-naive mice with the mild detergent digitonin, separation by BN-PAGE, and Coomassie staining (COOM) yields prominent bands corresponding to the established sizes for monomeric MRC and other proteins, as described in text. Additionally, differences in higher molecular weight (MW) bands consistent with supercomplex (SC) identity are apparent between the B6 and D2 strains. In-gel enzymatic activity (IGA) staining on the same samples verifies the presence of CI, CII, and CIV in monomeric (CI;CIV;CII), subcomplex (*1, *2) and SC (a-e) bands, and further highlights the genetic variation in higher order MRC. Representative samples are shown from gels stained independently for COOM, CI/CII, and CIV.

Due to our initial findings, we chose to focus these studies primarily on higher order (super- and sub-complex) structure. The lack of a favorable internal protein standard, however, complicated quantitative analysis of both SC amount and activity by traditional methods. While others attempting to use BN-PAGE quantitatively have relied on Coomassie-stained CV or CIII signals for normalization[206, 209], similar use here was precluded by current evidence demonstrating the interdependence of individual complex assembly and stability, as well as SC formation (Section III.A.5). Furthermore, all major MRC constituents appear to be affected at the protein level, either directly or indirectly, by alcohol exposure (Section III.A.2). In some studies[209, 210], the need for rigorous quantitation was transcended by a qualitatively obvious magnitude of effect. In these cases, the authors indicated that direct comparisons of raw IODs could be made due to equal protein loading between lanes. While all efforts to equalize protein-loading were made in our preparations, small inequities between lanes were still visible that precluded such assumptions; biochemical effects of strain or treatment are potentially subtle considering the phenotypic effect size of withdrawal, particularly between congenic and background strains (Section I.C). For these reasons, more precise quantitation requires the establishment of genotype- and treatment-independence for any potential normalization candidate, ideally using an identified non-MRC component present in crude mitochondrial preparations. Such procedures were beyond the scope of these studies intended as a survey possible MRC involvement in strain-specific predisposition or expression of vulnerability to ethanol withdrawal.

To this end, we first performed a semi-quantitative assessment by calculating the proportion of each dominant SC configuration (SC-c, SC-b, SC-a) within a single sample (lane) based on the ratios of raw IODs from Coomassie, CI-, and CIV-stained gels (Figure 6, A-C). Since SC-b is consistent with the predominant SC species reported in bovine heart ($I_1III_2IV_1$) and shown to possess superior stability and respiratory efficiency compared to SC-a[203], we chose to focus on potential strain or treatment effects in other SC amounts and activity relative to this band, i.e.,

b:c and b:a ratios. Additionally, the requirement for maximum development time to obtain comparable signals of CIV activity in SCs (Section III.B.5) resulted in an intense CIV-m signal that was more representative of protein amount rather than activity, *per se*. Since CIV-m abundance between strains in all treatments appeared qualitatively equivalent, we used this signal as a reasonable semi-quantitative standard for relative differences in higher order CIV-containing bands.

In a recent landmark report[158], supercomplex bands consistent with SC-b and SC-c were isolated with digitonin from mouse liver mitochondria and demonstrated true "respirasome" activity, i.e., they could transfer electrons from NADH to O_2 as detected by respirometry. Thus, we were most interested to further characterize SC-b and SC-c semi-quantitatively for inherent strain-dependent differences that may have considerable functional implications for respiratory activity. Relative quantitation of bands SC-b:c (Figure 6A) confirms qualitative observations that SC-b is the predominant configuration in B6 (Figure 5). As mentioned above, while Coomassie staining could not detect enough SC-c to obtain an IOD reading in this strain, SC-b was strongly visualized. In contrast, SC-c was clearly present in D2 with Coomassie (Figure 5), but at somewhat lower intensity than SC-b (mean b:c ratio=1.5). This was also the case for CI activity in D2 (mean b:c ratio=1.9). In B6, however, enzymatic staining revealed a considerable predominance of CI activity in SC-b (mean b:c ratio=7.8), almost four times the ratio in D2 ($p<0.0001$). Similarly, while SC-b still clearly predominates CIV activity in B6 (mean b:c ratio=1.3), SC-c possesses the majority of CIV activity in D2 (mean b:c ratio=0.3, $p<0.0001$).

Comparisons of CIV IGA confirmed the genotype-dependence and direction of b:c predominance in CIV activity (Figure 6C; mean B6 b=0.03, mean D2 b=0.02, $p<0.005$; mean B6 c=0.03, mean D2 c=0.05, $p<0.017$). Interestingly, two additional bands demonstrated strong CIV activity. The first (*1) co-migrates with the presumed CV band, and is consistent with a subcomplex previously reported to contain $CIII_2$ associated with CIV_2[205], while the second (*2) is smaller and likely represents the $CIII_2/CIV_1$ species. Relative quantitation of CIV IGA in *2 was

significantly greater in B6 than D2 (mean B6=0.13, mean D2=0.09, $p<0.02$), while the opposite was true for *1 (mean B6=0.09, mean D2=0.12, $p<0.001$).

Strain and/or treatment differences in the proportion of SC-b to SC-a may be functionally informative, since previous studies indicate limited or nonexistent true respiratory capacity of this band and suggest it may represent a “holding” configuration for immature respirasomes, or structurally or functionally impaired supercomplexes[158, 208]. We observed no significant strain differences in b:a ratios after staining for amount (COOM) or CI activity in naïve animals (Figure 6B), but a trend toward a greater predominance of SC-b in B6 may be present (COOM: mean B6=1.6, mean D2=1.1, $p<0.25$; CI: mean B6=1.4, mean D2=1.0, $p<0.25$).

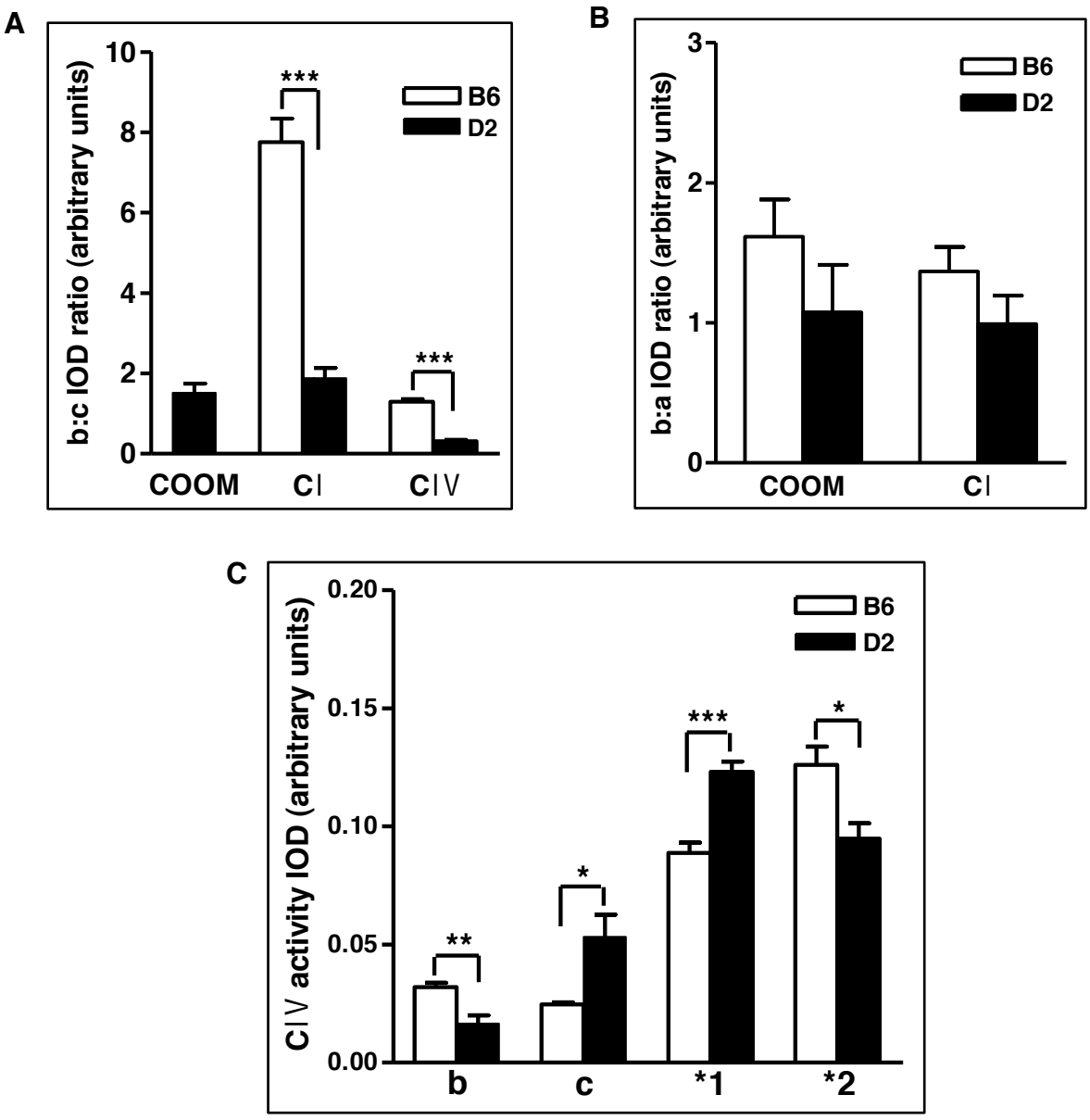

Figure 6. **Semi-quantitative assessment of MRC configurations in ethanol-naïve B6 and D2 mice.** Whole brain mitochondria were visualized after BN-PAGE and staining for amount (COOM) and activities of CI and CIV. Band integrated optical density (IOD) readings were obtained from digital images and compared as ratios of SC-b to SC-c (A), SC-b to SC-a (B), or normalized to monomeric CIV signal (C). All statistical comparisons were made within-gels. The same samples (n=5 per strain) were repeated on independent gels for each activity stain. *$p < 0.02$; **$p < 0.005$; ***$p < 0.0005$.

Taken together, these results suggest that higher order MRC organization in the CNS is genetically influenced and distinctly different at baseline between the B6 and D2 strains that vary greatly in a variety of behaviors, including ethanol withdrawal liability and other alcohol-related traits (Section I.E). These findings may have significant implications on the overall respiratory function inherent to these strains, as well as populations derived from them, and their levels of (or requirements for) oxidative homeostasis, metabolic energy production capacity, and innate ability to cope effectively with mitochondrial stressors such as alcohol.

R8 congenic vs. background B6 strain animals.

The R8 congenic demonstrates significantly greater withdrawal severity after both acute and chronic ethanol administration than background (B6) mice. This strain harbors the D2 allele for a Chr 1 interval limited to the *Alcw1/Alcdp1* QTL region on a uniform B6 genomic background. Since previous molecular analyses revealed an overrepresentation of mitochondria-related genes in this interval, several of which express genotype-dependent variation in ethanol-naïve R8 compared to background B6 mice, including a subunit each of CI and CII, we were particularly interested to see whether this strain exhibited any of the inherent structural MRC differences similar to those detected in D2 and B6 progenitor comparisons.

No qualitative differences were detected between strains on BN-PAGE under the same conditions in which B6 and D2 were compared; the R8 band pattern was indistinguishable from B6 (Figure 7A). Similarly, neither SC-c nor SC-d could be visualized by Coomassie, as in B6. These upper SC bands were detected by IGA staining in both strains, but the predominance of SC-b over SC-c was similar in these strains for both CI and CIV (Figure 7B) (mean CI b:c ratio: B6=11.1, R8=11.4, p=0.9; mean CIV b:c ratio: B6=2.5, R8=2.6, p=0.7). Similarly, relative amounts (COOM) and CI IGA were comparable between R8 and B6 strains for mean SC-b:a ratios (Figure 8C; mean COOM b:a ratio: B6=1.2, R8=1.3, p=0.45; mean CI b:a ratio: B6=0.5, R8=0.6, p=0.34). We also did not observe any genotype-dependent differences in normalized CIV IGA (Figure 8D) for SC-b (mean B6 and R8=0.03, p=0.20), SC-c (mean B6=0.01, mean

R8=0.03, p=0.65), or subcomplex bands *1 (mean B6=0.09, mean R8=0.09, p= 0.44), or *2 (mean B6=0.09, mean R8=0.13, p=0.25). These results indicate that the presence of the D2 allele only within the 1.1 Mb *Alcw1/Alcdp1* QTL interval does not by itself direct the formation of higher order MRC complexes substantially distinct from B6, and that these structural characteristics alone cannot explain the susceptibility of the R8 strain to more severe ethanol withdrawal. Alternatively, it is possible that a D2-like MRC configuration is actually present in R8 brain, but restricted to certain regions, and is therefore masked by the whole brain preparation used here. Additionally, increased amounts of SC-c, SC-d, CIV-containing subcomplexes, and CIV activity relative to SC-b may simply be the grossly observable portions of a likely multi-faceted *in vivo* MRC structural organization that can be detected by these methods. B6 vs R8 differences in similarly important, but subtler, features (e.g., absolute amounts of SC-b and SC-a) that also contribute to the global MRC configuration may require increased quantitative sensitivity and experimental power to detect. Considering the small phenotypic effect size of ethanol withdrawal in R8 mice (Section I.G), an even smaller underlying biochemical effect would not be surprising.

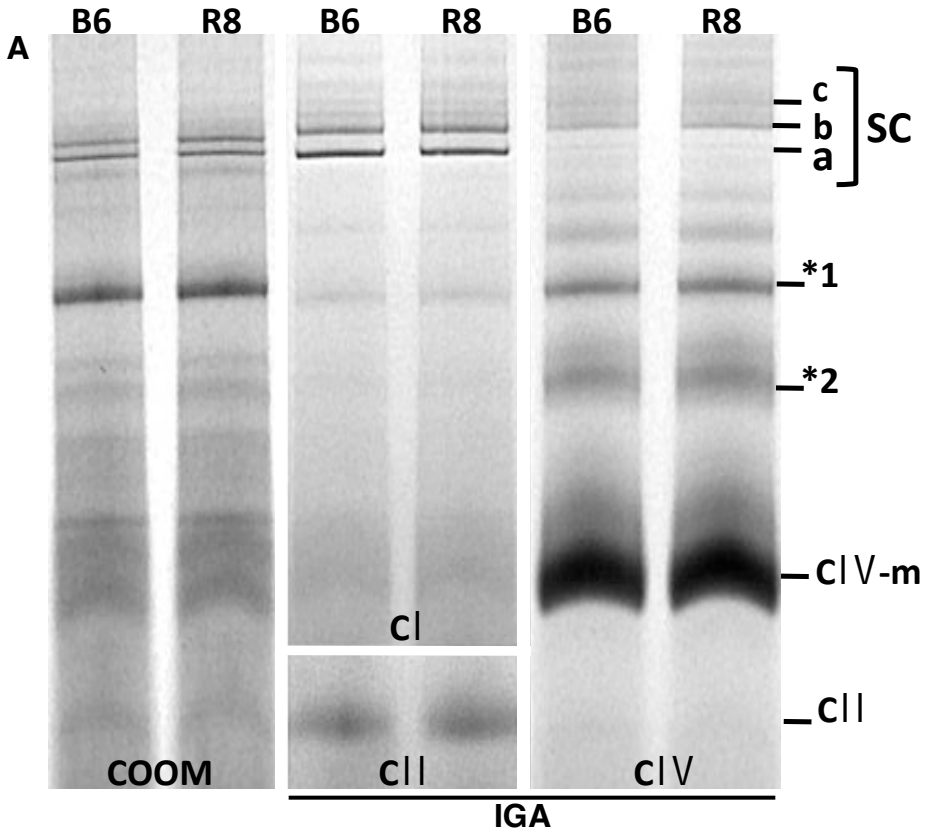

Figure 7. BN-PAGE comparisons of mitochondria from ethanol-naïve R8 congenic vs. B6 background strain mice. Digitonin solubilization of whole brain mitochondria and separation by BN-PAGE yields a band pattern after Coomassie (COOM), and CI, CII, and CIV in-gel activity (IGA) staining for ethanol-naïve R8 congenic mice that is qualitatively similar to B6 background strain mice (A). Conditions were identical to those described in Figure 5. Semi-quantitation was performed as in Figure 6 to derive proportional measures of genotype-dependent differences in SC-b:c (B), SC-b:a (C), and CIV-reactive (D) bands. Representative samples are shown of gels stained independently for COOM, CI/CII, and CIV activities. $p > 0.2$ for all comparisons, two tailed.

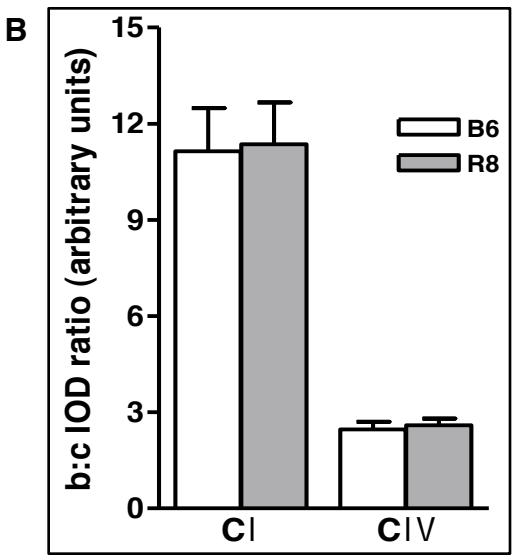

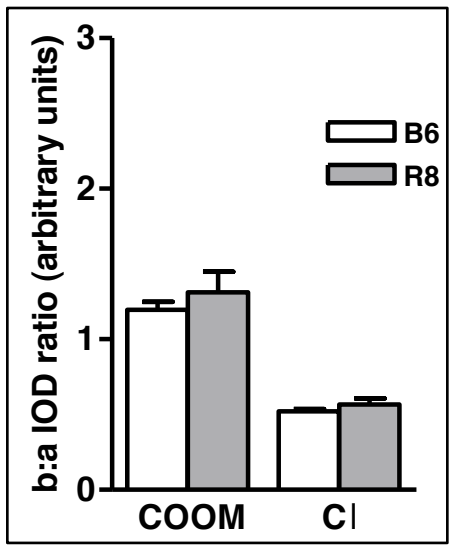

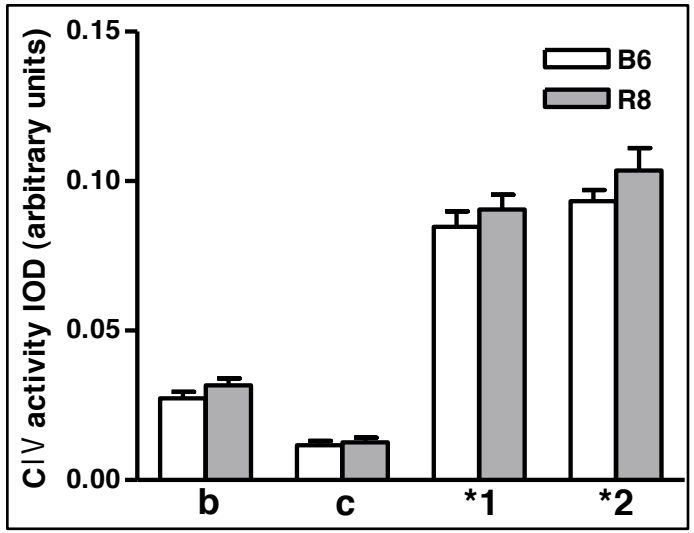

IV.C.2. Genotype-dependent differences in MRC organization and activity are preserved, and may be intensified, during chronic ethanol exposure and withdrawal

Chronic alcohol exposure is well-known to increase brain oxidative stress and damage mitochondria (Section III.A.2). Furthermore, a few studies have uncovered deleterious effects on respiratory activity, ROS, and oxidative damage during withdrawal above those produced by exposure alone (Section III.A.3). Here we sought to evaluate whether chronic ethanol exposure and/or withdrawal is associated with alterations in MRC structure and function, particularly in a genotype-dependent manner. Because the withdrawal phenotype is more robust in chronic than acute ethanol exposure paradigms (Section I.C), we chose first to investigate potential strain- or treatment-dependent MRC alterations in mice using this model.

Ethanol-dependent B6 and D2 animals.

Mice of each strain were exposed to three days of continuous ethanol (E) or air (AP) inhalation and administered pyrazole to maintain intoxicating BECs. Brain tissue from half of each group was obtained immediately upon vapor cessation. These mice are considered ethanol-dependent; pyrazole inhibition of ADH ensures no lapses in exposure, and thus relatively stable brain adaptation to moderate, unremitting ethanol that is intended to mimic human patterns of intake and dependence. BN-PAGE was performed identically as for naïve mice, and gels stained for COOM, and IGA of CI, CII, and CIV (Figure 8).

Qualitatively, ethanol-treated B6 and D2 mice exhibit similar differences in overall MRC organization after digitonin solubilization as their ethanol-naïve counterparts: B6 mitochondria have predominantly SC-b and SC-a configurations (Figure 8, left), while D2 display these, as well as a significant presence of SC-c and SC-d (Figure 8, right). Furthermore, in comparison to air-pyrazole controls, no rearrangement or structural aberrations in SC, subcomplex, or individual complexes could be observed, indicating that chronic ethanol exposure does not affect gross MRC organization of either strain.

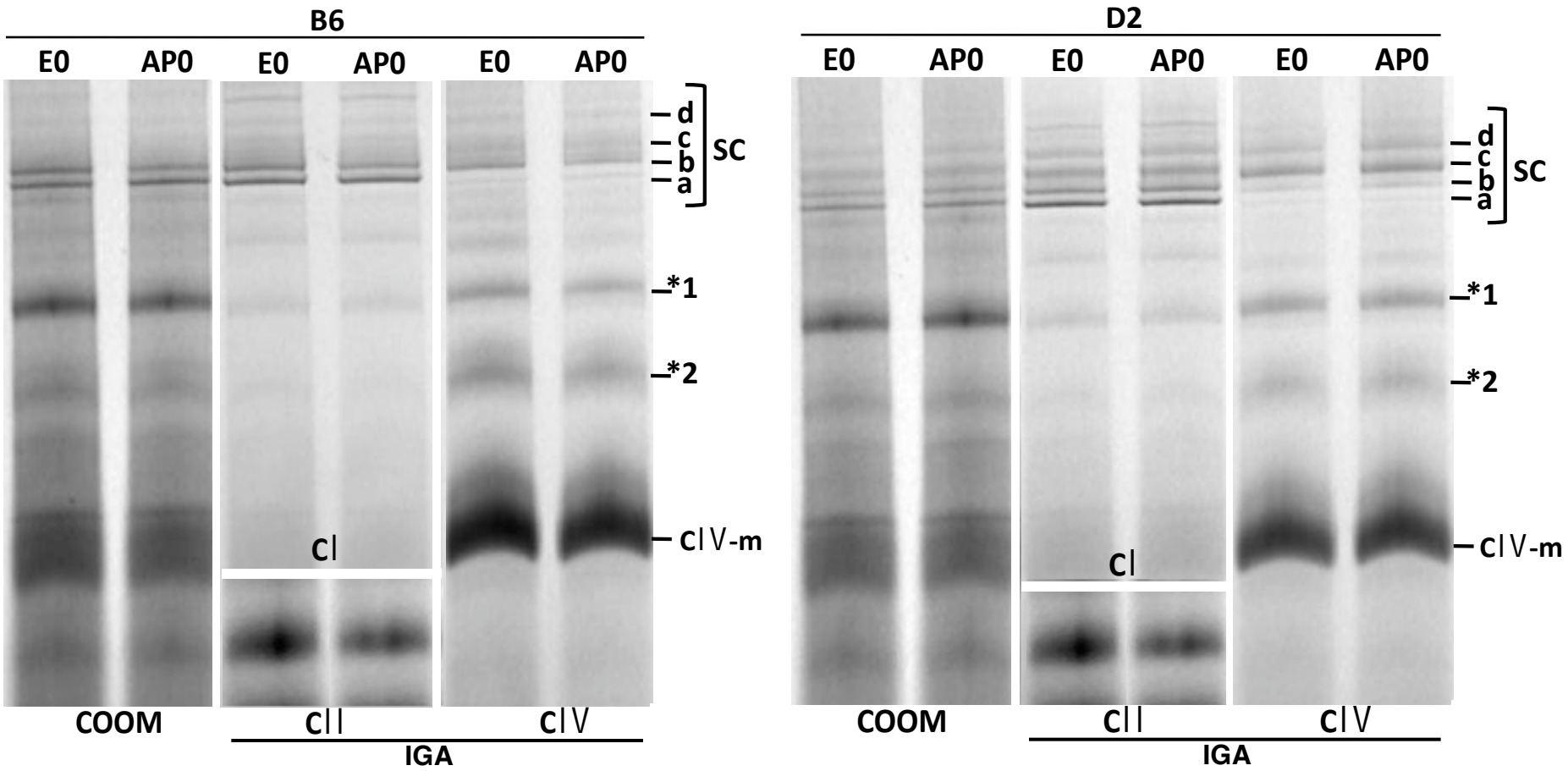

Figure 8. **BN-PAGE comparisons of mitochondria from ethanol-dependent B6 and D2 mice.** COOM, CI, CII, and CIV in-gel activity (IGA) staining of whole brain mitochondria from ethanol-dependent mice reveals no qualitative treatment effects on super-, sub-, or individual MRC complexes after BN-PAGE in either the B6 or D2 strains. Of note, however, is the distinct genotype-dependent band pattern revealed by digitonin solubilization, particularly for SCs (a-d). This pattern highly resembles that observed in ethanol-naïve mice, indicating that genetic influence on higher order MRC organization is preserved after chronic ethanol exposure. BN-PAGE was performed identically as for naïve mice. Representative samples are shown for gels stained independently for COOM, and CI/CII or CIV activities. E0 - ethanol-dependent; AP0 – air/pyrazole controls.

Semi-quantitative assessment of SC proportions (Figure 9, A-C) confirmed the apparent lack of an ethanol effect on MRC configurations, since neither the b:c (Figure 9A) nor b:a (Figure 9B) ratios was significantly different for amount present (COOM) or CI activity between ethanol-dependent and air control animals in either strain (mean D2 COOM b:c ratio: ETOH=0.73, AP=0.84, p=0.32; mean B6 CI b:c ratio: ETOH=4.6, AP=4.4, p=0.47; mean D2 CI b:c ratio: ETOH=1.4, AP=1.6, p=0.14; mean B6 COOM b:a ratio: ETOH=1.2, AP=1.3, p=0.85; mean D2 COOM b:a ratio: ETOH=0.58, AP=0.75, p=0.22; mean B6 CI b:a ratio: ETOH=0.85, AP=0.84, p=0.93; mean D2 CI b:a ratio: ETOH=0.70, AP=0.79, p=0.18).

Although amounts appeared unchanged, we observed an apparent effect of chronic ethanol exposure in D2 mice, which showed a trend (p=0.12) for decreased b:c CIV activity in the ethanol-treated group (Figure 9A, mean ETOH=0.28, mean AP=0.33) while treatment effects in B6 were clearly not significant (mean ETOH=1.8, mean AP=2.1, p=0.41). This result was further supported when CIV IGA of super- and sub-complexes was normalized to monomeric CIV activity (Figure 9C), as reduced signal/activity was found for D2 in ethanol-treated SC-b (mean ETOH=0.02, mean AP=0.03, $p<0.05$), SC-c (mean ETOH=0.07, mean AP=0.08, $p<0.05$), SC-d (mean ETOH=0.02, mean AP=0.03, $p<0.05$), and *2 (mean ETOH=0.05, mean AP=0.08, $p<0.02$). These results may suggest that CIV activity is compromised for the major SCs, and thus possibly overall, only in ethanol-dependent D2 animals. Alternatively, the integrity of CIV-containing super- or sub-complexes may be particularly vulnerable to the damaging effects of ethanol in D2, or experience increased or unique ethanol-related stress compared to B6 and thus increased turnover. If present, such effects might be more pronounced and accurately quantified with an appropriate internal mitochondrial protein standard.

For this group of experiments, we were primarily interested in whether we could observe ethanol treatment effects in either strain, and were limited in making direct comparisons between strains by methodological constraints, i.e., ten samples at most can be included on a single gel, and thus directly compared, since technical variation is large enough to preclude

statistical evaluation between gels. However, it is important to note that qualitative strain differences were apparent in mitochondria from both ethanol-dependent and air-pyrazole control mice, and in parallel with the significant genotype-dependence of these measures observed in naïve mice (Figure 6A); mean b:c ratios of CI and CIV activity in B6 are much greater (4.4-4.6 and 1.8-2.1, respectively) than in D2 (1.4-1.6 and 0.28-0.33, respectively), and SC-c retains the predominant CIV activity in D2 (mean b:c < 0.5). Considering these were entirely different experimental groups consisting of individuals separated by many generations, and samples obtained and prepared with the same protocol but entirely independently, we can be reasonably confident that the strain-specific MRC organization and activity detected are inherent and stable attributes with potentially substantial influence on many aspects of CNS mitochondrial function.

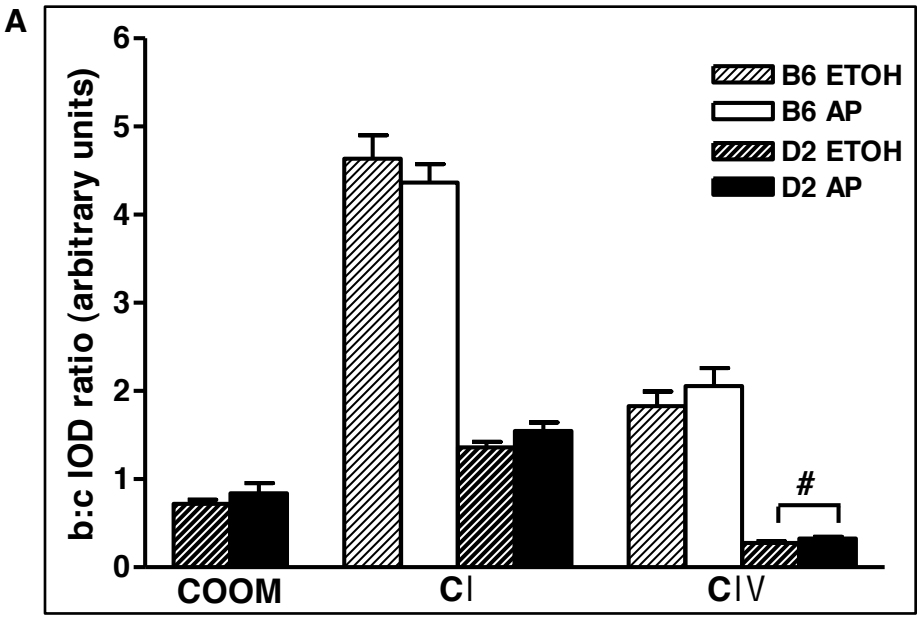

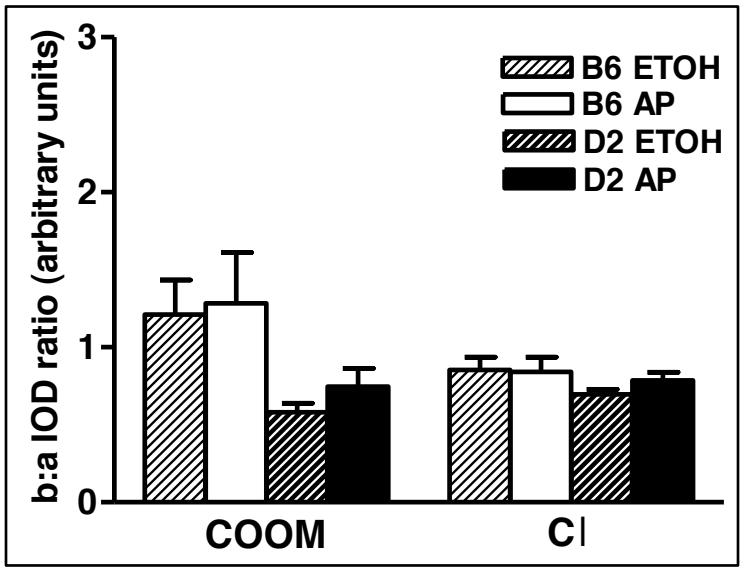

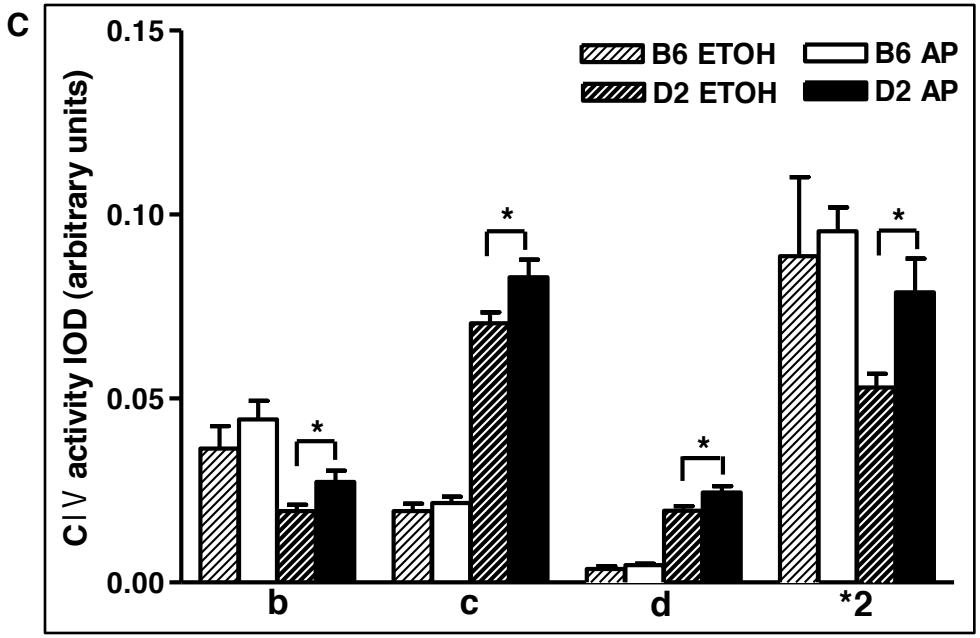

Figure 9. Semi-quantitative assessment of MRC configurations in ethanol-dependent (ETOH) and air-pyrazole control (AP) B6 and D2 mice. Staining for amount (COOM) and CI and CIV activities after BN-PAGE, and IOD ratios of SC-b:c (A), SC-b:a (B), or normalized to monomeric CIV signal (C) shows significantly decreased CIV activity only in mitochondria from ethanol-dependent D2 mice. Conditions were identical to those described for ethanol-naïve mice. To increase the power to detect ethanol effects (ETOH *vs.* AP), each strain was visualized on separate gels and only intra-strain statistical comparisons were made. n=4-5 per strain, per treatment. *p < 0.05, #p=0.12, two-tailed.

Ethanol-withdrawn B6 and D2 animals. While much evidence is available regarding the deleterious effects of ethanol exposure on mitochondria and the MRC, we were most interested in exploring whether this mechanism is associated with withdrawal neurobiology, and in a way that could be linked to genetic susceptibility. It is clear that withdrawal from ethanol is a unique neurobiological phenomenon involving mechanisms perhaps overlapping, but at least partially distinct, from that of exposure alone. The details of cellular and regional substrates of withdrawal, however, and specific genetic contributions to these, are still almost entirely unknown. Thus, we obtained whole-brain samples from mice withdrawn from ethanol following chronic exposure or air-pyrazole controls at the time of peak withdrawal (7 hrs post vapor cessation; Section IV.B.2) to assess for the presence of treatment effects on MRC organization and/or function that may potentially play a role in strain-specific ethanol withdrawal severity.

Mitochondria from ethanol-withdrawn (E7) and air-pyrazole control (AP) mice display a strain-specific band pattern on BN-PAGE (Figure 10) similar to ethanol-dependent and control animals, as well as ethanol-naïve mice. Again, the predominance of SC-b and SC-a, and lack of SC-c and SC-d, is clear in B6 after COOM staining (Figure 10, left), while all configurations are present in significant amounts in D2 mice (Figure 10, right). No obvious rearrangements or aberrations in super-, sub-, or individual complexes are apparent between ethanol-withdrawn and control mice of either strain, and the groups display qualitatively equivalent levels of CI, CIV, and CII activity for relative amounts of overall mitochondrial protein present.

No changes in SC proportions were observed after semi-quantitative assessment (Figure 11, A-C), indicating that ethanol withdrawal is not associated with gross MRC rearrangement in either strain compared to naïve animals. Within strains, there was no difference in the mean b:c ratios (Figure 11A) and b:a ratios (Figure 11B) after COOM or CI IGA between ethanol-withdrawn and control groups (D2 COOM mean b:c ratio: ETOH=1.4, AP=1.0, p=0.23; B6 CI mean b:c ratio: ETOH=7.1, AP=7.2, p=0.93; D2 CI mean b:c ratio ETOH=1.5, AP=1.3, p=0.26; B6 COOM mean b:a ratio: ETOH=1.3, AP=1.2, p=0.67; D2 COOM mean b:a ratio: ETOH=0.79,

AP=0.65, p=0.36; B6 CI mean b:a ratio: ETOH=1.2, AP-7=1.2, p=1.0; D2 b:a CI ratio: ETOH=1.1, AP=0.84, p=0.17). Contrary to ethanol-dependent D2 mice, we did not observe any effects of ethanol withdrawal on the mean b:c ratio of CIV IGA in D2 mice (Figure 11A; ETOH=0.39, AP=0.39, p=0.97), nor in B6 (ETOH=1.4, AP=1.5, p=0.75), indicating that if exposure does alter the proportional amount or activity of CIV- containing SCs, this effect has re-equilibrated by 7 hr post-ethanol. Similarly, no treatment effects were observed for normalized CIV IGA in any of the super- or sub-complexes (data not shown), reaffirming the apparent recovery of this activity in D2 during the withdrawal period.

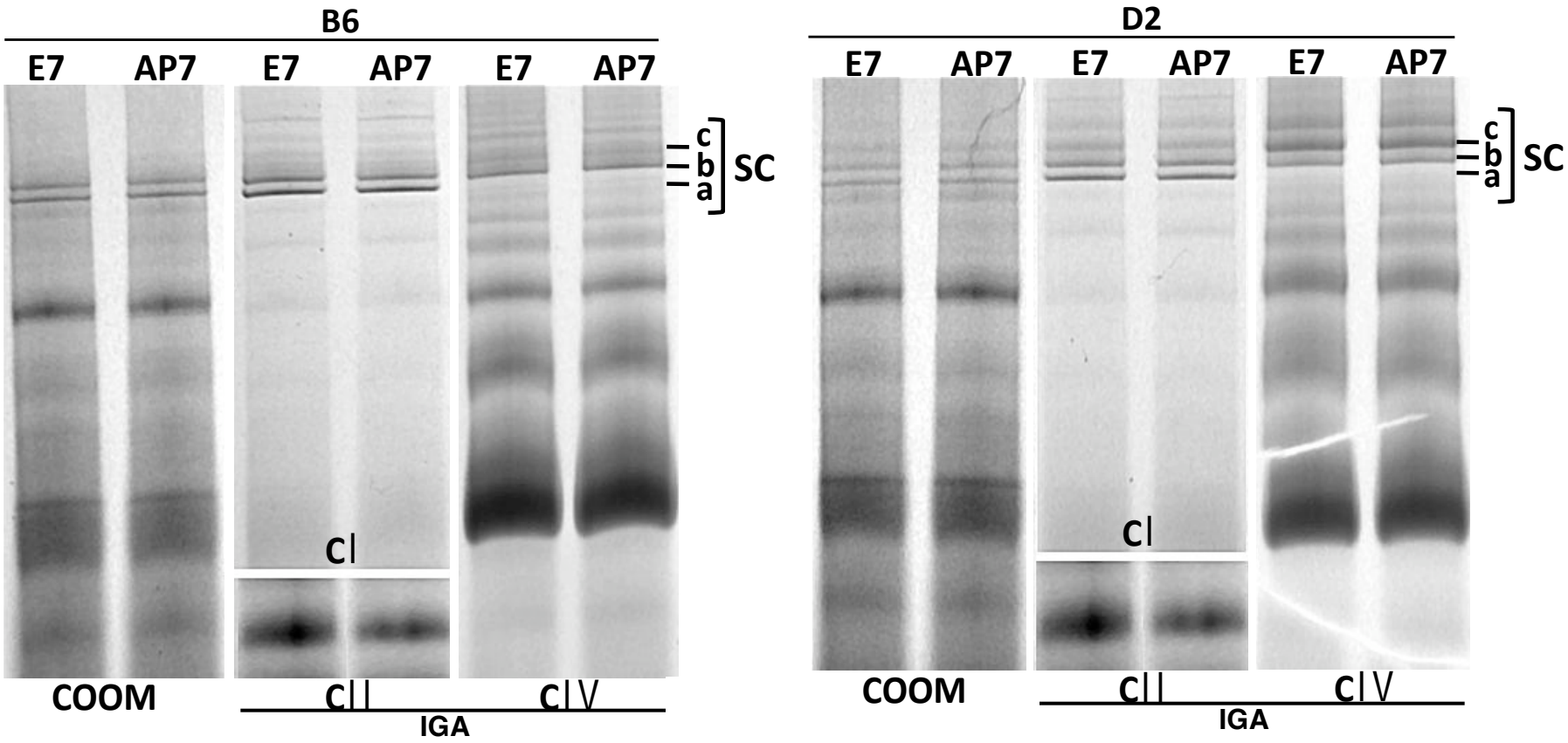

Figure 10. **BN-PAGE of mitochondria from ethanol-withdrawn B6 and D2 mice.** COOM, CI, CII, and CIV IGA staining of whole brain mitochondria 7 hr post-cessation of chronic ethanol (E7) reveals no qualitative differences in super-, sub-, or individual MRC complexes after BN-PAGE compared to controls (AP7) for either B6 or D2 mice. Of note, however, is the distinct strain-dependent band pattern revealed by digitonin solubilization, particularly for SCs (a-c), which is similar to that observed in naïve and ethanol–dependent mice and indicates the genetic influence on higher order MRC organization is preserved during ethanol withdrawal. BN-PAGE was performed identically as for naïve and ethanol-dependent mice. Samples shown are representative of n=3-5 per strain, per treatment. E7 - ethanol-withdrawn, AP7 – air/pyrazole controls.

Again, while direct strain comparisons were not made in these experiments due to the focus on a more thorough assessment of ethanol-specific effects within strains, clear genotype-dependent differences in the preferential SC configuration were observed qualitatively that are in line with both naïve and ethanol-dependent animals. SC-b strongly predominates SC-c in B6 mitochondria for amount present (no SC-c signal is visible in COOM), and IGA of CI (mean b:c ratio=7.14-7.2) and CIV (mean b:c=1.4-1.5). Conversely, D2 SC-c is present in almost equivalent amounts (mean COOM b:c=1.0-1.4) and retains comparable CI activity (mean b:c=1.3-1.5) to SC-b, yet possesses a much higher proportion of CIV activity (mean b:c=0.39). Like data from ethanol-dependent and naïve animals, these results substantiate the observation that brain MRC organization is inherently distinctly different in these two strains. Thus, while not apparently altered by ethanol-dependence or withdrawal, at least at the whole-brain level and as detectable by these methods, preferential MRC complex associations may still have important consequences for baseline mitochondrial function that can drastically affect behavioral responses to ethanol and other phenotypes.

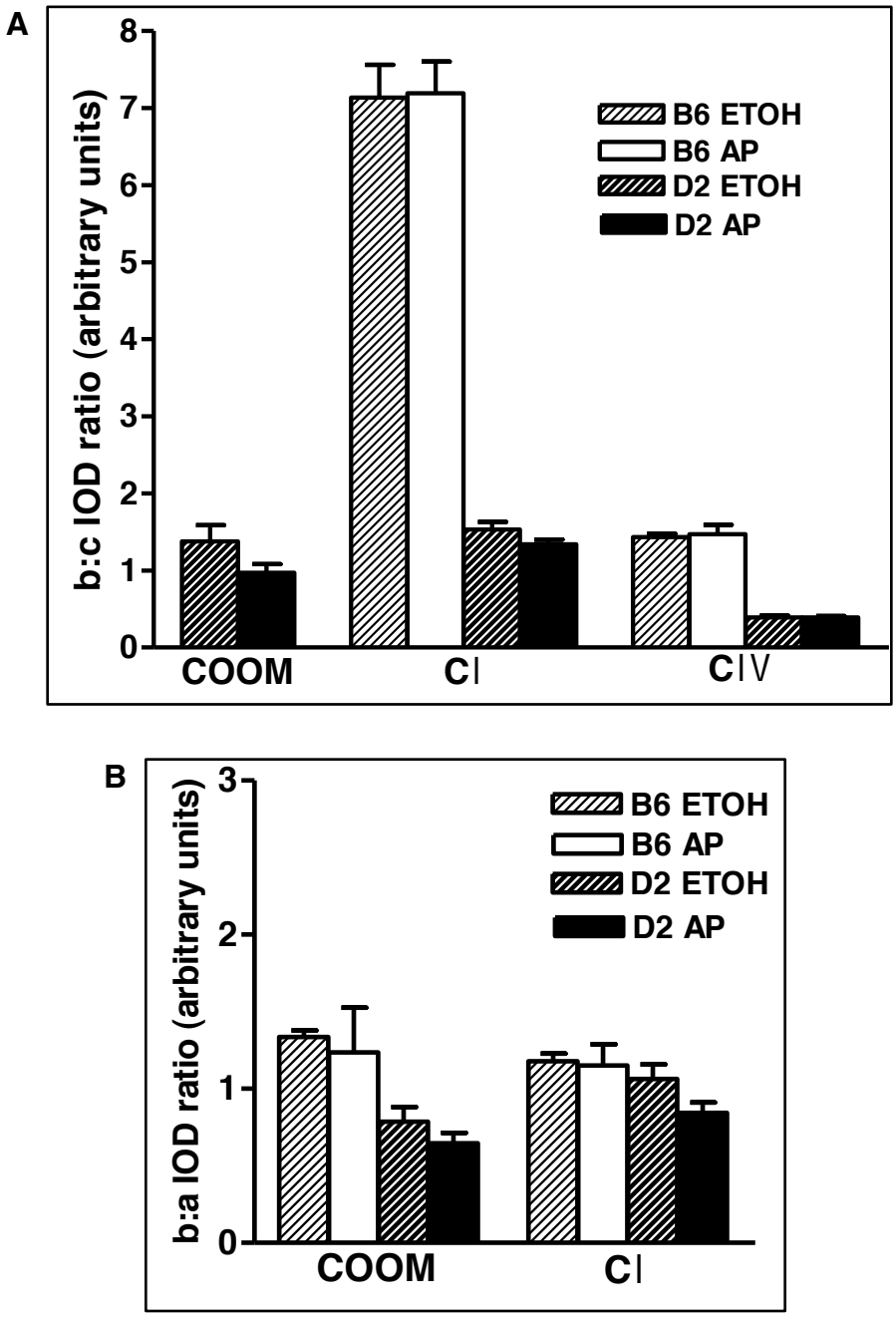

Figure 11. **Semi-quantitative assessment of MRC configurations in ethanol-withdrawn (ETOH) and air-pyrazole control (AP) B6 and D2 mice.** Staining for amount (COOM) and CI activity after BN-PAGE, and IOD ratios of SC-b:c (A) and SC-b:a (B) shows that ethanol withdrawal has no effect on MRC configurations in either strain. Conditions were identical to those described for ethanol-dependent and naïve mice. To increase the power to detect ethanol effects (ETOH *vs.* AP), each strain was visualized on separate gels and only intra-strain statistical comparisons were made. n=3-5 per strain, per treatment, $p < 0.2$ for all comparisons.

Ethanol-dependent and withdrawn R8 congenic animals.

Chronic ethanol withdrawal HIC scores are significantly greater for the R8 congenic than for B6 background strain animals (Section I.G), and of a similar magnitude as the much larger interval congenic, B6.D2*Mtv-7*. This suggests that a majority, if not all, of the genetic variance influenced by this QTL may be contained within the 1.1 Mb R8 interval. Brain mitochondria from ethanol-naïve R8 mice, however, display a qualitatively B6-, and not D2-, like band pattern after digitonin solubilization and BN-PAGE, indicating that this Chr 1 interval alone does not direct the aspects of MRC organization observable with the methods used here. Similarly, semi-quantitation to identify strain-specific preferential configurations did not detect any differences between naïve R8 and B6 mitochondria. It is possible, however, that more subtle strain differences are present, but require the stress of ethanol exposure and/or withdrawal to become apparent under these experimental conditions.

Qualitatively, mitochondria from ethanol-dependent (E0) and ethanol-withdrawn (E7) R8 congenic animals appear similar to mitochondria from appropriate controls (AP0, AP7, respectively) after COOM, CI and CIV IGA staining (Figure 12A). This indicates that there are no gross effects of ethanol treatment on MRC organization, consistent with qualitative observations in B6 and D2. Furthermore, like ethanol-naïve mice, the R8 band pattern is similar to that in B6 background mice with the absence of SC-c and SC-d visualization by COOM (Figure 12A, left lanes), but modest detection by CI and CIV IGA staining. Semi-quantitatively, the predominance of SC-b to SC-c in CI and CIV activities (Figure 12B) was not altered by ethanol exposure (CIV mean b:c ratio: ETOH=2.2, AP-0=2.1, p=0.39) or withdrawal (CI mean b:c ratio: ETOH=10.7; AP=10.4, p=0.89; CIV mean b:c ratio: ETOH=3.2, AP=3.1, p=0.77), nor was the proportion of SC-b to SC-a in amount (COOM mean b:a ratio: ETOH=0.96; AP=0.83, p=0.38) or CI activity (CI mean b:a ratio: ETOH=0.64, AP=0.56, p=0.17) (Figure 12C). Interestingly, comparisons of normalized CIV activity (Figure 12D) suggest decreases of SC-b (mean ETOH=0.04, AP-0=0.05, p=0.07), SC-c (mean ETOH=0.01, AP=0.02, p=0.04), and *2

(mean ETOH=0.07, mean AP=0.09, p=0.05) in ethanol-dependent R8 animals, an effect in the same direction as D2 and not present in B6 (Figure 9C).

It is important to note that, as in previous experiments using mitochondria from ethanol-dependent animals, only intra-strain statistical evaluation can be made reliably. BN-PAGE experiments for ethanol-dependent and ethanol-withdrawn were performed independently, thus direct comparisons of the magnitude of b:c ratios (e.g., in CIV activity) between ethanol-dependent and withdrawn animals cannot be obtained here. It is possible, however, that if more pronounced differences between these two strains emerge under ethanol stress than are observable in naïve animals, these may be readily detected by further experiments including both strains within a single treatment condition.

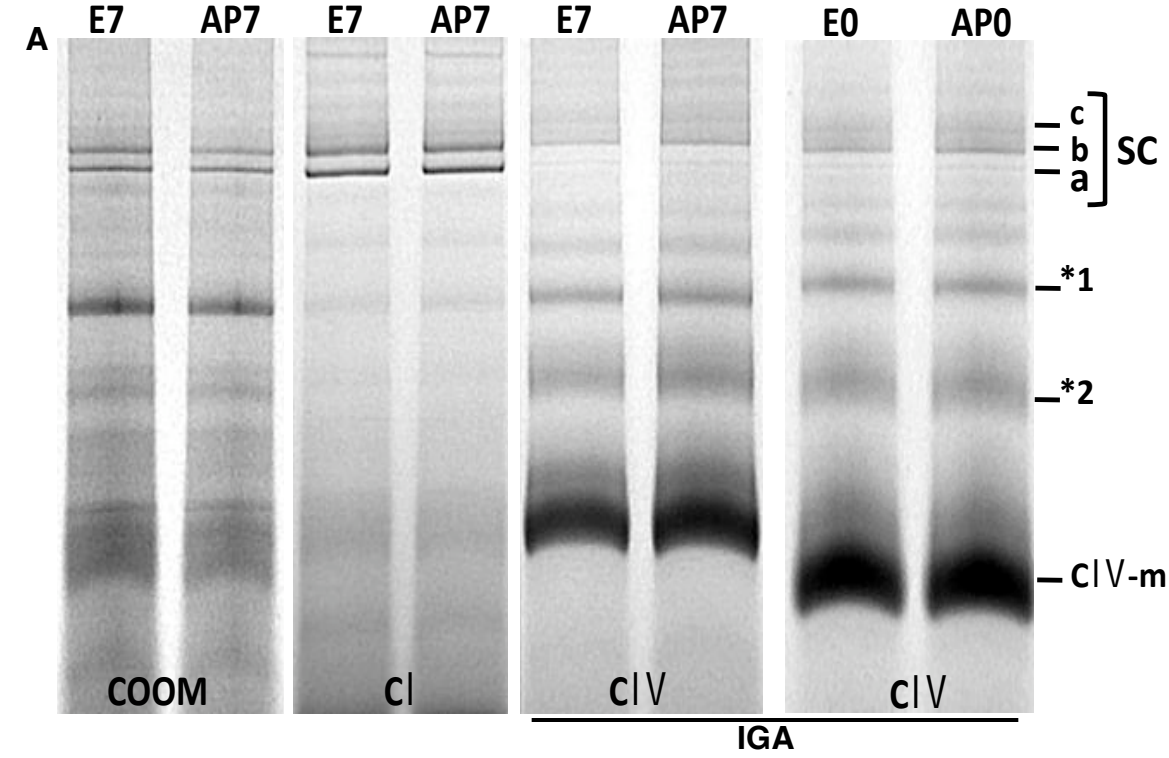

Figure 12. **BN-PAGE of R8 mice after chronic ethanol exposure.** COOM, CI, CII, and CIV IGA staining of mitochondria from ethanol-dependent (E0) and ethanol–withdrawn (E7) R8 congenic mice reveals no qualitative treatment effects (A). Semi-quantitation performed as in all B6 and D2, and ethanol-naïve R8, experiments also shows no effects of ethanol for SC-b:c (B) or SC-b:a (C). CIV-reactive (D) bands, however, suggest a decrease in ethanol-dependent animals over controls (D), similar to that seen for D2. n = 4-5 per treatment, *p < 0.05, #p < 0.07

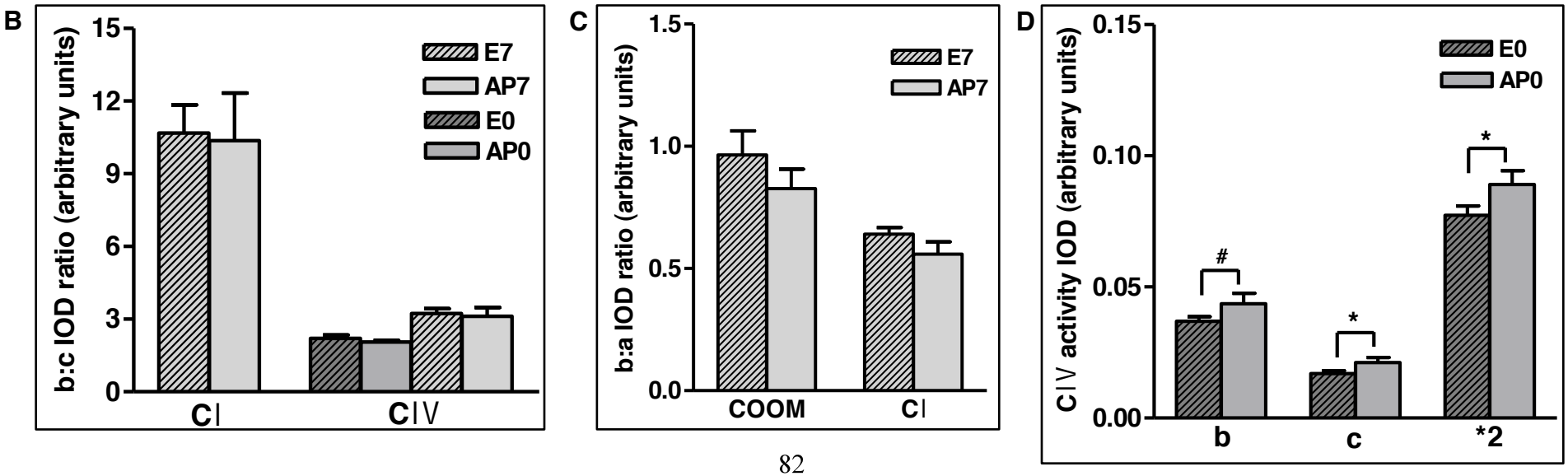

Along these lines, and because we are particularly interested in the neurobiological mechanism influenced by B6/D2 genetic variation at *Alcdp1/Alcw1* that is active during withdrawal, we began to assess whether more subtle strain-dependent differences could be detected after ethanol by directly comparing them within a single treatment condition on BN-PAGE. In these experiments, ethanol-withdrawn D2 and R8 congenic samples were run simultaneously with B6 (Figure 13A,B). While the proportional differences in b:c are large and obvious between ethanol-naïve B6 and D2 mice both qualitatively and semi-quantitatively, differences in b:a, if present, are more subtle.

Statistical comparisons for strain differences were not significant in either amounts (COOM) or CI activity of b:a in ethanol-naïve animals, but we noted a trend (B6 > D2) that was upheld in all ethanol experiments. Qualitatively (Figure 13A), we observed a clear difference in the proportion of SC-b to SC-a in both ethanol-withdrawn D2 (Figure 13A) and R8 congenics (Figure 13B) when compared directly to ethanol-withdrawn B6 after both COOM and CI IGA staining. Semi-quantitatively, these differences were significant (Figure 13C,D) and in the same direction as the previously noted trend. As might be predicted, the D2/B6 difference (Figure 13C) was larger in magnitude (COOM mean b:a ratio: B6=0.68, D2=0.26, $p<0.003$; CI mean b:a ratio: B6=0.50, D2=0.17; $p<0.0008$) than the R8/B6 (Figure 13D) (COOM mean b:a ratio: B6=0.93, R8=0.65, $p<0.05$; CI mean b:a ratio: B6=0.65, R8=0.43, $p<0.025$). These results indicate that small strain differences involving SC-a and/or SC-b may be present that require increased power to detect at statistical significance in naive animals, but become pronounced after ethanol exposure and/or withdrawal. That we observed no intra-strain treatment effect of chronic withdrawal on b:a may indicate that these changes are too subtle to detect with the current experimental power and/or methods. Alternatively, it is possible that any ethanol effects may have been masked by the requirement for pyrazole inhibition of ADH in all groups when using the chronic exposure model[35].

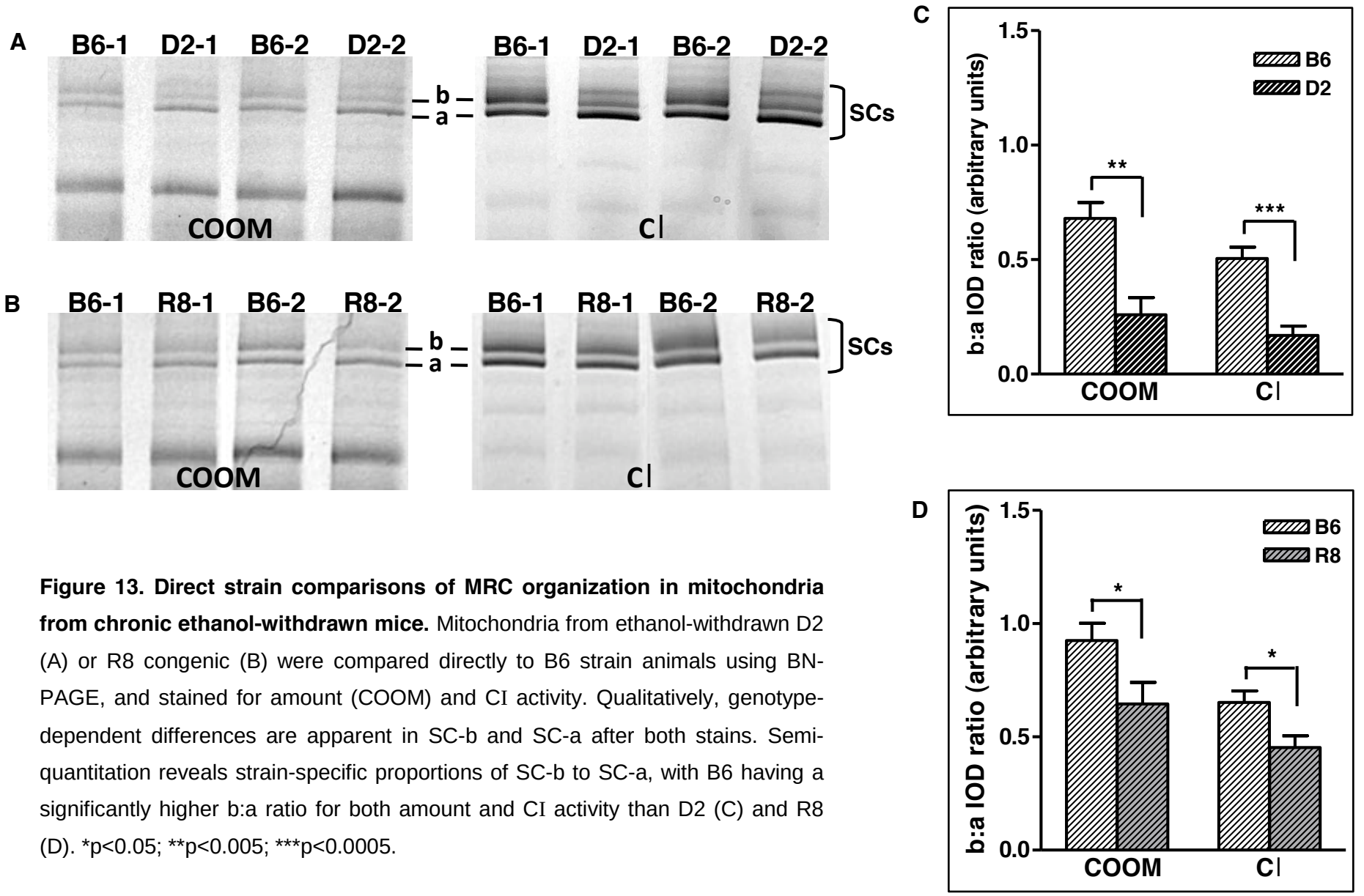

Figure 13. Direct strain comparisons of MRC organization in mitochondria from chronic ethanol-withdrawn mice. Mitochondria from ethanol-withdrawn D2 (A) or R8 congenic (B) were compared directly to B6 strain animals using BN-PAGE, and stained for amount (COOM) and CI activity. Qualitatively, genotype-dependent differences are apparent in SC-b and SC-a after both stains. Semi-quantitation reveals strain-specific proportions of SC-b to SC-a, with B6 having a significantly higher b:a ratio for both amount and CI activity than D2 (C) and R8 (D). *p<0.05; **p<0.005; ***p<0.0005.

As a step toward describing more thoroughly the genotype-dependent MRC organization we observed, and developing a plausible correlation of these findings to respiratory function at baseline and under ethanol stress, we began to assess BN-PAGE separated proteins with immunostaining by Western blot analysis. For initial experiments, we chose to first confirm the presence of CIII in both super- and CIV-containing sub-complexes utilizing a commercial antibody raised against the core 1 subunit (UQCRC1), particularly because no validated IGA enzymatic reaction is currently available. While a limited of number of samples (n=2 per strain, per treatment) were tested and only preliminary results obtained to date, these data indicate that CIII is indeed present in SCs a-d, as well as in subcomplex bands *1 and *2 (Figure 14). Interestingly, CIII immunoreactivity in *1 is present only for D2; there is effectively no signal in both R8 and B6, even though both strains show at least moderate CIV activity in naïve (Figure 14, center lanes; Figure 5) and ethanol-withdrawn animals (Figures 8 and 12). The lack of CIII may account for the qualitatively decreased amount and CIV IGA signal of *1 in B6 compared to D2 observed in all experiments. Furthermore, this absence may actually contribute functionally to the decreased CIV activity of this subcomplex seen in B6.

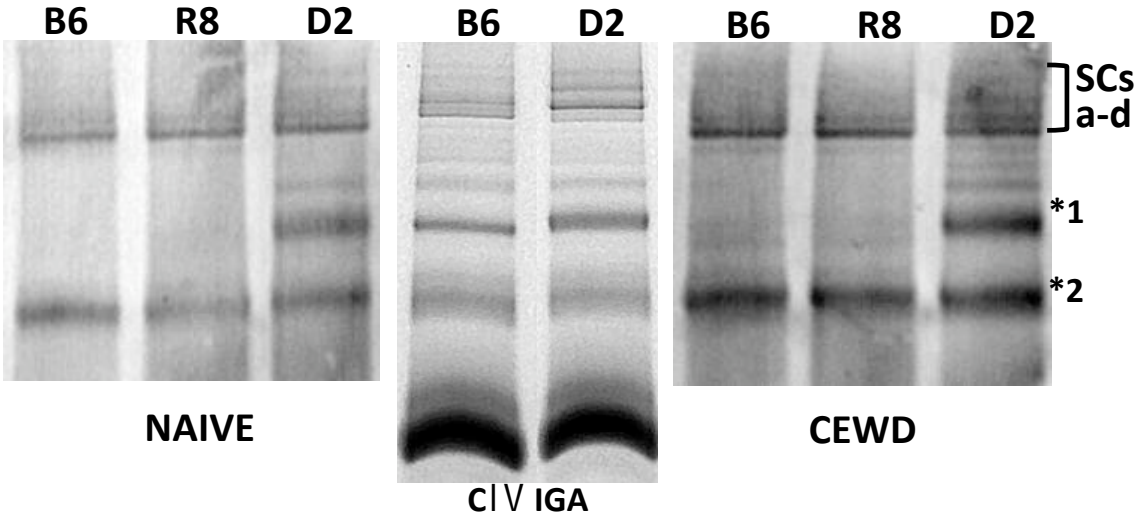

Figure 14. Western blot analysis confirms strain differences in MRC super- and sub-complexes and identifies a role for CIII. Mitochondria from ethanol-naïve and chronic ethanol-withdrawn (CEWD) B6, D2, and R8 congenic mice were separated by BN-PAGE and probed for immunoreactivity with the core 1 CIII subunit. Presence of CIII was indicated by significant signal in SCs a-d, as predicted by our experiments and previous reports of band identities (see text). CIII was also detected in subcomplexes *1 and *2, although only in D2 mice; signal is effectively absent for *1 in both B6 and R8 congenic strains. Levels of *2 appear qualitatively similar across all strains. A representative sample of B6 and D2 stained for CIV activity (IGA) is shown (center) for cross-reference of CIII immunoreactivity to CIV-containing bands. Representative blots are shown.

IV.C.3. Strain differences in MRC organization and activity are preserved during withdrawal following acute ethanol exposure

In the acute ethanol model, withdrawal is monitored over the 12-48 hr following a single hypnotic dose of ethanol (4 g/kg, i.p.)[34]. Since BECs vary little across genotype after a single injection, neither monitoring nor stabilization of BECs with ADH inhibition is necessary. While D2 and R8 congenic mice still experience significantly more severe withdrawal than B6 in these conditions, the phenotype is less robust (Section I.G). Furthermore, while there are clearly some common genetic mechanisms, acute ethanol activates modest brain gene expression changes[53], has lower heritability (Section I.C), and activates some distinct neurocircuitry compared to chronic exposure[6, 211]. Since the minimal 1.1 Mb Chr 1 QTL interval shows capture for both chronic and acute withdrawal, however, we were interested to see if any strain-specific MRC differences could be detected after a single ethanol injection. Additionally, the chronic alcohol exposure model used in these experiments requires concomitant pyrazole administration, a known biological stressor. While we were unable to determine whether this indeed impacted our previous results, it is certainly possible that the presence of pyrazole in both ethanol-treated and control groups precluded our ability to detect any MRC effects due strictly to ethanol. Thus, applying BN-PAGE to animals exposed in the acute model can directly test whether withdrawal from ethanol is associated with observable, and perhaps strain-dependent, effects on MRC organization.

Qualitatively, the strain-dependent MRC organization we observed in ethanol-naïve and chronic ethanol-exposed animals was apparent after staining for amount (COOM), and CI, CII, and CIV activities (Figure 15), with SC-b and SC-a the predominant configurations in B6 (Figure 15, left) and additional prominent SCs clearly visible in D2 (Figure 15, right). There appears to be no intra-strain effect of acute ethanol withdrawal for either B6 or D2, however, which is confirmed in semi-quantitation of SC-b to SC-c (Figure 16A) (COOM mean b:c ratio: D2-E=0.9, D2-S=1.0, p=0.72; CI mean b:c ratio: B6-E=4.7, B6-S=4.8, p=0.74; D2-E=1.5, D2-S=1.4,

p=0.82; CIV mean b:c ratio: B6-E=2.6, B6-S=2.7, p=0.70; D2-E=0.49, D2-S=0.54, p=0.37), and SC-b to SC-a (Figure 16B) (COOM mean b:a ratio; B6-E=1.5, B6-S=1.5, p=1.0; D2-E=1.2, D2-S=1.2, p=0.85; CI mean b:a ratio: B6-E=0.9, B6-S=1.0, p=0.71; D2-E=0.9, D2-S=1.0, p=0.85). Normalized CIV activity also showed no effects of acute ethanol withdrawal on any CIV-containing super- or sub-complex for either strain (data not shown), indicating that a single ethanol injection does not affect the aspects of higher order MRC organization that can be detected with these methods in either strain. It is important to note, however, that the D2 sample size was small in these experiments (n=3 per strain, per treatment); thus, it will be necessary to repeat these experiments with increased power, particularly considering the effect size of the acute ethanol withdrawal phenotype.

During the course of these experiments, we obtained information from a recent report detecting, for the first time, the presence of CII in both super- and sub-complexes of mammalian mitochondria[158]. Thus, we applied staining for CII activity (IGA) to the entire gel in an attempt to detect signal in bands other than the established monomer. Indeed, while faint, a purple color indicative of CII activity was apparent in both strains in the band consistent with subcomplex *1 (Figure 16, bottom middle lanes), which also possesses significant CIV activity. To confirm this result, we performed immunostaining on BN-PAGE gels of naïve and ethanol-withdrawn B6, D2, and R8 congenic mitochondria with an antibody to the 30 kDa subunit of CII (succinate dehydrogenase, iron-sulfur protein; SDHB), and again detected an unambiguous signal at the level of *1 in all strains (data not shown). Furthermore, we also obtained a specific, albeit faint, signal in SCs of the D2 and R8 strains. While these data are preliminary, and we were not yet able to determine if quantitative strain differences exist, the indication that these higher order MRC configurations may include CII is supported by a recent report[158], and is a new and exciting finding for the field that has to date considered CII structurally and functionally independent in mammals (reviewed in[208]).

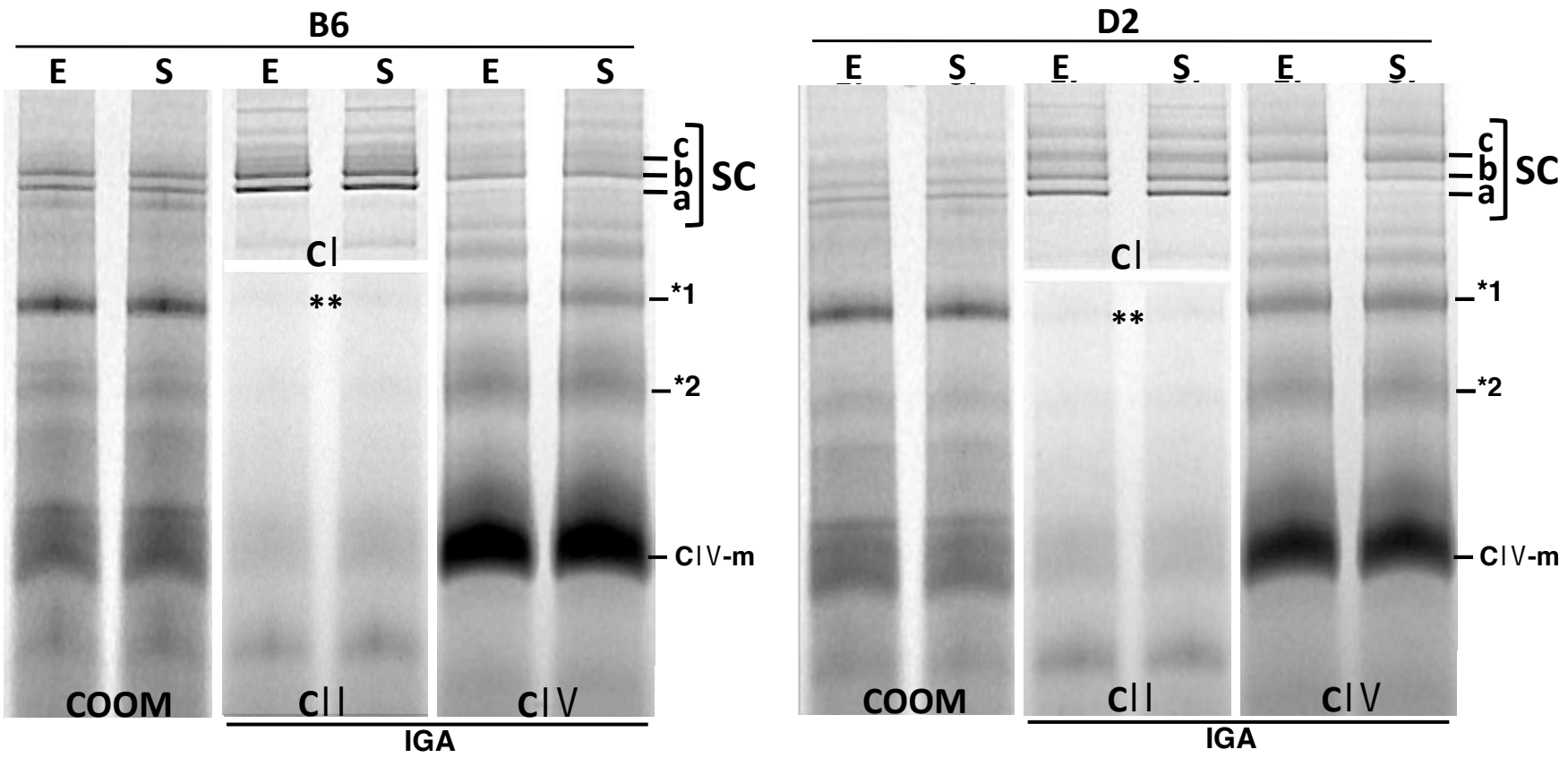

Figure 15. **BN-PAGE comparisons of mitochondria from acute ethanol-withdrawn and saline control B6 and D2 mice.** COOM, and CI, CII, and CIV activity (IGA) staining of whole-brain mitochondria after BN-PAGE reveals no qualitative changes associated with acute ethanol withdrawal (i.e., 7 hrs post, 4 g/kg i.p.) in super-, sub-, or individual MRC complexes for either strain. A prominent strain-dependent SC (a-c) band pattern is revealed by digitonin solubilization, and resembles that observed in independent groups of naïve and chronic ethanol-exposed mice. IGA staining applied to the entire gel reveals a faint signal (**) in subcomplex *1, indicating CII activity. Samples shown are representative of gels stained independently for COOM, and CI, CII, and CIV activities. E - ethanol-injected; S - saline controls.

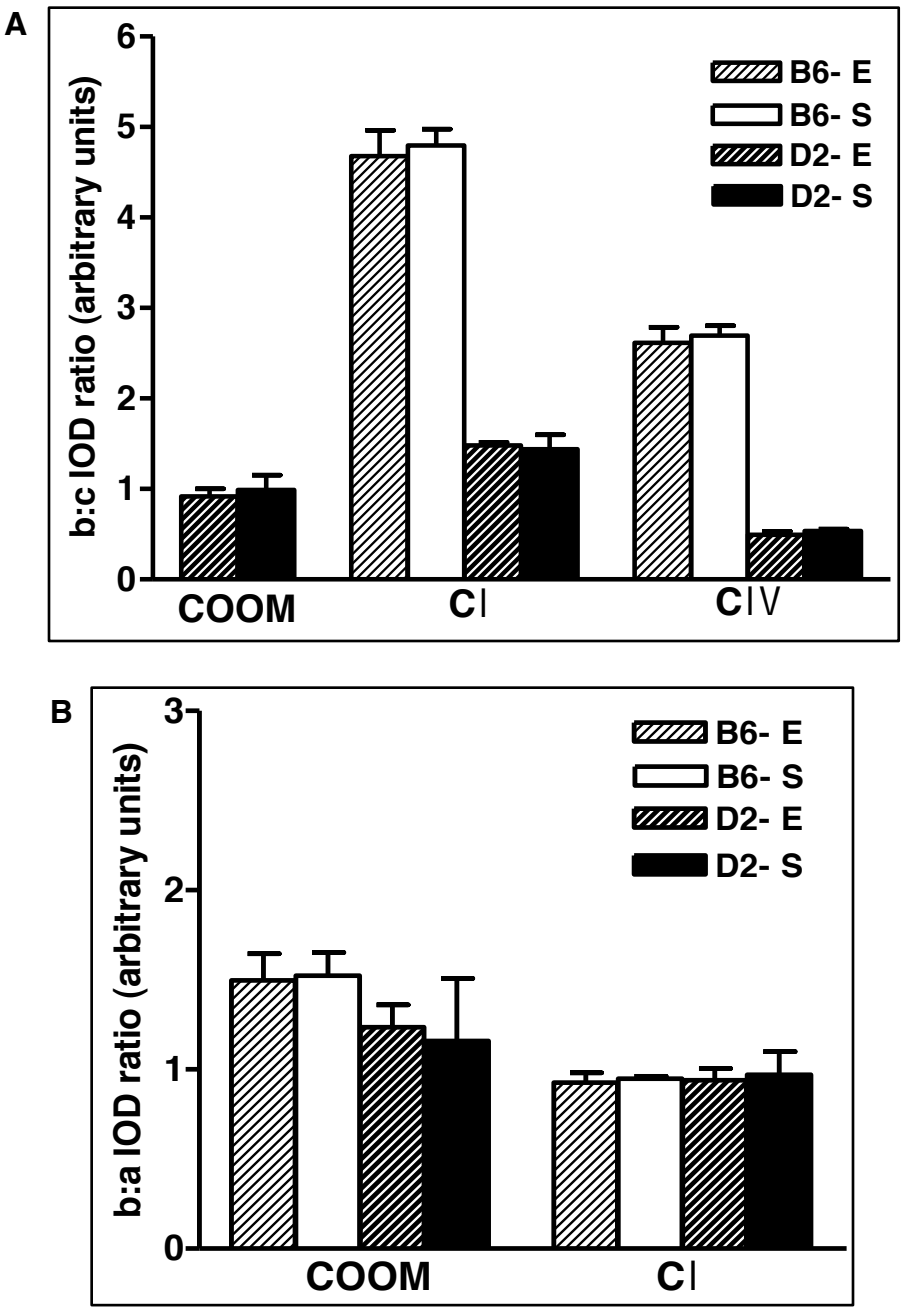

Figure 16. **Semi-quantitative assessment of MRC configurations from acute ethanol-withdrawn and saline control B6 and D2 mice.** Staining for amount (COOM) and specific activity of CI and CIV after BN-PAGE on mitochondria obtained 7 hrs post-injection (ethanol-E, 4 g/kg, or saline-S, i.p.) reveals no treatment differences in proportions of SC-b:c (A) or SC-b:a (B). Conditions were identical to those described for naïve and chronic ethanol-exposed mice. Statistical comparisons were made within strains to increase the power to detect effects associated with ethanol withdrawal (E *vs*. S), and B6 and D2 visualized on separate gels. n = 3-4 per strain, per treatment. $p > 0.2$ for all comparisons.

IV.D. DISCUSSION

In a systematic molecular analysis of the fine-mapped QTL influencing both acute (*Alcw1*) and chronic (*Alcdp1*) alcohol withdrawal on distal mouse Chr 1, we identified several MRC-related genes as particularly promising candidates to underlie this QTL. Since mitochondrial function and oxidative stress pathways were overrepresented among the entire group of genes within the QTL interval, as well as the 17 high priority candidates identified, and because B6 and D2 have been shown to differ inherently in several aspects of mitochondrial and oxidative stress biology (Section I.E), we sought to explore biochemically whether an MRC-related mechanism may be involved in genetic vulnerability to alcohol withdrawal, particularly that directed by the Chr 1 QTL.

Here, we took advantage of BN-PAGE to simultaneously evaluate both structure and activity of the MRC. We determined the identities of B6 and D2 whole-brain SCs based on COOM band patterns, IGA and immunodetection for specific complexes, as well as comparison with extensive previous reports of mammalian SCs isolated with digitonin (Section III.C.2). Thus, we can be reasonably certain SC-a is the CI/$CIII_2$ association, and that SC-b, SC-c, and SC-d consist of this primary configuration with additional copies of CIV (1, 2, and 3, respectively). To our knowledge, there has been no similar report to date, in mice or in brain, and particularly involving genetic influence on such MRC organization.

These studies readily determined that the MRC retains distinctly different structural and functional properties in B6 and D2 mice. In B6, SC-b clearly predominates in amount and activity of CI and CIV: levels of SC-c are beneath detection threshold by COOM, and there is at least twice as much CIV activity, and almost 8 times as much CI activity, in SC-b than SC-c. A much different pattern is present in D2 mice in that SC-c is clearly visualized by COOM, and while SC-b CI activity is still slightly greater than SC-c, the substantial majority of CIV activity resides in SC-c. A fourth high molecular weight band, SC-d, also displays significant COOM signal and CI and CIV activity in D2 mice, but no COOM and minimal CI and CIV IGA signals in

B6. The maintenance of additional SC associations in D2 with substantial enzymatic activity may suggest a compensatory need in this strain for supplemental respiratory capacity. Alternatively, the presence of these configurations may confer inherently higher respiratory activity in this strain over B6. In each scenario, a higher baseline level of oxidative stress is predicted, since both respiratory compromise and increased activity generate additional ROS. Furthermore, both situations would result in an enhanced vulnerability to a mitochondrial and oxidative stressor such as ethanol.

Interestingly, we also observed qualitatively more of the CIV-containing subcomplex (*1) comigrating with monomeric CV (ATP synthase) in naïve D2 than B6 animals. This band is consistent in size with a subcomplex previously reported to consist of $CIII_2$/CIV_2[212], as well as with a CII-containing subcomplex reported by Acin-Perez *et al.*[158] Our preliminary experiments demonstrated both CII immunoreactivity and IGA activity for this band in ethanol-naïve and withdrawn animals of both strains, confirming supramolecular assocation of CII. Perhaps most surprisingly, while D2 mice showed strong CIII immunoreactivity in the *1 band, effectively no signal was detected in B6. This result may account for the relatively lesser amount observed in B6 after COOM and CIV IGA staining, and while indicating that some form of the *1 subcomplex may be present, this formation is almost certainly not capable of respiratory activity without associated CIII. While a specific function has not yet been demonstrated in mammals, this configuration is the predominant respiratory SC in yeast and requires direct lipid-binding (e.g., CL) at both CIII and CIV for structural stability and catalytic activity[213]. An increased amount of this subcomplex in D2, and the presence of all obligatory MRC constituents, may thus suggest that this strain possesses a unique requirement for supported respiratory capacity, or maintains a state of increased respiratory activity even under normal conditions.

In a recent landmark publication[158], SCs from mouse liver and cell-line mitochondria corresponding to SC-b and SC-c directly demonstrated respiratory capability. Intriguingly, these results also strongly support the presence of a significant portion of CII in association with SCs

evidenced by: 1) immunodetection of CII subunits in association with CI, CIII, and CIV, 2) partner dependence of BN-PAGE CII comigration with particular sub- and supercomplexes containing CIII and CIV, and 3) the demonstration that certain SC bands are able to respire when fueled with succinate. These are remarkable findings considering the decades-long acceptance of CII as structurally and functionally independent of other MRC constituents. Here, we obtained immunoblot evidence that, although preliminary, also indicates the presence of CII in both sub- (*1) and supercomplexes. This result was further supported by detection of band *1 CII IGA in mice withdrawing from acute ethanol. Combined with the evidence presented here that B6 and D2 mice have inherently different proportions of these higher order CII-containing configurations, these results may suggest critical strain-specific implications for brain MRC function and perhaps a mechanism of genetic predisposition to metabolic, respiratory, and oxidative stressors such as ethanol.

In future investigations, it will be important to determine whether there is indeed a preference for CII association with certain SCs, as suggested by the higher proportion of immunoreactivity and succinate-driven respiration reported by Acin-Perez *et al.*[158] for the band corresponding to SC-c. In combination with our results showing a predominant SC-c configuration in D2 mitochondria, and CII immunoreactivity and enhanced CIV IGA in this band, these lines of evidence may support the idea that this strain maintains potentially increased respiratory capacity and/or a need to supplement activity by CII-afforded utilization of succinate as an additional respiratory substrate to NADH. That SC-d is also prominent in D2 and not B6 may further indicate a requirement for functional reinforcement by enhanced structural association of MRC constituents.

CI and CII can complement and support function of the other, since substrates enter the MRC at both sites. Succinate, in contrast to NADH, can be generated non-enzymatically[214] as well as from TCA cycle activity, such that an increased capacity of the MRC to use this substrate would be an efficient means to support respiratory function. One drawback to

increased CII employment is amplified ROS production; electrons are transported via CII to CoQ in both forward and reverse directions, causing additional leakage at CI. This is propagated by high membrane potential and electron transport compromise at CII[215]. In brain, reverse electron transport is a substantial source of mitochondrial-linked ROS since conditions of "dual electron entry," in which both NAD- and FAD-linked substrates are present, are widespread[199]. Additionally, free fatty acids can have an uncoupling effect on the MRC, thereby decreasing ROS production, but only under conditions of RET[216].

Acin-Perez *et al.*[158] also demonstrated for the first time the integration of the small molecule electron carriers (CoQ and cytochrome *c*) into MRC SCs; CoQ was found in the SC-b corresponding band, while a sizeable majority of cytochrome *c* associated with SC-c species. These carriers are also known to affect apparent SC molecular weight[217], which may explain the relative upward shift observed in B6 SC-c and SC-d. Utilization of specific carrier reserve pools is one way the MRC can maintain such a profound compensatory capacity in the face of perturbation[215]. If this feature is yet another aspect of higher order MRC structure, our studies identify these electron carriers as an additional potentially informative direction for future investigation of genotype-dependent SC organization.

In previous molecular analyses, we found higher whole-brain gene expression in R8 congenic than B6 background only for the genes encoding the MRC subunits (*Ndufs2* and *Sdhc*; Section II) – all other candidates were decreased in R8 vs. B6, including the third MRC-related gene (*Ppox*) whose role in heme biosynthesis is critical to maintenance of mitochondrial *cyt c* levels. Furthermore, progenitor coding sequence comparisons revealed predicted amino acid changes in D2 vs. B6 for the mitochondrial-targeting portion of *Ndufs2* and the highly conserved ubiquinone binding site of *Sdhc*. One possible interpretation is that a degree of respiratory compromise pre-exists with a D2 allele that requires support of CI and CII through compensatory increases in mRNA. Alternatively, or perhaps as a result, these genetic variations may lead to a hyper- and/or dysfunctional MRC that would produce increased ROS even at

baseline, but particularly in the context of respiratory stress. In both scenarios, overproduction of mitochondrial ROS would be a prominent feature likely to have significant cell-wide repercussions and perhaps create a unique vulnerability to multi-faceted stressors such as ethanol.

We did not, however, observe a gross D2-like deviation in SC organization when comparing naïve R8 congenic mice to B6; SC-b was qualitatively the predominant configuration in both strains and no statistical differences in SC ratios were detected semi-quantitatively. There was also a similar absence of CIII signal in the *1 subcomplex in R8 as observed for B6. These results suggest that loci other than *Alcdp1/Alcw1* influence the aspects of MRC organization observable with these methods, at least at the whole-brain level, which is not surprising considering the centrality of the MRC to overall cell function and vitality. The higher order structure that can be observed here is likely the combined result of several interrelated components, most of which will require additionally methods to investigate. Additionally, phenotypic QTL effect sizes for complex traits are typically quite small, even when the proportion of associated genetic variance is relatively high[38]. Thus, more subtle differences between the R8 congenic and B6 background strains may be present (e.g., in total amount of SC-b or CIV activity) that require increased power or precision to detect. Future investigations using immunochemical normalization, and downstream applications such as 2D or 3D PAGE to examine specific subunits and/or additional associated proteins, are needed to confidently determine how the *Alcdp1/Alcw1* QTL may influence MRC structure and/or function.

The large-scale strain differences displayed by naïve B6 and D2 animals were also present in dependent and withdrawn animals after chronic ethanol exposure, indicating that these aspects of MRC organization are stable inherent characteristics consistent across generations, and not artifacts of sample preparation. We did not detect an effect of ethanol on overall MRC organization or SC-b/SC-c proportions in any strain. We did, however, observe a suggestive decrease in the CIV activity of both sub- and supercomplexes in both D2 and R8 ethanol-

dependent mice that was not present in controls or B6 animals. This may indicate a diminished capacity to support the transfer of electrons to O_2 in these strains, and thus potentially directly have affect ATP production. Decreases in brain CIV activity, but not protein levels, have been repeatedly observed after chronic ethanol[183-185], and some of a larger magnitude in ethanol-withdrawn than even dependent animals[183, 185]. In our experiments, CIV IGA was not different between ethanol-withdrawn and control animals, suggesting that any potential effects of ethanol dependence had normalized at the time of peak withdrawal. It is entirely feasible, however, that chronic exposure strain-specifically induces a state of respiratory compromise that may also act as a contributing mechanism to the development of severe withdrawal even when amounts and/or activity have re-equilibrated.

These results were obtained from relative measures on particular intermolecular assemblies, and thus do not reveal whether overall CIV activity is indeed diminished in the more vulnerable strains. Future quantitative studies to determine the total activity and amount of CIV present in each strain, and comparisons with control mice, will be necessary to elucidate whether ethanol-dependence and/or withdrawal may have a more global effect on CIV function. Combined with evidence that specific higher order MRCs assemblies may be affected, and in a genotype-dependent manner, however, this information will be extremely useful for further elucidating respiratory chain involvement in the brain's response to ethanol. Additionally, regional assessment of CIV activity may be informative considering the tight coupling between MRC function and neuronal activity, and can be readily performed qualitatively and quantitatively in brain sections using the IGA stain used here[218]. Regional CI and CII activities can be similarly evaluated and may be a critical future strategy since withdrawal circuitry displays genotype dependence (Section I.B), and may act in part through *Alcdp1/Alcw1* (Chen G. *et al.*, in preparation).

While SC proportions were not apparently altered by chronic ethanol exposure or withdrawal, we observed a potential exacerbation of trending differences involving SC-a in naïve

animals that may have functional relevance. Levels of the SC-b:a ratio were higher in B6 than both D2 and R8 at peak withdrawal that appear, qualitatively, a result of increases in SC-a concomitant with decreases in SC-b. The $CI/CIII_2$ configuration (SC-a) has frequently been considered a stable, yet respiratorily non-functional, portion of the respirasome generated either during the purification process or in turnover. Recent pulse-chase evidence[158], however, suggests its role as a synthesis intermediate in SC formation, as does the presence of the proposed MRC chaperone, prohibitin[219], observed in the band corresponding to SC-a of the same study. Interestingly, increases in prohibitin have been detected in rat liver after chronic ethanol exposure, concurrent with specific decreases in subunits of CI and CIV[220]. Thus, our results may indicate the presence of a pre-existing genetic vulnerability to increases of a non-functional SC species during withdrawal from chronic ethanol. Additionally, it is possible that the presence of pyrazole, a strong metabolic stressor, obscured detection of any specific ethanol effects since both treatment and control groups received ADH inhibition. That changes in SC-b:a were not observed in acute ethanol-withdrawn mice may suggest these results were due only to pyrazole administration, although acute studies were underpowered. In any case, that strains vulnerable to more severe withdrawal (D2 and R8) show a shift away from active, toward non-functional, MRC configurations compared to a less vulnerable strain (B6) may indicate a genetic influence on MRC stability with possible associated functional effects in withdrawn animals.

A major limitation of these studies, and in BN-PAGE, in general, is the lack of an internal mitochondrial protein standard. Whereas others have used an individual complex for normalization[206, 209], we determined that the interdependence of individual MRC complexes to assemble and interact appropriately to form functional associations (Section III.A.5), and the reported ethanol effects on MRC complexes as well as the mtDNA partially encoding them (Section III.A.5), precluded such a similar use here. While COOM is useful for visualizing general patterns, it is relatively insensitive to small changes in SC amounts using digitonin

solubilization due to moderate background levels and run-to-run technical variation. Immunochemical determination of protein amounts using relative quantitation with a non-OXPHOS standard will thus be highly useful in future studies examining total SC amounts, and may help reveal whether they retain true strain- or treatment-dependent activity independent of complex amount. Additionally, while the substrates utilized for IGA staining are reportedly complex-specific, inhibition is an important biochemical confirmation for future studies that may also be exploited to test genotype-dependent sensitivity.

These results provide evidence for genetic influence on brain MRC organization likely to have consequences in the face of ethanol, and offer a new and promising direction for further investigations on withdrawal neurobiology. Future testing of genotype dependence in baseline and ethanol-induced oxidative stress, both globally and specifically in mitochondria, will be important next steps. In many cases, functionally harmful oxidative modification has no effect on SC stability[221]; thus potentially significant strain or treatment differences would not be detected here. Straightforward gel-based applications downstream of BN-PAGE are available (e.g., immunodetection of lipid peroxidation product, 4-HNE), however, and will likely be useful in further investigations. Since digitonin disrupts the mitochondrial membrane by interaction with cholesterol, strain variation in cholesterol content may also influence MRC configurations as observed through BN-PAGE. Interestingly, the D2 allele confers highly reduced brain expression (50-100X less than B6) of a cholesterol transport gene (*Apoa2*) identified as a promising candidate for *Alcdp1/Alcw1* (Section II). Considering that genetic factors are an important determinant of brain regional fatty acid composition in B6 and D2[222], some of these are more vulnerable to oxidative modification than others[223], intricate lipid-MRC dynamics exist[196], and lipid peroxidation has been observed during withdrawal[187], this may be a critical line of investigation for further studies.

V. GENERAL CONCLUSIONS AND FUTURE DIRECTIONS

The path of gene identification, i.e., moving from QTL to QTG, is one of the most challenging and unrealized objectives for modern medical geneticists. Several levels of proof are generally required, including multiple sources of molecular and behavioral evidence to confidently exclude the possibility of a false positive result[38, 78]. In many cases, convincing candidates from animal models have emerged only after congenics were used to significantly narrow an interval, and have demonstrated appropriate differences in expression and/or sequence between inbred progenitor strains, as well as in the congenics used for fine mapping[66, 67]. Only then is it reasonable to proceed with direct testing (e.g., genetic manipulation) that may more definitively reveal a candidate's true phenotypic impact. The work described here contributes significantly to such efforts by integrating the use of congenic animals with an unbiased molecular strategy to identify the most promising QTG candidates for *Alcdp1/Alcw1,* and a biochemical approach to implicate a potential neurobiological mechanism by which the QTL may exert at least part of its effect.

The *Alcdp1/Alcw1* ethanol withdrawal QTL resides within a highly gene-dense and polymorphic stretch of mouse Chr 1 that has been recently referred to as a "QTL hotspot" due to its involvement in a large number of behavioral and physiological traits[75]. Perhaps not surprisingly then, the abundance of promising candidates remaining even after a rigorous systematic molecular assessment precluded the advancement of any to behavioral level testing, and necessitated approaches to identify a mechanism of genetic influence before focusing on any one candidate. As recent complex trait QTG studies in both humans and animal models indicate[58, 59], ethanol withdrawal susceptibility conferred by the Chr 1 QTL may be the combined result of several sources of genetic variation associated with this region, perhaps involving a larger network of loci distributed throughout the genome (Section III) whose interactions on molecular, epistatic, protein, metabolic, and other levels in aggregate direct the overall phenotype. Thus, future investigations utilizing the R8 congenic to assess whether this interval

influences other traits both ethanol-related and not, and can regulate larger gene networks in *trans*, as well as directly testing *in vivo* the contribution of oxidative and/or mitochondrial mechanisms suggested by this work, will help elucidate how the Chr 1 QTL exerts its effect and whether it is due a single or multiple linked QTGs.

The finding that *Alcdp1/Alcw1* apparently does not influence withdrawal from pentobarbital (Section I.G) or zolpidem[69] may be a crucial clue for QTG(s) identification. Although there is considerable evidence that withdrawal vulnerability to a variety of sedative-hypnotics has some genetic factors in common[27, 29], the large effect pentobarbital withdrawal QTL (*Pbw1*) originally mapped as broadly overlapping initial *Alcw1* and *Alcdp1* regions on distal Chr 1[71] was most recently localized to a 0.44-Mb interval immediately distal to, but excluding, the R8 introgressed interval[74]. Similar to the ethanol withdrawal QTLs, an ISCS harboring the D2 allele only within this interval (R9) was critical to fine mapping *Pbw1*. These results highlight the complexity of genetic architecture commonly underlying quantitative traits, particularly in this region of Chr 1, and the utility of ISCS panels to dissociate the individual effects of closely linked QTL. Clearly, identification of the specific cellular mechanisms associated with withdrawal from different sedative-hypnotics, and the utilization of congenics in experiments directly testing these mechanisms, can be powerful support for a particular candidate(s) as a more likely true QTG. For example, contrary to the multiple pathways of increased oxidative stress and mitochondrial compromise produced by ethanol, we are aware of no evidence that barbiturates or zolpidem affect brain oxidative status and/or respiratory function. If future experiments reveal an effect of ethanol and/or withdrawal on MRC organization and function in R8 congenic animals, the demonstration of no such effects in pentobarbital or zolpidem-exposed mice would provide further support for the involvement of genes related to oxidative and mitochondrial mechanisms in the Chr 1 QTL effect.

Along these lines, we have begun to explore *in vivo* the potential role of a mitochondrial/ oxidative stress mechanism in contributing to genetic susceptibility conferred by the D2 allele

(Kozell, L.B., Denmark, D.L., unpublished). In pilot experiments, groups of D2 mice were pretreated for two days with moderate doses (300 mg/kg, i.p.) of N-acetylcysteine (NAC), a blood-brain-barrier-soluble[224] glutathione precursor well-known for its free radical scavenging and other antioxidative properties, or saline. On the third day, all mice were subjected to acute ethanol challenge (4 mg/kg, i.p.) and scored for withdrawal severity over the following 12 hr period. While not yet statistically significant, comparisons of both raw and corrected HIC scores indicate a trend toward decreased ethanol withdrawal severity in mice pretreated with NAC ($p=0.09$, ANOVA, *one-tailed*). These results predict that with increased power using larger experimental groups, antioxidant administration may demonstrate protection from more severe ethanol withdrawal in genetically vulnerable strains. Results from similar experiments using the R8 strain will be further evidence of the importance of an oxidative stress mechanism particularly for withdrawal susceptibility driven by *Alcdp1/Alcw1*.

Attempting to induce withdrawal vulnerability in converse experiments using a resistant strain like B6 may be another powerful way to demonstrate the contribution of oxidative and mitochondrial pathways to this phenotype. Agents that increase oxidative stress directly through mitochondrial dysfunction would be optimal tools for such experiments. A vast array of inhibitors specific to MRC complexes (e.g., rotenone – CI), or for more general respiratory function (e.g., 2,4-dinitrophenol – uncouples OXPHOS from ATP production) have been shown to induce significant oxidative challenge, and are widely utilized for contemporary studies investigating the role of mitochondrial-related oxidative stress in common neuropathological conditions. Incorporation of recent data elucidating neurocircuitry that is strain-dependently activated during ethanol withdrawal[6, 7, 211] may enhance the power of such studies since they suggest brain regions (e.g., substantia nigra pars reticulata, hippocampal dentate gyrus) likely to retain especially heightened sensitivity to stressors. For example, the demonstration that B6 mice have increased withdrawal severity after nigral microinjection of ROS-inducing mitochondrial inhibitors would be compelling evidence to both support a critical role for this region in

underlying the severe withdrawal phenotype, as well as identify a cellular mechanism by which it is expressed.

A similar experiment can be envisioned to examine a prospective role in withdrawal for the cellular stress gene network suggested as associated *in trans* with B6/D2 variation at *Alcdp1/Alcw1* (Section III). Both microarray and qRT-PCR expression data reveal increased pre-existing brain expression of stress response genes in Chr 1 congenic compared to background B6 mice. Chen *et al.*[152] showed that ethanol could potentiated an ATF4-mediated cellular stress response pathway (Section III) in cells previously sensitized by a small ER challenge, and that this occurred through a ROS-dependent mechanism. Salubrinal is a small-molecule inhibitor of eIF2α dephosphorylation that prevents initiation of some intracellular stress signaling cascades and can counteract ER stress-induced cell degeneration in culture[225], as well as excitotoxic hippocampal neuronal death after kainic acid exposure *in vivo*[226]. Thus, like protection with antioxidants, direct inhibition of these potentially deleterious stress response pathways in withdrawal susceptible strains *in vivo* may be an effective way to prevent their severe reactions to exposure and abrupt cessation of ethanol. Such findings would be entirely novel additions to the understanding of withdrawal neurobiology and present an array of promising targets for exploration of therapeutic potential.

In retrospect, our original microarray studies comparing whole-brain gene expression between Chr 1 congenic (R4) and background B6 mice were underpowered (N=6 arrays per strain each representing one individual). Despite this, preliminary results indicated the presence of network structure, and identified oxidative stress and mitochondrial-related genes as overrepresented among those with coordinated pre-existing gene expression differences associated with introgression of the D2-derived R4 interval. Based on literature evidence and *in silico* analyses of public genome-wide brain expression data on mapping populations derived from B6 and D2 (Gene Network, www.genenetwork.org), a small number of genes from the larger network were selected and determined by qRT-PCR as influenced specifically by

Alcdp1/Alcw1, i.e., significantly increased expression in R8 congenic *vs* B6 background strain animals. These results corroborate initial findings that expression of cellular stress response pathway genes may be upregulated at baseline in Chr 1 congenic strains. Clearly, future microarray studies using larger comparisons groups (n=24 arrays per strain) of R8 congenic and B6 background strain mice will be highly informative for elucidating the extent of *trans*-regulatory *Alcdp1/Alcw1* influence suggested by these studies and others (Section III), and identify specific mechanisms by which this network may be tested for contribution to the withdrawal susceptibility phenotype.

The *Alcdp1/Alcw1* QTL interval is syntenic with human Chr 1q23.2-23.3. While still only coarsely localized to a much larger interval on 1q, this region has been repeatedly implicated as associated with alcohol dependence in clinical populations (Section II.A). Thus, these studies identifying promising QTG candidates in a robust animal model, and implicating larger gene networks involving cellular pathways related to mitochondrial function and stress responses, designate *Alcdp1/Alcw1* a region of high priority for further investigation aimed at the discovery and understanding the genetic determinants of human alcoholism.

REFERENCES

1. Bice, P., W. Valdar, L. Zhang, L. Liu, D. Lai, N. Grahame, J. Flint, T.K. Li, L. Lumeng, and T. Foroud, *Genomewide SNP screen to detect quantitative trait loci for alcohol preference in the high alcohol preferring and low alcohol preferring mice.* Alcohol Clin Exp Res, 2009. **33**(3): p. 531-7.
2. Rogawski, M.A., *Update on the neurobiology of alcohol withdrawal seizures.* Epilepsy Curr, 2005. **5**(6): p. 225-30.
3. Faingold, C.L. and A. Riaz, *Ethanol withdrawal induces increased firing in inferior colliculus neurons associated with audiogenic seizure susceptibility.* Exp Neurol, 1995. **132**(1): p. 91-8.
4. Hunter, B.E., C.A. Boast, D.W. Walker, and S.F. Zornetzer, *Alcohol withdrawal syndrome in rats: neural and behavioral correlates.* Pharmacol Biochem Behav, 1973. **1**(6): p. 719-25.
5. Hitzemann, B. and R. Hitzemann, *Genetics ethanol and the Fos response: a comparison of the C57BL/6J and DBA/2J inbred mouse strains.* Alcohol Clin Exp Res, 1997. **21**(8): p. 1497-507.
6. Kozell, L.B., R. Hitzemann, and K.J. Buck, *Acute alcohol withdrawal is associated with c-Fos expression in the basal ganglia and associated circuitry: C57BL/6J and DBA/2J inbred mouse strain analyses.* Alcohol Clin Exp Res, 2005. **29**(11): p. 1939-48.
7. Chen, G., L.B. Kozell, R. Hitzemann, and K.J. Buck, *Involvement of the limbic basal ganglia in ethanol withdrawal convulsivity in mice is influenced by a chromosome 4 locus.* J Neurosci, 2008. **28**(39): p. 9840-9.
8. Mayfield, R.D., R.A. Harris, and M.A. Schuckit, *Genetic factors influencing alcohol dependence.* Br J Pharmacol, 2008. **154**(2): p. 275-87.
9. Goldman, D., G. Oroszi, and F. Ducci, *The genetics of addictions: uncovering the genes.* Nat Rev Genet, 2005. **6**(7): p. 521-32.
10. Strat, Y.L., N. Ramoz, G. Schumann, and P. Gorwood, *Molecular genetics of alcohol dependence and related endophenotypes.* Curr Genomics, 2008. **9**(7): p. 444-51.
11. Reich, T., et al., *Genome-wide search for genes affecting the risk for alcohol dependence.* Am J Med Genet, 1998. **81**(3): p. 207-15.
12. Hinrichs, A.L., et al., *Functional variant in a bitter-taste receptor (hTAS2R16) influences risk of alcohol dependence.* Am J Hum Genet, 2006. **78**(1): p. 103-11.
13. Wang, J.C., et al., *Evidence of common and specific genetic effects: association of the muscarinic acetylcholine receptor M2 (CHRM2) gene with alcohol dependence and major depressive syndrome.* Hum Mol Genet, 2004. **13**(17): p. 1903-11.
14. Lutz, U.C., A. Batra, W. Kolb, F. Machicao, S. Maurer, and M.D. Kohnke, *Methylenetetrahydrofolate reductase C677T-polymorphism and its association with alcohol withdrawal seizure.* Alcohol Clin Exp Res, 2006. **30**(12): p. 1966-71.
15. van Munster, B.C., J.C. Korevaar, S.E. de Rooij, M. Levi, and A.H. Zwinderman, *Genetic polymorphisms related to delirium tremens: a systematic review.* Alcohol Clin Exp Res, 2007. **31**(2): p. 177-84.
16. Schuckit, M.A., *Alcohol sensitivity and dependence.* Exs, 1994. **71**: p. 341-8.
17. Barry, H., 3rd, *Childhood family influences on risk of alcoholism.* Prog Neuropsychpharm, 1979. **3**(5-6): p. 601-12.
18. Friedman, H.J., *Assesment of physical dependence on and withdrawal from ethanol in animals*, in *Alcohol Tolerance and Dependence*, H. Rigter and J.C. Crabbe, Editors. 1980, Elsevier: Amsterdam. p. 93-121.
19. Belknap, J.K., S.E. Laursen, and J.C. Crabbe, *Ethanol and nitrous oxide produce withdrawal-induced convulsions by similar mechanisms in mice.* Life Sci, 1987. **41**(17): p. 2033-40.

20. Kosobud, A. and J.C. Crabbe, *Ethanol withdrawal in mice bred to be genetically prone or resistant.* JPET, 1986. **238**(1): p. 170-7.
21. Goldstein, D.B. and N. Pal, *Alcohol dependence produced in mice by inhalation of ethanol.* Science, 1971. **172**(980): p. 288-90.
22. Terdal, E.S. and J.C. Crabbe, *Indexing withdrawal in mice: matching genotypes for exposure in studies using ethanol vapor inhalation.* Alcohol Clin Exp Res, 1994. **18**(3): p. 542-7.
23. Buck, K.J. and et al, *Mapping murine loci for physical dependence on ethanol.* Psychopharmacology (Berl), 2002. **160**(4): p. 398-407.
24. Crabbe, J.C., *Provisional mapping of QTL for chronic ethanol withdrawal severity in BXD RI mice.* JPET, 1998. **286**(1): p. 263-71.
25. Buck, K.J. and et al, *QTL involved in genetic predisposition to acute alcohol withdrawal in mice.* J Neurosci, 1997. **17**(10): p. 3946-55.
26. Metten, P. and J.C. Crabbe, *Alcohol withdrawal severity in inbred mouse strains.* Behav Neurosci, 2005. **119**(4): p. 911-25.
27. Belknap, J.K., P. Metten, E.H. Beckley, and J.C. Crabbe, *Multivariate analyses reveal common and drug-specific genetic influences on responses to four drugs of abuse.* Trends Pharmacol Sci, 2008. **29**(11): p. 537-43.
28. Crabbe, J.C., J.K. Belknap, and K.J. Buck, *Genetic animal models of alcohol and drug abuse.* Science, 1994. **264**(5166): p. 1715-23.
29. Metten, P. and J.C. Crabbe, *Common genetic determinants of severity of acute withdrawal from ethanol, pentobarbital and diazepam in inbred mice.* Behav Pharmacol, 1994. **5**(4 And 5): p. 533-547.
30. Fehr, C., R.L. Shirley, J.K. Belknap, J.C. Crabbe, and K.J. Buck, *Congenic mapping of alcohol and pentobarbital withdrawal liability loci to a <1 centimorgan interval of murine chromosome 4: identification of Mpdz as a candidate gene.* J Neurosci, 2002. **22**(9): p. 3730-8.
31. Hood, H.M., P. Metten, J.C. Crabbe, and K.J. Buck, *Fine mapping of a sedative-hypnotic drug withdrawal locus on mouse chromosome 11.* Genes Brain Behav, 2006. **5**(1): p. 1-10.
32. Metten, P., T.J. Phillips, J.C. Crabbe, L.M. Tarantino, G.E. McClearn, R. Plomin, V.G. Erwin, and J.K. Belknap, *High genetic susceptibility to ethanol withdrawal predicts low ethanol consumption.* Mamm Genome, 1998. **9**(12): p. 983-90.
33. Metten, P. and J.C. Crabbe, *Alcohol withdrawal severity in inbred mouse (Mus musculus) strains.* Behav Neurosci, 2005. **119**(4): p. 911-25.
34. Buck, K.J., P. Metten, J.K. Belknap, and J.C. Crabbe, *Quantitative trait loci involved in genetic predisposition to acute alcohol withdrawal in mice.* J Neurosci, 1997. **17**(10): p. 3946-55.
35. Buck, K.J., B.S. Rademacher, P. Metten, and J.C. Crabbe, *Mapping murine loci for physical dependence on ethanol.* Psychopharmacology (Berl), 2002. **160**(4): p. 398-407.
36. Gilad, Y., S.A. Rifkin, and J.K. Pritchard, *Revealing the architecture of gene regulation: the promise of eQTL studies.* Trends Genet, 2008. **24**(8): p. 408-15.
37. Cookson, W., L. Liang, G. Abecasis, M. Moffatt, and M. Lathrop, *Mapping complex disease traits with global gene expression.* Nat Rev Genet, 2009. **10**(3): p. 184-94.
38. Flint, J., W. Valdar, S. Shifman, and R. Mott, *Strategies for mapping and cloning quantitative trait genes in rodents.* Nat Rev Genet, 2005. **6**(4): p. 271-86.
39. Mc, C.G., *The genetics of mouse behavior in novel situations.* J Comp Physiol Psychol, 1959. **52**(1): p. 62-7.
40. Phillips, T.J., M. Huson, C. Gwiazdon, S. Burkhart-Kasch, and E.H. Shen, *Effects of acute and repeated ethanol exposures on the locomotor activity of BXD recombinant inbred mice.* Alcohol Clin Exp Res, 1995. **19**(2): p. 269-78.

41. Crabbe, J.C., P. Metten, I. Ponomarev, C.A. Prescott, and D. Wahlsten, *Effects of genetic and procedural variation on measurement of alcohol sensitivity in mouse inbred strains.* Behav Genet, 2006. **36**(4): p. 536-52.
42. Crabbe, J.C., P. Metten, C.H. Yu, J.P. Schlumbohm, A.J. Cameron, and D. Wahlsten, *Genotypic differences in ethanol sensitivity in two tests of motor incoordination.* J Appl Physiol, 2003. **95**(4): p. 1338-51.
43. Cunningham, C.L., D.R. Niehus, D.H. Malott, and L.K. Prather, *Genetic differences in the rewarding and activating effects of morphine and ethanol.* Psychopharmacology (Berl), 1992. **107**(2-3): p. 385-93.
44. Misra, V., H. Lee, A. Singh, K. Huang, R.K. Thimmulappa, W. Mitzner, S. Biswal, and C.G. Tankersley, *Global expression profiles from C57BL/6J and DBA/2J mouse lungs to determine aging-related genes.* Physiol Genomics, 2007. **31**(3): p. 429-40.
45. Roeder, I. and R. Lorenz, *Asymmetry of stem cell fate and the potential impact of the niche: observations, simulations, and interpretations.* Stem Cell Rev, 2006. **2**(3): p. 171-80.
46. Rebrin, I., M.J. Forster, and R.S. Sohal, *Effects of age and caloric intake on glutathione redox state in different brain regions of C57BL/6 and DBA/2 mice.* Brain Res, 2007. **1127**(1): p. 10-8.
47. Ferguson, M., I. Rebrin, M.J. Forster, and R.S. Sohal, *Comparison of metabolic rate and oxidative stress between two different strains of mice with varying response to caloric restriction.* Exp Gerontol, 2008. **43**(8): p. 757-63.
48. Lynn, S., E.J. Huang, S. Elchuri, M. Naeemuddin, Y. Nishinaka, J. Yodoi, D.M. Ferriero, C.J. Epstein, and T.T. Huang, *Selective neuronal vulnerability and inadequate stress response in superoxide dismutase mutant mice.* Free Radic Biol Med, 2005. **38**(6): p. 817-28.
49. Hitzemann, R., C. Reed, B. Malmanger, M. Lawler, B. Hitzemann, B. Cunningham, S. McWeeney, J. Belknap, C. Harrington, K. Buck, T. Phillips, and J. Crabbe, *On the integration of alcohol-related quantitative trait loci and gene expression analyses.* Alcohol Clin Exp Res, 2004. **28**(10): p. 1437-48.
50. Kerns, R.T., A. Ravindranathan, S. Hassan, M.P. Cage, T. York, J.M. Sikela, R.W. Williams, and M.F. Miles, *Ethanol-responsive brain region expression networks: implications for behavioral responses to acute ethanol in DBA/2J versus C57BL/6J mice.* J Neurosci, 2005. **25**(9): p. 2255-66.
51. Chesler, E.J., L. Lu, S. Shou, Y. Qu, J. Gu, J. Wang, H.C. Hsu, J.D. Mountz, N.E. Baldwin, M.A. Langston, D.W. Threadgill, K.F. Manly, and R.W. Williams, *Complex trait analysis of gene expression uncovers polygenic and pleiotropic networks that modulate nervous system function.* Nat Genet, 2005. **37**(3): p. 233-42.
52. Gatti, D., A. Maki, E.J. Chesler, R. Kirova, O. Kosyk, L. Lu, K.F. Manly, R.W. Williams, A. Perkins, M.A. Langston, D.W. Threadgill, and I. Rusyn, *Genome-level analysis of genetic regulation of liver gene expression networks.* Hepatology, 2007. **46**(2): p. 548-57.
53. Daniels, G.M. and K.J. Buck, *Expression profiling identifies strain-specific changes associated with ethanol withdrawal in mice.* Genes Brain Behav, 2002. **1**(1): p. 35-45.
54. Bhave, S.V., P.L. Hoffman, N. Lassen, V. Vasiliou, L. Saba, R.A. Deitrich, and B. Tabakoff, *Gene array profiles of alcohol and aldehyde metabolizing enzymes in brains of C57BL/6 and DBA/2 mice.* Alcohol Clin Exp Res, 2006. **30**(10): p. 1659-69.
55. Toye, A.A., J.D. Lippiat, P. Proks, K. Shimomura, L. Bentley, A. Hugill, V. Mijat, M. Goldsworthy, L. Moir, A. Haynes, J. Quarterman, H.C. Freeman, F.M. Ashcroft, and R.D. Cox, *A genetic and physiological study of impaired glucose homeostasis control in C57BL/6J mice.* Diabetologia, 2005. **48**(4): p. 675-86.
56. Loney, K.D., K.R. Uddin, and S.M. Singh, *Strain-specific brain metallothionein II (MT-II) gene expression, its ethanol responsiveness, and association with ethanol preference in mice.* Alcohol Clin Exp Res, 2003. **27**(3): p. 388-95.

57. Harrison, M. and S.M. Singh, *Genetics and differential expression of NADH:ubiquinone oxidoreductase B8 subunit in brains of genetic strains of mice differing in voluntary alcohol consumption.* Biochim Biophys Acta, 2002. **1579**(2-3): p. 164-72.
58. Flint, J. and T.F. Mackay, *Genetic architecture of quantitative traits in mice, flies, and humans.* Genome Res, 2009. **19**(5): p. 723-33.
59. Mackay, T.F., E.A. Stone, and J.F. Ayroles, *The genetics of quantitative traits: challenges and prospects.* Nat Rev Genet, 2009. **10**(8): p. 565-77.
60. Darvasi, A., *Strategies for the dissection of complex traits in animal models.* Nat Genet, 1998. **18**(1): p. 19-24.
61. Denmark, D.L., L.C. Milner, and K.J. Buck, *Interval-specific congenic animals for high-resolution quantitative trait loci mapping.* Alcohol Research & Health, 2008. **31**(3): p. 266-9.
62. Flint, J., W. Valdar, S. Shifman, and R. Mott, *Strategies for mapping and cloning QTGs in rodents.* Nat Rev Genet, 2005. **6**(4): p. 271-86.
63. Korstanje, R. and B. Paigen, *From QTL to gene: the harvest begins.* Nat Genet, 2002. **31**(3): p. 235-6.
64. Belknap, J.K., R. Hitzemann, J.C. Crabbe, T.J. Phillips, K.J. Buck, and R.W. Williams, *QTL analysis and genomewide mutagenesis in mice: complementary genetic approaches to the dissection of complex traits.* Behav Genet, 2001. **31**(1): p. 5-15.
65. Cicila, G.T., M.R. Garrett, S.J. Lee, J. Liu, H. Dene, and J.P. Rapp, *High-resolution mapping of the blood pressure QTL on chromosome 7 using Dahl rat congenic strains.* Genomics, 2001. **72**(1): p. 51-60.
66. Liang, Y., M. Jansen, B. Aronow, H. Geiger, and G. Van Zant, *The quantitative trait gene latexin influences the size of the hematopoietic stem cell population in mice.* Nat Genet, 2007. **39**(2): p. 178-88.
67. Shirley, R.L., N.A. Walter, M.T. Reilly, C. Fehr, and K.J. Buck, *Mpdz is a quantitative trait gene for drug withdrawal seizures.* Nat Neurosci, 2004. **7**(7): p. 699-700.
68. Wolfer, D.P., W.E. Crusio, and H.P. Lipp, *Knockout mice: simple solutions to the problems of genetic background and flanking genes.* Trends Neurosci, 2002. **25**(7): p. 336-40.
69. Kozell, L., J.K. Belknap, J.R. Hofstetter, A. Mayeda, and K.J. Buck, *Mapping a locus for alcohol physical dependence and associated withdrawal to a 1.1 Mb interval of mouse chromosome 1 syntenic with human chromosome 1q23.2-23.3.* Genes Brain Behav, 2008. **7**(5): p. 560-7.
70. Walter, N.A., D. Bottomly, T. Laderas, M.A. Mooney, P. Darakjian, R.P. Searles, C.A. Harrington, S.K. McWeeney, R. Hitzemann, and K.J. Buck, *High throughput sequencing in mice: a platform comparison identifies a preponderance of cryptic SNPs.* BMC Genomics, 2009. **10**(1): p. 379.
71. Buck, K., P. Metten, J. Belknap, and J. Crabbe, *Quantitative trait loci affecting risk for pentobarbital withdrawal map near alcohol withdrawal loci on mouse chromosomes 1, 4, and 11.* Mamm Genome, 1999. **10**(5): p. 431-7.
72. Ferraro, T.N., G.T. Golden, G.G. Smith, J.F. Martin, F.W. Lohoff, T.A. Gieringer, D. Zamboni, C.L. Schwebel, D.M. Press, S.O. Kratzer, H. Zhao, W.H. Berrettini, and R.J. Buono, *Fine mapping of a seizure susceptibility locus on mouse Chromosome 1: nomination of Kcnj10 as a causative gene.* Mamm Genome, 2004. **15**(4): p. 239-51.
73. Ferraro, T.N., G.G. Smith, C.L. Schwebel, F.W. Lohoff, P. Furlong, W.H. Berrettini, and R.J. Buono, *Quantitative trait locus for seizure susceptibility on mouse chromosome 5 confirmed with reciprocal congenic strains.* Physiol Genomics, 2007. **31**(3): p. 458-62.
74. Kozell, L.B., N.A. Walter, L.C. Milner, K. Wickman, and K.J. Buck, *Mapping a barbiturate withdrawal locus to a 0.44 Mb interval and analysis of a novel null mutant identify a role for Kcnj9 (GIRK3) in withdrawal from pentobarbital, zolpidem, and ethanol.* J Neurosci, 2009. **29**(37): p. 11662-73.

75. Mozhui, K., D.C. Ciobanu, T. Schikorski, X. Wang, L. Lu, and R.W. Williams, *Dissection of a QTL hotspot on mouse distal chromosome 1 that modulates neurobehavioral phenotypes and gene expression.* PLoS Genet, 2008. **4**(11): p. e1000260.
76. Mogil, J.S., S.G. Wilson, E.J. Chesler, A.L. Rankin, K.V. Nemmani, W.R. Lariviere, M.K. Groce, and et al., *The melanocortin-1 receptor gene mediates female-specific mechanisms of analgesia in mice and humans.* PNAS, 2003. **100**(8): p. 4867-72.
77. Collins, F.S., E.D. Green, A. Guttmacher, and M.S. Guyer, *A vision for the future of genomics research.* Nature, 2003. **422**(6934): p. 835-47.
78. Churchill, G.A., et al., *The Collaborative Cross, a community resource for the genetic analysis of complex traits.* Nat Genet, 2004. **36**(11): p. 1133-7.
79. Dick, D.M. and T. Foroud, *Candidate genes for alcohol dependence: a review of genetic evidence from human studies.* Alcohol Clin Exp Res, 2003. **27**(5): p. 868-79.
80. Edenberg, H.J. and T. Foroud, *The genetics of alcoholism: identifying specific genes through family studies.* Addict Biol, 2006. **11**(3-4): p. 386-96.
81. Risinger, F.O. and C.L. Cunningham, *Ethanol-induced conditioned taste aversion in BXD recombinant inbred mice.* Alcohol Clin Exp Res, 1998. **22**(6): p. 1234-44.
82. Tarantino, L.M., G.E. McClearn, L.A. Rodriguez, and R. Plomin, *Confirmation of quantitative trait loci for alcohol preference in mice.* Alcohol Clin Exp Res, 1998. **22**(5): p. 1099-105.
83. Demarest, K., J. McCaughran, Jr., E. Mahjubi, L. Cipp, and R. Hitzemann, *Identification of an acute ethanol response quantitative trait locus on mouse chromosome 2.* J Neurosci, 1999. **19**(2): p. 549-61.
84. Guerrini, I., C.C. Cook, W. Kest, A. Devitgh, A. McQuillin, D. Curtis, and H.M. Gurling, *Genetic linkage analysis supports the presence of two susceptibility loci for alcoholism and heavy drinking on chromosome 1p22.1-11.2 and 1q21.3-24.2.* BMC Genet, 2005. **6**(1): p. 11.
85. Dick, D.M., J. Nurnberger, Jr., H.J. Edenberg, A. Goate, R. Crowe, J. Rice, K.K. Bucholz, J. Kramer, M.A. Schuckit, T.L. Smith, B. Porjesz, H. Begleiter, V. Hesselbrock, and T. Foroud, *Suggestive linkage on chromosome 1 for a quantitative alcohol-related phenotype.* Alcohol Clin Exp Res, 2002. **26**(10): p. 1453-60.
86. Turecki, G., G.A. Rouleau, and M. Alda, *Family density of alcoholism and linkage information in the analysis of the COGA data.* Genet Epidemiol, 1999. **17**(Suppl 1): p. S361-6.
87. Aragaki, C., F. Quiaoit, L. Hsu, and L.P. Zhao, *Mapping alcoholism genes using linkage/linkage disequilibrium analysis.* Genet Epidemiol, 1999. **17 Suppl 1**: p. S43-8.
88. Collins, F.S., E.D. Green, A.E. Guttmacher, and M.S. Guyer, *A vision for the future of genomics research.* Nature, 2003. **422**(6934): p. 835-47.
89. Zhang, L., M.F. Miles, and K.D. Aldape, *A model of molecular interactions on short oligonucleotide microarrays.* Nat Biotechnol, 2003. **21**(7): p. 818-21.
90. Mehrabian, M., H. Allayee, J. Stockton, P.Y. Lum, T.A. Drake, L.W. Castellani, M. Suh, C. Armour, S. Edwards, J. Lamb, A.J. Lusis, and E.E. Schadt, *Integrating genotypic and expression data in a segregating mouse population to identify 5-lipoxygenase as a susceptibility gene for obesity and bone traits.* Nat Genet, 2005. **37**(11): p. 1224-33.
91. Livak, K.J. and T.D. Schmittgen, *Analysis of relative gene expression data using real-time quantitative PCR and the 2(-Delta Delta C(T)) Method.* Methods, 2001. **25**(4): p. 402-8.
92. Walter, N.A., S.K. McWeeney, S.T. Peters, J.K. Belknap, R. Hitzemann, and K.J. Buck, *SNPs matter: impact on detection of differential expression.* Nat Methods, 2007. **4**(9): p. 679-80.
93. Waterston, R.H., et al., *Initial sequencing and comparative analysis of the mouse genome.* Nature, 2002. **420**(6915): p. 520-62.
94. Crabbe, J.C., *Sensitivity to ethanol in inbred mice: genotypic correlations among several behavioral responses.* Behav Neurosci, 1983. **97**(2): p. 280-9.

95. Allison, D.B., X. Cui, G.P. Page, and M. Sabripour, *Microarray data analysis: from disarray to consolidation and consensus.* Nat Rev Genet, 2006. **7**(1): p. 55-65.
96. Bethune, J., F. Wieland, and J. Moelleken, *COPI-mediated transport.* J Membr Biol, 2006. **211**(2): p. 65-79.
97. Brock, C., L. Boudier, D. Maurel, J. Blahos, and J.P. Pin, *Assembly-dependent surface targeting of the heterodimeric GABAB Receptor is controlled by COPI but not 14-3-3.* Mol Biol Cell, 2005. **16**(12): p. 5572-8.
98. Keller, S.H., J. Lindstrom, M. Ellisman, and P. Taylor, *Adjacent basic amino acid residues recognized by the COP I complex and ubiquitination govern endoplasmic reticulum to cell surface trafficking of the nicotinic acetylcholine receptor alpha-Subunit.* J Biol Chem, 2001. **276**(21): p. 18384-91.
99. Margeta-Mitrovic, M., Y.N. Jan, and L.Y. Jan, *A trafficking checkpoint controls GABA(B) receptor heterodimerization.* Neuron, 2000. **27**(1): p. 97-106.
100. O'Kelly, I., M.H. Butler, N. Zilberberg, and S.A. Goldstein, *Forward transport. 14-3-3 binding overcomes retention in endoplasmic reticulum by dibasic signals.* Cell, 2002. **111**(4): p. 577-88.
101. Vivithanaporn, P., S. Yan, and G.T. Swanson, *Intracellular trafficking of KA2 kainate receptors mediated by interactions with coatomer protein complex I (COPI) and 14-3-3 chaperone systems.* J Biol Chem, 2006. **281**(22): p. 15475-84.
102. Yuan, H., K. Michelsen, and B. Schwappach, *14-3-3 dimers probe the assembly status of multimeric membrane proteins.* Curr Biol, 2003. **13**(8): p. 638-46.
103. Pascual, M., S.L. Valles, J. Renau-Piqueras, and C. Guerri, *Ceramide pathways modulate ethanol-induced cell death in astrocytes.* J Neurochem, 2003. **87**(6): p. 1535-45.
104. Minana, R., E. Climent, D. Barettino, J.M. Segui, J. Renau-Piqueras, and C. Guerri, *Alcohol exposure alters the expression pattern of neural cell adhesion molecules during brain development.* J Neurochem, 2000. **75**(3): p. 954-64.
105. Tomas, M., P. Marin, L. Megias, G. Egea, and J. Renau-Piqueras, *Ethanol perturbs the secretory pathway in astrocytes.* Neurobiol Dis, 2005. **20**(3): p. 773-84.
106. Chow, V.T. and H.H. Quek, *Alpha coat protein COPA (HEP-COP): presence of an Alu repeat in cDNA and identity of the amino terminus to xenin.* Ann Hum Genet, 1997. **61**(Pt 4): p. 369-73.
107. Kinkead, B. and C.B. Nemeroff, *Novel treatments of schizophrenia: targeting the neurotensin system.* CNS Neurol Disord Drug Targets, 2006. **5**(2): p. 205-18.
108. Hamscher, G., H.E. Meyer, J.W. Metzger, and G.E. Feurle, *Distribution, formation, and molecular forms of the peptide xenin in various mammals.* Peptides, 1995. **16**(5): p. 791-7.
109. Alexiou, C., J.P. Zimmermann, R.R. Schick, and V. Schusdziarra, *Xenin--a novel suppressor of food intake in rats.* Brain Res, 1998. **800**(2): p. 294-9.
110. Erwin, V.G., V.M. Gehle, K. Davidson, and R.A. Radcliffe, *Confirmation of correlations and common quantitative trait loci between neurotensin receptor density and hypnotic sensitivity to ethanol.* Alcohol Clin Exp Res, 2001. **25**(12): p. 1699-707.
111. Radcliffe, R.A., P. Bludeau, W. Asperi, T. Fay, X.S. Deng, V.G. Erwin, and R.A. Deitrich, *Confirmation of quantitative trait loci for ethanol sensitivity and neurotensin receptor density in crosses derived from the inbred high and low alcohol sensitive selectively bred rat lines.* Psychopharmacology (Berl), 2006. **188**(3): p. 343-54.
112. Erwin, V.G., A. Korte, and M. Marty, *Neurotensin selectively alters ethanol-induced anesthesia in LS/Ibg and SS/Ibg lines of mice.* Brain Res, 1987. **400**(1): p. 80-90.
113. Erwin, V.G., R. Radcliffe, and R.A. Deitrich, *Neurotensin levels in specific brain regions and hypnotic sensitivity to ethanol and pentobarbital as a function of time after haloperidol administration in selectively bred rat lines.* J Pharmacol Exp Ther, 2001. **299**(2): p. 698-704.
114. Smits, S.M., A.F. Terwisscha van Scheltinga, A.J. van der Linden, J.P. Burbach, and M.P. Smidt, *Species differences in brain pre-pro-neurotensin/neuromedin N mRNA distribution:*

the expression pattern in mice resembles more closely that of primates than rats. Brain Res Mol Brain Res, 2004. **125**(1-2): p. 22-8.
115. Elde, R., M. Schalling, S. Ceccatelli, S. Nakanishi, and T. Hokfelt, *Localization of neuropeptide receptor mRNA in rat brain: initial observations using probes for neurotensin and substance P receptors.* Neurosci Lett, 1990. **120**(1): p. 134-8.
116. Mazella, J., J.M. Botto, E. Guillemare, T. Coppola, P. Sarret, and J.P. Vincent, *Structure, functional expression, and cerebral localization of the levocabastine-sensitive neurotensin/neuromedin N receptor from mouse brain.* J Neurosci, 1996. **16**(18): p. 5613-20.
117. Bailey, S.M., *A review of the role of reactive oxygen and nitrogen species in alcohol-induced mitochondrial dysfunction.* Free Radic Res, 2003. **37**(6): p. 585-96.
118. Sun, A.Y. and G.Y. Sun, *Ethanol and oxidative mechanisms in the brain.* J Biomed Sci, 2001. **8**(1): p. 37-43.
119. Almaas, R., O.D. Saugstad, D. Pleasure, and T. Rootwelt, *Effect of barbiturates on hydroxyl radicals, lipid peroxidation, and hypoxic cell death in human NT2-N neurons.* Anesthesiology, 2000. **92**(3): p. 764-74.
120. Smith, D.S., S. Rehncrona, and B.K. Siesjo, *Barbiturates as protective agents in brain ischemia and as free radical scavengers in vitro.* Acta Physiol Scand Suppl, 1980. **492**: p. 129-34.
121. Ueda, Y., T. Doi, K. Nagatomo, and A. Nakajima, *Protective role of pentobarbital pretreatment for NMDA-R activated lipid peroxidation is derived from the synergistic effect on endogenous anti-oxidant in the hippocampus of rats.* Neurosci Lett, 2007. **417**(1): p. 46-9.
122. Vallett, M., T. Tabatabaie, R.J. Briscoe, T.J. Baird, W.W. Beatty, R.A. Floyd, and D.V. Gauvin, *Free radical production during ethanol intoxication, dependence, and withdrawal.* Alcohol Clin Exp Res, 1997. **21**(2): p. 275-85.
123. Dahchour, A., F. Lallemand, R.J. Ward, and P. De Witte, *Production of reactive oxygen species following acute ethanol or acetaldehyde and its reduction by acamprosate in chronically alcoholized rats.* Eur J Pharmacol, 2005. **520**(1-3): p. 51-8.
124. Kashani-Poor, N., K. Zwicker, S. Kerscher, and U. Brandt, *A central functional role for the 49-kDa subunit within the catalytic core of mitochondrial complex I.* J Biol Chem, 2001. **276**(26): p. 24082-7.
125. Sun, F., X. Huo, Y. Zhai, A. Wang, J. Xu, D. Su, M. Bartlam, and Z. Rao, *Crystal structure of mitochondrial respiratory membrane protein complex II.* Cell, 2005. **121**(7): p. 1043-57.
126. Morgan, P.G. and M.M. Sedensky, *Mutations affecting sensitivity to ethanol in the nematode, Caenorhabditis elegans.* Alcohol Clin Exp Res, 1995. **19**(6): p. 1423-9.
127. Kayser, E.B., P.G. Morgan, C.L. Hoppel, and M.M. Sedensky, *Mitochondrial expression and function of GAS-1 in Caenorhabditis elegans.* J Biol Chem, 2001. **276**(23): p. 20551-8.
128. Kayser, E.B., P.G. Morgan, and M.M. Sedensky, *GAS-1: a mitochondrial protein controls sensitivity to volatile anesthetics in the nematode Caenorhabditis elegans.* Anesthesiology, 1999. **90**(2): p. 545-54.
129. Kayser, E.B., C.L. Hoppel, P.G. Morgan, and M.M. Sedensky, *A mutation in mitochondrial complex I increases ethanol sensitivity in Caenorhabditis elegans.* Alcohol Clin Exp Res, 2003. **27**(4): p. 584-92.
130. Ugalde, C., R.J. Janssen, L.P. van den Heuvel, J.A. Smeitink, and L.G. Nijtmans, *Differences in assembly or stability of complex I and other mitochondrial OXPHOS complexes in inherited complex I deficiency.* Hum Mol Genet, 2004. **13**(6): p. 659-67.
131. Gonzalez-Arriaza, H.L. and J.M. Bostwick, *Acute porphyrias: a case report and review.* Am J Psychiatry, 2003. **160**(3): p. 450-9.

132. Flatscher-Bader, T., M.P. van der Brug, N. Landis, J.W. Hwang, E. Harrison, and P.A. Wilce, *Comparative gene expression in brain regions of human alcoholics.* Genes Brain Behav, 2006. **5 Suppl 1**: p. 78-84.
133. Liu, J., J.M. Lewohl, R.A. Harris, V.R. Iyer, P.R. Dodd, P.K. Randall, and R.D. Mayfield, *Patterns of gene expression in the frontal cortex discriminate alcoholic from nonalcoholic individuals.* Neuropsychopharmacology, 2006. **31**(7): p. 1574-82.
134. Yuan, W., R.T. Matthews, J.D. Sandy, and P.E. Gottschall, *Association between protease-specific proteolytic cleavage of brevican and synaptic loss in the dentate gyrus of kainate-treated rats.* Neuroscience, 2002. **114**(4): p. 1091-101.
135. Held-Feindt, J., E.B. Paredes, U. Blomer, C. Seidenbecher, A.M. Stark, H.M. Mehdorn, and R. Mentlein, *Matrix-degrading proteases ADAMTS4 and ADAMTS5 (disintegrins and metalloproteinases with thrombospondin motifs 4 and 5) are expressed in human glioblastomas.* Int J Cancer, 2006. **118**(1): p. 55-61.
136. Mayer, J., M.G. Hamel, and P.E. Gottschall, *Evidence for proteolytic cleavage of brevican by the ADAMTSs in the dentate gyrus after excitotoxic lesion of the mouse entorhinal cortex.* BMC Neurosci, 2005. **6**: p. 52.
137. De Strooper, B., P. Saftig, K. Craessaerts, H. Vanderstichele, G. Guhde, W. Annaert, K. Von Figura, and F. Van Leuven, *Deficiency of presenilin-1 inhibits the normal cleavage of amyloid precursor protein.* Nature, 1998. **391**(6665): p. 387-90.
138. De Strooper, B., W. Annaert, P. Cupers, P. Saftig, K. Craessaerts, J.S. Mumm, E.H. Schroeter, V. Schrijvers, M.S. Wolfe, W.J. Ray, A. Goate, and R. Kopan, *A presenilin-1-dependent gamma-secretase-like protease mediates release of Notch intracellular domain.* Nature, 1999. **398**(6727): p. 518-22.
139. Kislinger, T., B. Cox, A. Kannan, C. Chung, P. Hu, A. Ignatchenko, M.S. Scott, A.O. Gramolini, Q. Morris, M.T. Hallett, J. Rossant, T.R. Hughes, B. Frey, and A. Emili, *Global survey of organ and organelle protein expression in mouse: combined proteomic and transcriptomic profiling.* Cell, 2006. **125**(1): p. 173-86.
140. Herz, J. and Y. Chen, *Reelin, lipoprotein receptors and synaptic plasticity.* Nat Rev Neurosci, 2006. **7**(11): p. 850-9.
141. Thomas, E.A., D.L. Copolov, and J.G. Sutcliffe, *From pharmacotherapy to pathophysiology: emerging mechanisms of apolipoprotein D in psychiatric disorders.* Curr Mol Med, 2003. **3**(5): p. 408-18.
142. Bergeson, S.E., R. Kyle Warren, J.C. Crabbe, P. Metten, V. Gene Erwin, and J.K. Belknap, *Chromosomal loci influencing chronic alcohol withdrawal severity.* Mamm Genome, 2003. **14**(7): p. 454-63.
143. Clancy, J.L., M. Nousch, D.T. Humphreys, B.J. Westman, T.H. Beilharz, and T. Preiss, *Methods to analyze microRNA-mediated control of mRNA translation.* Methods Enzymol, 2007. **431**: p. 83-111.
144. Holcik, M. and N. Sonenberg, *Translational control in stress and apoptosis.* Nat Rev Mol Cell Biol, 2005. **6**(4): p. 318-27.
145. Davenport, E.L., G.J. Morgan, and F.E. Davies, *Untangling the unfolded protein response.* Cell Cycle, 2008. **7**(7): p. 865-9.
146. Pan, Y., H. Chen, F. Siu, and M.S. Kilberg, *Amino acid deprivation and endoplasmic reticulum stress induce expression of multiple activating transcription factor-3 mRNA species that, when overexpressed in HepG2 cells, modulate transcription by the human asparagine synthetase promoter.* J Biol Chem, 2003. **278**(40): p. 38402-12.
147. Shih, A.Y., S. Imbeault, V. Barakauskas, H. Erb, L. Jiang, P. Li, and T.H. Murphy, *Induction of the Nrf2-driven antioxidant response confers neuroprotection during mitochondrial stress in vivo.* J Biol Chem, 2005. **280**(24): p. 22925-36.
148. Bugiani, M., F. Invernizzi, S. Alberio, E. Briem, E. Lamantea, F. Carrara, I. Moroni, L. Farina, M. Spada, M.A. Donati, G. Uziel, and M. Zeviani, *Clinical and molecular findings in children with complex I deficiency.* Biochim Biophys Acta, 2004. **1659**(2-3): p. 136-47.

149. Grad, L.I. and B.D. Lemire, *Mitochondrial complex I mutations in Caenorhabditis elegans produce cytochrome c oxidase deficiency, oxidative stress and vitamin-responsive lactic acidosis.* Hum Mol Genet, 2004. **13**(3): p. 303-14.
150. Harding, H.P., et al., *An integrated stress response regulates amino acid metabolism and resistance to oxidative stress.* Mol Cell, 2003. **11**(3): p. 619-33.
151. Green, T.A., I.N. Alibhai, S. Unterberg, R.L. Neve, S. Ghose, C.A. Tamminga, and E.J. Nestler, *Induction of activating transcription factors (ATFs) ATF2, ATF3, and ATF4 in the nucleus accumbens and their regulation of emotional behavior.* J Neurosci, 2008. **28**(9): p. 2025-32.
152. Chen, G., C. Ma, K.A. Bower, X. Shi, Z. Ke, and J. Luo, *Ethanol promotes endoplasmic reticulum stress-induced neuronal death: involvement of oxidative stress.* J Neurosci Res, 2008. **86**(4): p. 937-46.
153. Hitzemann, R., S. Edmunds, W. Wu, B. Malmanger, N. Walter, J. Belknap, P. Darakjian, and S. McWeeney, *Detection of reciprocal quantitative trait loci for acute ethanol withdrawal and ethanol consumption in heterogeneous stock mice.* Psychopharmacology (Berl), 2009. **203**(4): p. 713-22.
154. Lin, J.H., P. Walter, and T.S. Yen, *Endoplasmic reticulum stress in disease pathogenesis.* Annu Rev Pathol, 2008. **3**: p. 399-425.
155. Peirce, J.L., H. Li, J. Wang, K.F. Manly, R.J. Hitzemann, J.K. Belknap, G.D. Rosen, S. Goodwin, T.R. Sutter, R.W. Williams, and L. Lu, *How replicable are mRNA expression QTL?* Mamm Genome, 2006. **17**(6): p. 643-56.
156. Petkov, P.M., J.H. Graber, G.A. Churchill, K. DiPetrillo, B.L. King, and K. Paigen, *Evidence of a large-scale functional organization of mammalian chromosomes.* PLoS Genet, 2005. **1**(3): p. e33.
157. Treadwell, J.A. and S.M. Singh, *Microarray analysis of mouse brain gene expression following acute ethanol treatment.* Neurochem Res, 2004. **29**(2): p. 357-69.
158. Acin-Perez, R., P. Fernandez-Silva, M.L. Peleato, A. Perez-Martos, and J.A. Enriquez, *Respiratory active mitochondrial supercomplexes.* Mol Cell, 2008. **32**(4): p. 529-39.
159. Boekema, E.J. and H.P. Braun, *Supramolecular structure of the mitochondrial oxidative phosphorylation system.* J Biol Chem, 2007. **282**(1): p. 1-4.
160. Reifschneider, N.H., S. Goto, H. Nakamoto, R. Takahashi, M. Sugawa, N.A. Dencher, and F. Krause, *Defining the mitochondrial proteomes from five rat organs in a physiologically significant context using 2D blue-native/SDS-PAGE.* J Proteome Res, 2006. **5**(5): p. 1117-32.
161. Ardehali, H., Z. Chen, Y. Ko, R. Mejia-Alvarez, and E. Marban, *Multiprotein complex containing succinate dehydrogenase confers mitochondrial ATP-sensitive K+ channel activity.* Proc Natl Acad Sci U S A, 2004. **101**(32): p. 11880-5.
162. Dubinsky, J.M., *Heterogeneity of nervous system mitochondria: Location, location, location!* Exp Neurol, 2009. **218**(2): p. 293-307.
163. Gusnard, D.A. and M.E. Raichle, *Searching for a baseline: functional imaging and the resting human brain.* Nat Rev Neurosci, 2001. **2**(10): p. 685-94.
164. Buzsaki, G., K. Kaila, and M. Raichle, *Inhibition and brain work.* Neuron, 2007. **56**(5): p. 771-83.
165. Gruetter, R., E.R. Seaquist, and K. Ugurbil, *A mathematical model of compartmentalized neurotransmitter metabolism in the human brain.* Am J Physiol Endocrinol Metab, 2001. **281**(1): p. E100-12.
166. Davey, G.P. and J.B. Clark, *Threshold effects and control of oxidative phosphorylation in nonsynaptic rat brain mitochondria.* J Neurochem, 1996. **66**(4): p. 1617-24.
167. Kiebish, M.A., X. Han, H. Cheng, J.H. Chuang, and T.N. Seyfried, *Cardiolipin and electron transport chain abnormalities in mouse brain tumor mitochondria: lipidomic evidence supporting the Warburg theory of cancer.* J Lipid Res, 2008. **49**(12): p. 2545-56.

168. Tan, D.X., L.C. Manchester, M.P. Terron, L.J. Flores, and R.J. Reiter, *One molecule, many derivatives: a never-ending interaction of melatonin with reactive oxygen and nitrogen species?* J Pineal Res, 2007. **42**(1): p. 28-42.
169. Green, D.R. and J.C. Reed, *Mitochondria and apoptosis.* Science, 1998. **281**(5381): p. 1309-12.
170. Bailey, S., *Reactive oxygen & nitrogen species in alcohol-induced mitochondrial dysfunction.* Free Radic Res, 2003. **37**(6): p. 585-96.
171. Hipolito, L., M.J. Sanchez, A. Polache, and L. Granero, *Brain metabolism of ethanol and alcoholism: an update.* Curr Drug Metab, 2007. **8**(7): p. 716-27.
172. Upadhya, S.C. and V. Ravindranath, *Detection and localization of protein-acetaldehyde adducts in rat brain after chronic ethanol treatment.* Alcohol Clin Exp Res, 2002. **26**(6): p. 856-63.
173. Venkatraman, A., A. Landar, A.J. Davis, E. Ulasova, G. Page, M.P. Murphy, V. Darley-Usmar, and S.M. Bailey, *Oxidative modification of hepatic mitochondria protein thiols: effect of chronic alcohol consumption.* Am J Physiol Gastrointest Liver Physiol, 2004. **286**(4): p. G521-7.
174. Carini, R., M.G. De Cesaris, R. Splendore, D. Vay, C. Domenicotti, M.P. Nitti, D. Paola, M.A. Pronzato, and E. Albano, *Signal pathway involved in the development of hypoxic preconditioning in rat hepatocytes.* Hepatology, 2001. **33**(1): p. 131-9.
175. Fernandez-Checa, J.C., C. Garcia-Ruiz, M. Ookhtens, and N. Kaplowitz, *Impaired uptake of glutathione by hepatic mitochondria from chronic ethanol-fed rats. Tracer kinetic studies in vitro and in vivo and susceptibility to oxidant stress.* J Clin Invest, 1991. **87**(2): p. 397-405.
176. Piruat, J.I. and J. Lopez-Barneo, *Oxygen tension regulates mitochondrial DNA-encoded complex I gene expression.* J Biol Chem, 2005. **280**(52): p. 42676-84.
177. Cahill, A., S. Hershman, A. Davies, and P. Sykora, *Ethanol feeding enhances age-related deterioration of the rat hepatic mitochondrion.* Am J Physiol Gastrointest Liver Physiol, 2005. **289**(6): p. G1115-23.
178. Mansouri, A., C. Demeilliers, S. Amsellem, D. Pessayre, and B. Fromenty, *Acute ethanol administration oxidatively damages and depletes mitochondrial dna in mouse liver, brain, heart, and skeletal muscles: protective effects of antioxidants.* J Pharmacol Exp Ther, 2001. **298**(2): p. 737-43.
179. Albano, E., *Alcohol, oxidative stress and free radical damage.* Proc Nutr Soc, 2006. **65**(3): p. 278-90.
180. Mansouri, A., C. Demeilliers, S. Amsellem, D. Pessayre, and B. Fromenty, *Acute ethanol administration oxidatively damages and depletes mitochondrial dna in mouse liver, brain, heart, and skeletal muscles.* JPET, 2001. **298**(2): p. 737-43.
181. Renis, M. and et al, *Nuclear DNA strand breaks during ethanol-induced oxidative stress in rat brain.* FEBS Lett, 1996. **390**(2): p. 153-6.
182. Bailey, S.M., E.C. Pietsch, and C.C. Cunningham, *Ethanol stimulates the production of reactive oxygen species at mitochondrial complexes I and III.* Free Radic Biol Med, 1999. **27**(7-8): p. 891-900.
183. Jung, M.E., R. Agarwal, and J.W. Simpkins, *Ethanol withdrawal posttranslationally decreases the activity of cytochrome c oxidase in an estrogen reversible manner.* Neurosci Lett, 2007. **416**(2): p. 160-4.
184. Jaatinen, P., J. Riikonen, P. Riihioja, O. Kajander, and A. Hervonen, *Interaction of aging and intermittent ethanol exposure on brain cytochrome c oxidase activity levels.* Alcohol, 2003. **29**(2): p. 91-100.
185. Jung, M.E., J.W. Simpkins, A.M. Wilson, H.F. Downey, and R.T. Mallet, *Intermittent hypoxia conditioning prevents behavioral deficit and brain oxidative stress in ethanol-withdrawn rats.* J Appl Physiol, 2008. **105**(2): p. 510-7.

186. Jung, M.E., L.J. Yan, M.J. Forster, and J.W. Simpkins, *Ethanol withdrawal provokes mitochondrial injury in an estrogen preventable manner.* J Bioenerg Biomembr, 2008. **40**(1): p. 35-44.
187. Milne, G.L., J.D. Morrow, and M.J. Picklo, Sr., *Elevated oxidation of docosahexaenoic acid, 22:6 (n-3), in brain regions of rats undergoing ethanol withdrawal.* Neurosci Lett, 2006. **405**(3): p. 172-4.
188. Vallett, M. and et al, *Free radical production during ethanol intoxication, dependence, and withdrawal.* Alcohol Clin Exp Res, 1997. **21**(2): p. 275-85.
189. Jung, M.E., L.J. Yan, M.J. Forster, and et al, *Ethanol withdrawal provokes mitochondrial injury in an estrogen preventable manner.* J Bioenerg Biomembr, 2008. **40**(1): p. 35-44.
190. Patel, M., *Mitochondrial dysfunction and oxidative stress in epileptic seizures.* Free Radic Biol Med, 2004. **37**(12): p. 1951-62.
191. Kudin, A.P., G. Zsurka, C.E. Elger, and W.S. Kunz, *Mitochondrial involvement in temporal lobe epilepsy.* Exp Neurol, 2009. **218**(2): p. 326-32.
192. Kunz, W.S., *The role of mitochondria in epileptogenesis.* Curr Opin Neurol, 2002. **15**(2): p. 179-84.
193. Lenaz, G. and M.L. Genova, *Kinetics of integrated electron transfer in the mitochondrial respiratory chain: random collisions vs. solid state electron channeling.* Am J Physiol Cell Physiol, 2007. **292**(4): p. C1221-39.
194. Vonck, J. and E. Schafer, *Supramolecular organization of protein complexes in the mitochondrial inner membrane.* Biochim Biophys Acta, 2009. **1793**(1): p. 117-24.
195. Genova, M.L., A. Baracca, A. Biondi, G. Casalena, M. Faccioli, A.I. Falasca, G. Formiggini, G. Sgarbi, G. Solaini, and G. Lenaz, *Is supercomplex organization of the respiratory chain required for optimal electron transfer activity?* Biochim Biophys Acta, 2008. **1777**(7-8): p. 740-6.
196. Seelert, H., D.N. Dani, S. Dante, T. Hauss, F. Krause, E. Schafer, M. Frenzel, A. Poetsch, S. Rexroth, H.J. Schwassmann, T. Suhai, J. Vonck, and N.A. Dencher, *From protons to OXPHOS supercomplexes and Alzheimer's disease: Structure-dynamics-function relationships of energy-transducing membranes.* Biochim Biophys Acta, 2009. **1787**(6): p. 657-671.
197. Zhang, M., E. Mileykovskaya, and W. Dowhan, *Gluing the respiratory chain together. Cardiolipin is required for supercomplex formation in the inner mitochondrial membrane.* J Biol Chem, 2002. **277**(46): p. 43553-6.
198. McKenzie, M., M. Lazarou, D.R. Thorburn, and M.T. Ryan, *Mitochondrial respiratory chain supercomplexes are destabilized in Barth Syndrome patients.* J Mol Biol, 2006. **361**(3): p. 462-9.
199. Tahara, E.B., F.D. Navarete, and A.J. Kowaltowski, *Tissue-, substrate-, and site-specific characteristics of mitochondrial reactive oxygen species generation.* Free Radic Biol Med, 2009. **46**(9): p. 1283-97.
200. Schug, Z.T. and E. Gottlieb, *Cardiolipin acts as a mitochondrial signalling platform to launch apoptosis.* Biochim Biophys Acta, 2009.
201. Schagger, H. and G. von Jagow, *Blue native electrophoresis for isolation of membrane protein complexes in enzymatically active form.* Anal Biochem, 1991. **199**(2): p. 223-31.
202. Wittig, I., H.P. Braun, and H. Schagger, *Blue native PAGE.* Nat Protoc. , 2006. **1**(1): p. 418-28.
203. Schagger, H. and K. Pfeiffer, *The ratio of oxidative phosphorylation complexes I-V in bovine heart mitochondria and the composition of respiratory chain supercomplexes.* J Biol Chem, 2001. **276**(41): p. 37861-7.
204. Jung, C., C.M. Higgins, and Z. Xu, *Measuring the quantity and activity of mitochondrial electron transport chain complexes in tissues of central nervous system using blue native polyacrylamide gel electrophoresis.* Anal Biochem, 2000. **286**(2): p. 214-23.

205. Schagger, H., R. de Coo, M.F. Bauer, S. Hofmann, C. Godinot, and U. Brandt, *Significance of respirasomes for the assembly/stability of human respiratory chain complex I.* J Biol Chem, 2004. **279**(35): p. 36349-53.
206. Sabar, M., J. Balk, and C.J. Leaver, *Histochemical staining and quantification of plant mitochondrial respiratory chain complexes using blue-native polyacrylamide gel electrophoresis.* Plant J, 2005. **44**(5): p. 893-901.
207. Krause, F., C.Q. Scheckhuber, A. Werner, S. Rexroth, N.H. Reifschneider, N.A. Dencher, and H.D. Osiewacz, *Supramolecular organization of cytochrome c oxidase- and alternative oxidase-dependent respiratory chains in the filamentous fungus Podospora anserina.* J Biol Chem, 2004. **279**(25): p. 26453-61.
208. Schafer, E., H. Seelert, N.H. Reifschneider, F. Krause, N.A. Dencher, and J. Vonck, *Architecture of active mammalian respiratory chain supercomplexes.* J Biol Chem, 2006. **281**(22): p. 15370-5.
209. Zerbetto, E., L. Vergani, and F. Dabbeni-Sala, *Quantification of muscle mitochondrial oxidative phosphorylation enzymes via histochemical staining of blue native polyacrylamide gels.* Electrophoresis, 1997. **18**(11): p. 2059-64.
210. Dabbeni-Sala, F., S. Di Santo, D. Franceschini, S.D. Skaper, and P. Giusti, *Melatonin protects against 6-OHDA-induced neurotoxicity in rats: a role for mitochondrial complex I activity.* Faseb J, 2001. **15**(1): p. 164-170.
211. Chen, G., M.T. Reilly, L.B. Kozell, R. Hitzemann, and K.J. Buck, *Differential activation of limbic circuitry associated with chronic ethanol withdrawal in DBA/2J and C57BL/6J mice.* Alcohol, 2009. **43**(6): p. 411-20.
212. Pfeiffer, K., V. Gohil, R.A. Stuart, C. Hunte, U. Brandt, M.L. Greenberg, and H. Schagger, *Cardiolipin stabilizes respiratory chain supercomplexes.* J Biol Chem, 2003. **278**(52): p. 52873-80.
213. Wenz, T., R. Hielscher, P. Hellwig, H. Schagger, S. Richers, and C. Hunte, *Role of phospholipids in respiratory cytochrome bc(1) complex catalysis and supercomplex formation.* Biochim Biophys Acta, 2009. **1787**(6): p. 609-16.
214. Fedotcheva, N.I., A.P. Sokolov, and M.N. Kondrashova, *Nonezymatic formation of succinate in mitochondria under oxidative stress.* Free Radic Biol Med, 2006. **41**(1): p. 56-64.
215. Benard, G., B. Faustin, A. Galinier, C. Rocher, N. Bellance, K. Smolkova, L. Casteilla, R. Rossignol, and T. Letellier, *Functional dynamic compartmentalization of respiratory chain intermediate substrates: implications for the control of energy production and mitochondrial diseases.* Int J Biochem Cell Biol, 2008. **40**(8): p. 1543-54.
216. Schonfeld, P. and L. Wojtczak, *Fatty acids decrease mitochondrial generation of reactive oxygen species at the reverse electron transport but increase it at the forward transport.* Biochim Biophys Acta, 2007. **1767**(8): p. 1032-40.
217. Vempati, U.D., X. Han, and C.T. Moraes, *Lack of cytochrome c in mouse fibroblasts disrupts assembly/stability of respiratory complexes I and IV.* J Biol Chem, 2009. **284**(7): p. 4383-91.
218. Nie, F. and M.T. Wong-Riley, *Double labeling of GABA and cytochrome oxidase in the macaque visual cortex: quantitative EM analysis.* J Comp Neurol, 1995. **356**(1): p. 115-31.
219. Artal-Sanz, M., W.Y. Tsang, E.M. Willems, L.A. Grivell, B.D. Lemire, H. van der Spek, and L.G. Nijtmans, *The mitochondrial prohibitin complex is essential for embryonic viability and germline function in Caenorhabditis elegans.* J Biol Chem, 2003. **278**(34): p. 32091-9.
220. Bailey, S.M., G. Robinson, A. Pinner, L. Chamlee, E. Ulasova, M. Pompilius, G.P. Page, D. Chhieng, N. Jhala, A. Landar, K.K. Kharbanda, S. Ballinger, and V. Darley-Usmar, *S-adenosylmethionine prevents chronic alcohol-induced mitochondrial dysfunction in the rat liver.* Am J Physiol Gastrointest Liver Physiol, 2006. **291**(5): p. G857-67.
221. Acin-Perez, R., M.P. Bayona-Bafaluy, M. Bueno, C. Machicado, P. Fernandez-Silva, A. Perez-Martos, J. Montoya, M.J. Lopez-Perez, J. Sancho, and J.A. Enriquez, *An intragenic*

suppressor in the cytochrome c oxidase I gene of mouse mitochondrial DNA. Hum Mol Genet, 2003. **12**(3): p. 329-39.
222. McNamara, R.K., J. Able, R. Jandacek, T. Rider, and P. Tso, *Inbred C57BL/6J and DBA/2J mouse strains exhibit constitutive differences in regional brain fatty acid composition.* Lipids, 2009. **44**(1): p. 1-8.
223. Kiebish, M.A., X. Han, H. Cheng, A. Lunceford, C.F. Clarke, H. Moon, J.H. Chuang, and T.N. Seyfried, *Lipidomic analysis and electron transport chain activities in C57BL/6J mouse brain mitochondria.* J Neurochem, 2008. **106**(1): p. 299-312.
224. Farr, S.A., H.F. Poon, D. Dogrukol-Ak, J. Drake, W.A. Banks, E. Eyerman, D.A. Butterfield, and J.E. Morley, *The antioxidants alpha-lipoic acid and N-acetylcysteine reverse memory impairment and brain oxidative stress in aged SAMP8 mice.* J Neurochem, 2003. **84**(5): p. 1173-83.
225. Boyce, M., K.F. Bryant, C. Jousse, K. Long, H.P. Harding, D. Scheuner, R.J. Kaufman, D. Ma, D.M. Coen, D. Ron, and J. Yuan, *A selective inhibitor of eIF2alpha dephosphorylation protects cells from ER stress.* Science, 2005. **307**(5711): p. 935-9.
226. Sokka, A.L., N. Putkonen, G. Mudo, E. Pryazhnikov, S. Reijonen, L. Khiroug, N. Belluardo, D. Lindholm, and L. Korhonen, *Endoplasmic reticulum stress inhibition protects against excitotoxic neuronal injury in the rat brain.* J Neurosci, 2007. **27**(4): p. 901-8.